國立台灣大學醫學院解剖學暨細胞生物學研究所

博士論文

Graduate Institute of Anatomy and Cell Biology

Cillege of Medicine

National Taiwan University

Doctoral Dissertation

研究 Eupafolin 和山苦瓜對腫瘤壞死因子刺激肺臟發

炎之影響及相關機轉

To study the protective effects of eupafolin and wild

bitter gourd on TNF-α-induced lung inflammation and

the related mechanisms

宋欣錦

Hsin-Ching Sung

指導教授：陳玉怜 博士

Advisor: Yuh-Lien Chen, Ph.D.

中華民國 106 年 7 月

July 2017

國立臺灣大學博士學位論文
口試委員會審定書

研究 Eupafolin 和山苦瓜對腫瘤壞死因子刺激肺臟發
炎之影響及相關機轉

To study the protective effects of eupafolin and wild
bitter gourd on TNF-α-induced lung inflammation and
the related mechanisms

本論文係宋欣錦君（學號:D01446002）在國立臺灣大學
解剖學暨細胞生物學研究所、所完成之博士學位論文，於民
國 106 年 7 月 17 日承下列考試委員審查通過及口試及格，
特此證明

口試委員：

陳玉怜 _____（簽名）

（指導教授）

吳建春 _____   林燕彥 _____

_____   陳永祥 _____

系主任、所長 謝松蒼 _____（簽名）

誌 謝 (Acknowledgment)

首先我要由衷地感謝我的博士班指導老師—陳玉怜教授，在她的耐心指導下，讓我在研究的這條道路上能順利的往前邁進。老師不僅指引我研究的方向，也不斷的協助我突破實驗上的困境，同時嚴格要求論文的撰寫，使其精益求精。這段求學時間，老師的支持和鼓勵，讓我有勇氣堅持到最後，逐步完成我的夢想。

誠摯的感謝梁展榮博士及劉振偉博士在實驗過程中，給予諸多的建議與提點，減少我可能嘗試錯誤的時間，同時也感謝這些年來一起在實驗室互相支持的夥伴—顏郁秀醫師、蒲啟明醫師、沈紋君博士、明憲、又溱、雅君、柏志、俊威、哲宇、紫琳及奕潔等，也因為有您們的陪伴，讓我的研究生活多采多姿。

此外，感謝長庚的同事在工作上的體諒與協助，讓我無後顧之憂。更重要的是要感謝我的家人在這段時間包容，尤其在工作和求學同時要兼顧的這段重要時刻，父親和先生對家庭事務的分擔和關懷，以及兩位可愛小孩對忙碌媽媽的體諒，都是讓我放心完成學業重要的動力和支持。

承蒙吳建春教授、江美治教授、陳永祥教授與林豐彥教授於百忙中撥冗參與論文及口試指導，在此致上最誠摯的謝意。

最後還是感謝所有協助過我的朋友，讓我能夠順利完成學業。未來希望在這條學術研究的道路上，可以跟指導教授和許多前輩看齊，期許自己在這浩瀚的醫學領域中，不斷地讓研究有所精進和突破。

<div align="right">

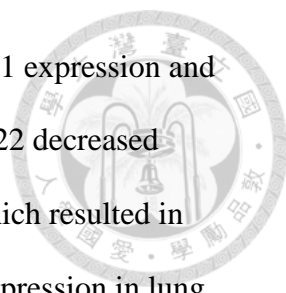宋 欣 錦　謹誌於

國立台灣大學　解剖暨細胞生物學研究所

中華民國一零六年七月

</div>

中文摘要

在肺臟相關的發炎疾病中，白血球會經由與呼吸道上皮細胞的細胞黏附因子黏著而移動，因此細胞黏附因子對發炎疾病具有重要的功能。Eupafolin 是一種類黃酮，也是鴨舌癀(*Phyla nodiflora*)中的主要活性物質，具有抗發炎的能力。另外，山苦瓜萃取物也具有許多藥理上的活性。本文主要目的在探討，在經過 TNF-α 刺激肺泡上皮細胞、C57BL/6 小鼠以及 miRNA-221/222 基因剔除小鼠中，eupafolin 及山苦瓜萃取物對細胞黏附因子表現的影響。研究中首先利用西方點墨法及免疫螢光染色法，觀察 eupafolin 及山苦瓜萃取物對 TNF-α 刺激 A549 細胞後 ICAM-1 及相關蛋白表現的影響。另外小鼠以腹腔注射 eupafolin 3 天(第一部分)，或是給予 C57BL/6 小鼠及 miRNA-221/222 基因剔除小鼠口服 5 天山苦瓜萃取物(第二部分)後，再以插管方式給予 TNF-α 1 天後取出肺臟。接著再以西方點墨法及組織免疫染色觀察 ICAM-1 表現的改變。第一部分實驗結果顯示，eupafolin 確實可降低因 TNF-α 刺激引起的 ICAM-1 表現，而此作用是經由抑制 ERK1/2、JNK、p38 和 AKT/PI3K 的磷酸化。然而，加入 p38 和 PI3K 的抑制劑並不會改變 ICAM-1 的表現。再者，eupafolin 同時降低了 TNF-α 所引起之 NF-κB 的活化及核轉移。在小鼠肺臟組織中，受 TNF-α 刺激而表現量增加的 ICAM-1 會受到 eupafolin 的抑制。第二部分實驗結果顯示，在 A549 細胞中，山苦瓜萃取物確實可經由抑制 PI3K/AKT/NF-κB/IκB 的磷酸化作用而減緩因 TNF-α 引起的 ICAM-1 表現，並且減少了白血球的黏附作用。除此之外，山苦瓜萃取物也會降低內生性的 ICAM-1 表現且會增加 miRNA -221/-222 的表現。讓細胞過度表現 miRNA 222 也可降低 PI3K/AKT/NF-κB/IκB 的磷酸化及 ICAM-1 表現量與白血球的黏附作用。另外，在小鼠肺臟組織中，山苦瓜萃取物可抑制 TNF-α 刺激或沒刺激而表現的 ICAM-1 以及增加 miRNA -221/-222 的表現；但並不影響 miRNA-221/222 基因剔除小鼠之 miRNA-221/-222 但些微影響 ICAM-1 的表現。此結果顯示，eupafolin 及山苦瓜萃取物在細胞及動物實驗中皆可降低 ICAM-1 的表現。Eupafolin 可降低因 TNF-α 引起的 ICAM-1 表現以及白血球的黏附作用，且是經由抑制 AKT/ERK1/2/JNK 的磷酸化作用以及 NF-κB 的核轉移所致；而山苦瓜萃取物則是經由 miR-221/-222/PI3K/AKT/NF-κB 這條路徑來控制。因此，eupafolin 及山苦瓜萃取物也提供了另一種治療肺臟發炎相關疾病的藥物的另一種新選擇。

英文摘要

The deregulation of cell adhesion molecules associated with the epithelium-leukocyte interaction plays the important role in the pathogenesis of lung airway inflammatory disorders. Eupafolin, a major bioactive compound found in *Phyla nodiflora,* has been reported to have the anti-inflammatory property. In addition, the extracts from wild bitter gourd fruit (WBGE) also possess numerous pharmacological activities. The purpose of this study was to investigate the effects of eupafolin or WBGE on intercellular adhesion molecule-1 (ICAM-1) expression in epithelial cells, C57BL/6 wild-type (WT) mice or microRNA (miR)-221/-222 knockout (KO) mice with or without tumor necrosis factor-α treatment and the related mechanisms. At first, the effects of eupafolin and WBGE on ICAM-1 expression and the related signals in A549 cells were examined by western blot and immunofluorescent staining. The part of the manuscript is the mice were injected intraperitoneally with or without eupafolin and then left untreated or injected intratracheally with TNF-α. The part section of them, WT mice and miR-221/-222 KO mice were orally treated with or without WBGE and then left untreated or injected intratracheally with TNF-α. The expression levels and patterns of ICAM-1 in the lung tissues were examined by western blot and immunohistochemical staining. In part one, eupafolin pretreatment reduced the TNF-α-induced ICAM-1 expression and also the ERK, JNK, p38, and AKT/ PI3K phosphorylation. However, the increase in ICAM-1 expression with TNF-α treatment was unaffected by p38 and PI3K inhibitors. Moreover, eupafolin decreased the TNF-α-induced NF-κB p65 activation and its nuclear translocation. Furthermore, eupafolin reduced ICAM-1 expression in the lung tissues of TNF-α-treated mice. In part two, WBGE significantly decreased the TNF-α-induced ICAM-1 expression in A549 cells through the inhibition of PI3K/ AKT/ NF-κB /IκB phosphorylation and decreased

leukocyte adhesion. In addition, WBGE reduced endogenous ICAM-1 expression and upregulated miR-221/-222 expression. The overexpression of miR-222 decreased PI3K/AKT/NF-κB/IκB phosphorylation and ICAM-1 expression, which resulted in reducing monocyte adhesion. Moreover, WBGE reduced ICAM-1 expression in lung tissues of WT mice with or without TNF-α treatment and upregulated miR-221/222. WBGE did not affect the miR-221/-222 level and had little effect on ICAM-1 expression in miR-221/-222 KO mice. These results suggest that eupafolin and WBGE reduced ICAM-1 expression both under *in vitro* and *in vivo* conditions. The protective effects of eupafolin were mediated via AKT/ERK1/2/JNK phosphorylation and nuclear translocation of NF-κB. Furthermore, WBGE were mediated partly through the miR-221/-222/PI3K/AKT/NF-κB pathway. Therefore, eupafolin and WBGE may represent novel therapeutic agents targeting epithelial activation in lung inflammation.

簡介

The dysregulated, chronic inflammation is a critical risk factor in the initiation and development of pulmonary diseases, such as asthma and chronic obstructive pulmonary disease (Barnes, 2011; Lee and Yang, 2013). The expression of adhesion molecules on airway epithelial cells was important for selective recruitment of effector cells onto epithelial cells (Chen et al., 2001). Intercellular adhesion molecule-1 (ICAM-1) which is an adhesion molecule, has long been known for its importance in mediating cell-cell interactions. Its expression is increased by the stimulation of inflammatory cytokines and enhances adhered leukocytes that migrated across the vascular endothelial cells and then interacted with epithelial cells at sites of inflammatory airways (Lee and Yang, 2013). The clinical study has also showed that the ICAM-1 level was much higher in plasma of patients with pulmonary diseases (Demir et al., 2002). ICAM-1 was shown to be upregulated in epithelial cells by the stimulation of several pro-inflammatory cytokines such as tumor necrosis factor-α (TNF-α), interleukin-1β, and interferon-γ (IFN-γ) (Kim et al., 2008; Wang et al., 2014). Currently available therapies for inflammation include corticosteroids and CXC chemokine receptor antagonists (Durham et al., 2015). However, many of these agents have a number of serious adverse effects. Modulation of the ICAM-1 expression provides a rationale for the development of therapeutic agents against a variety of inflammatory lung diseases.
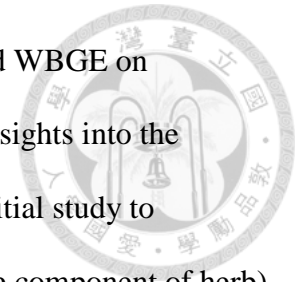
Herbs have been extensively used in foods and in traditional medicines in oriental countries for centuries. The active components of herbs may provide a useful platform for the development of effective pharmacological agents. *Phyla nodiflora*, which belongs to the Verbenaceae family, is a common ingredient of herbal tea for the treatment of inflammation, menstrual disorders, and infectious diseases (Yang et al.,

1998). Eupafolin (6-methoxy-5, 7, 3′, 4′-tetrahydroxyflavone), the major bioactive flavonoid isolated from the dried aerial parts of *P. nodiflora*, inhibits the NO release in LPS-stimulated macrophages (Maas et al., 2011). These results indicate that eupafolin has antioxidative and anti-inflammatory effects on macrophages (Ko et al., 2014; Lai et al., 2011; Maas et al., 2011).

Wild bitter gourds (WBG, *Momordica charantia* L.) are consumed as a vegetable and have been used as a traditional herbal medicine in Asia (Chao et al., 2014). The noticeable pharmacological properties of WBG fruit extract (WBGE) are anti-diabetic (Chaturvedi, 2012), anti-inflammatory (Chao et al., 2014, Lii et al., 2009), anti-tumor (Bai et al., 2016; Somasagara et al., 2015) and anti-oxidative actions (Lu et al., 2014). However, the anti-inflammatory effects of both eupafolin and WBGE on human lung epithelial cells and the underlying mechanisms have not been investigated.

The intracellular signaling pathways by which TNF-α causes ICAM-1 expression are, in the main, not well understood, but certain have been proposed, including mitogen-activated protein kinases (MAPKs), PI3K/AKT and transcriptional factors (Binion et al., 2009; Chen et al., 2001). In addition, evidence also suggested that miRNA was involved in lung inflammation (Alipoor et al., 2016). MiRNAs, which are a new class of non-coding small RNAs, are 19-25 nucleotides in length (Alipoor et al.2016). They target mRNAs through complementarity between the miRNAs and the 3'-untranslated regions (3'UTRs) of target mRNAs, which causes either mRNA cleavage or translational suppression and results in gene silencing (Hu et al., 2010). Additionally, recent studies have shown that miR-221 or miR-222 can suppress ICAM-1 translation and regulate ICAM-1 expression (Hu et al., 2010; Gong et al., 2011; Jansen et al., 2015). However, the relationship between miRNAs and ICAM-1 in lung inflammation is still unclear.
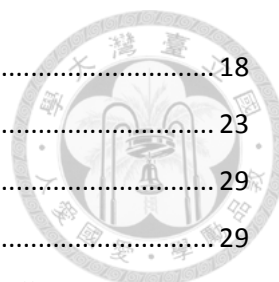
Therefore, a better understanding of the effects of eupafolin and WBGE on ICAM-1 expression and the mechanisms might provide important insights into the prevention of airway inflammation. Accordingly, this study is the initial study to elucidate the anti-inflammatory effects of both eupafolin (a bioactive component of herb) and WBGE (a common vegetable in Asia), and the related mechanisms on TNF-α-treated A549 cells and mice.

目錄

PART I

中文摘要

Eupafolin 是一種類黃酮，也是鴨舌癀(*Phyla nodiflora*.)中的主要活性物質。在肺臟相關的發炎疾病中，白血球會經由與呼吸道上皮細胞的細胞黏附因子黏著而移動，因此細胞黏附因子對發炎疾病具有重要的功能。本文研究主要目的在探討，eupafolin 對肺臟上皮細胞被腫瘤壞死因子(tumor necrosis factor-α, TNF-α)刺激後所引起之細胞黏附因子(intercellular cell adhesion molecule-1, ICAM-1)的表現量影響及其作用機轉。研究中利用西方點墨法及免疫螢光染色實驗，觀察 TNF-α 刺激人類呼吸道上皮細胞(A549 cells)後 ICAM-1 的表現以及影響的相關蛋白表現。在動物實驗部分，小鼠以腹腔注射 eupafolin 3 天，再以插管方式給予 TNF-α 1 天後取出肺臟。然後利用西方點墨法及組織免疫染色觀察 eupafolin 對 ICAM-1 表現的影響。細胞實驗結果顯示，eupafolin 可降低因 TNF-α 引起的 ICAM-1 表現，而此作用是經過抑制 ERK1/2、JNK、p38 和 AKT/PI3K 的磷酸化作用。然而，加入 p38 和 PI3K 的抑制劑並不會改變 ICAM-1 的表現。再者，eupafolin 同時降低了 TNF-α 所引起之 NF-κB 的活化及核轉移。動物的實驗結果顯示，在小鼠肺臟組織中，受 TNF-α 刺激而表現量增加的 ICAM-1 會受到 eupafolin 的抑制。Eupafolin 可降低因 TNF-α 引起的 ICAM-1 表現以及白血球的黏附作用，且是經由抑制 AKT/ERK1/2/JNK 的磷酸化作用以及 NF-κB 的核轉移所致。因此，eupafolin 對呼吸道上皮細胞具有抗發炎的能力；而此實驗結果也提供了另一種治療肺臟發炎相關疾病的藥物的新選擇。

關鍵字: eupafolin; 細胞黏附因子-1; MAPKs; AKT; 發炎

英文摘要

Eupafolin, a major bioactive compound found in *Phyla nodiflora*, has the anti-inflammatory property. Upregulation of cell adhesion molecules in the lung airway epithelium is associated with the epithelium-leukocyte interaction and plays a critical role in the pathogenesis of lung airway inflammatory disorders. To investigate the effects of eupafolin on tumor necrosis factor-α (TNF-α)-induced intercellular cell adhesion molecule-1 (ICAM-1) expression in A549 human lung airway epithelial cells and the underlying mechanisms. The effect of eupafolin on ICAM-1 expression in A549 cells were examined by Western blotting and immunofluorescent staining. The mice were injected intraperitoneally with or without eupafolin and then were left untreated or were injected intratracheally with TNF-α. To detect the effect of eupafolin on ICAM-1 expression, the lung tissues were also examined by Western blotting and immunohistochemical staining. Eupafolin pretreatment reduced the TNF-α-induced ICAM-1 expression and also the ERK1/2, JNK, p38, and AKT/PI3K phosphorylation. However, the increase in ICAM-1 expression with TNF-α treatment was unaffected by p38 and PI3K inhibitors. Eupafolin decreased the TNF-α-induced NF-κB p65 activation and its nuclear translocation. Furthermore, eupafolin reduced ICAM-1 expression in the lung tissues of TNF-α-treated mice. Eupafolin exerts its anti-inflammatory activity by suppressing the TNF-α-induced ICAM-1 expression and subsequent monocyte adhesion via AKT/ERK1/2/JNK phosphorylation and nuclear translocation of NF-κB p65. These results suggest that eupafolin may represent a novel therapeutic agent targeting epithelial activation in lung inflammation.
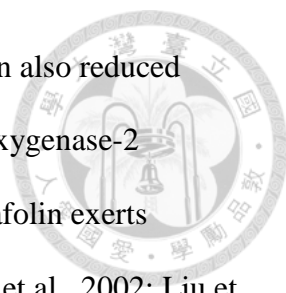
Keywords: eupafolin; intercellular cell adhesion molecule-1; MAPKs; AKT; inflammation

第一章　簡介

The dysregulated, chronic inflammation is a critical risk factor in the initiation and development of pulmonary diseases, such as asthma and chronic obstructive pulmonary disease (Barnes, 2011; Lee and Yang, 2013). The increased adhesion molecules and inflammatory chemokines on airway epithelial cells would be important in the selective recruitment of effector cells onto epithelial cells (Rosseau et al., 2000). Among the cell adhesion molecules, intercellular cell adhesion molecule-1 (ICAM-1), a cell surface glycoprotein that belongs to the immunoglobulin supergene family, is overexpressed on airway epithelial cells during inflammation, which enhances the adherence and infiltration of leukocytes across the endothelial cells and epithelial cells at sites of inflammatory airways. The clinical study has also showed that the ICAM-1 level was much higher in plasma of patients with pulmonary diseases (Demir et al., 2002). ICAM-1 was shown to be upregulated in epithelial cells by the stimulation of several pro-inflammatory cytokines such as tumor necrosis factor-α (TNF-α), interleukin-1β, and interferon-γ (IFN-γ) (Kim et al., 2008; Wang et al., 2014). Modulation of the ICAM-1 expression provides a rationale for the development of therapeutic agents against a variety of inflammatory lung diseases.

Herbs have been extensively used in foods and in traditional medicines in oriental countries for centuries. The active components of herbs may provide a useful platform for the development of effective pharmacological agents. *Phyla nodiflora*, which belongs to the Verbenaceae family, is a common ingredient of herbal tea for the treatment of inflammation, menstrual disorders, and infectious diseases (Yang et al., 1998). Eupafolin (6-methoxy-5, 7, 3′, 4′-tetrahydroxyflavone; Fig. 1), the major bioactive flavonoid isolated from the dried aerial parts of *P. nodiflora*, inhibits the NO

release in LPS-stimulated macrophages (Maas et al., 2011). Eupafolin also reduced

pro-inflammatory inducible nitric oxide synthase (iNOS) and cyclooxygenase-2

(COX-2) expression in these cells (Lai et al., 2011). In addition, eupafolin exerts

anti-tumor activity by the inhibition of cancer cell proliferation (Abe et al., 2002; Liu et

al., 2014). These results indicate that eupafolin has antioxidative and anti-inflammatory

effects on macrophages (Ko et al., 2014; Lai et al., 2011; Maas et al., 2011). However,

the anti-inflammatory effects of eupafolin on human lung epithelial cells and the related

mechanisms have not been investigated. The intracellular signaling pathways by which

TNF-α causes ICAM-1 expression are, in the main, not well understood, but certain

have been proposed, including mitogen-activated protein kinases (MAPKs), PI3K/AKT

and transcriptional factors (Binion et al., 2009; Chen et al., 2001). Little is known about

the effects of eupafolin on ICAM-1 expression and the mechanisms of these effects, and

a better understanding of this might provide important insights into the prevention of

airway inflammation. In the present study, we showed that eupafolin reduced

AKT/ERK1/2/JNK phosphorylation in TNF-α-treated A549 cells (a human airway type

II alveolar epithelial cells), resulting in the reduced activation of NF-κB in the ICAM-1

promoter, which is followed by the reduction of ICAM-1 expression and monocyte

adhesion. Moreover, we found that TNF-α-induced ICAM-1 expression was also

suppressed in lung tissues of C57BL/6J mice by eupafolin treatment.

第二章 材料與方法
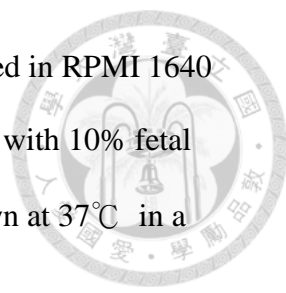
2.1. Extraction and purification of eupafolin

P. nodiflora was collected from a local farm (Tainan, Taiwan). The authenticity of the plant species was identified by a pharmacognosist, Professor Ih-sheng Chen, and stored as a voucher specimen (2007-02-PNM) in the Herbarium of the Department of Fragrance and Cosmetic Science, Kaohsiung Medical University, Kaohsiung, Taiwan. Eupafolin was purified from the plant as described previously (Ko et al., 2014). In brief, dried aerial part of *P. nodiflora* was chopped and immersed in methanol at room temperature. The methanol extract was filtered and concentrated by rotary vacuum evaporation. The crude methanolic extract was suspended in water and successively portioned with an equivalent volume of n-hexane, chloroform, and ethyl acetate. The partition was subjected to silica gel column chromatography, purified with a mixture of n-hexane and ethyl acetate, and followed by purification with methanol. The purified fraction was recrystallized to obtain eupafolin. Eupafolin was stored at −20℃ until further use. The chemical structure and purity of eupafolin (Fig. 1) was identified by ^{1}H-NMR. Eupafolin was dissolved in dimethylsulfoxide (DMSO) and then further diluted with the assay medium (1-50 μM). Solvent controls with DMSO were carried out in each assay.

2.2. Cell culture
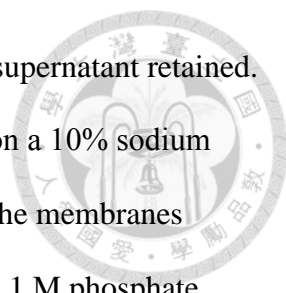
Human lung epithelial alveolar cells (A549 cells) and human monocytic leukemia cells (U937 cells) were obtained from American Type Culture Collection (Manassas, VA, USA). A549 cells were cultured in Dulbecoo's Modified Eagle Medium (DMEM) (Gibco, Life Technology, Grand Island, NY, USA) supplemented with 10% fetal bovine

serum(FBS) and 1% penicillin-streptomycin. U937 cells were cultured in RPMI 1640

medium (M.A. Bioproducts, Walkersville, MD, USA) supplemented with 10% fetal

bovine serum and 1% penicillin-streptomycin. These cells were grown at 37℃ in a

humidified atmosphere of 95% air and 5% CO_2. The

3-(4,5-dimethylthiazol-2-yl)-2,5-diphenyl tetrazolium bromide (MTT) assay was used

to measure cell viability. The principle of this assay is that mitochondrial

dehydrogenase in viable cells reduces MTT to a blue formazan. Briefly, cells were

grown in 96-well plates and incubated with various concentrations of TNF-α (0.1-10

ng/mL) or eupafolin (1-50 μM) for 24 h, then 100 μL of MTT (0.5 mg/mL) was added

to each well and incubation continued at 37℃ for an additional 4 h. The medium was

then carefully removed, so as not to disturb the formazan crystals formed. Dimethyl

sulphoxide (DMSO; 100 μL), which solubilizes the formazan crystals, was added to

each well and the absorbance of the solubilized blue formazan read at 530 nm (reaction)

and 690 nm (background) using a DIAS Microplate Reader (Dynex Technologies,

U.S.A.). The reduction in optical density caused by cytokine and eupafolin was used as

a measurement of cell viability, normalized to cells incubated in control medium, which

were considered 100% viable. In the present study, A549 cells treated with 0.1-10

ng/mL of TNF-α or 1-50 μM of eupafolin for 24 h did not cause the cytotoxicity.

2.3. Preparation of cell lysates and Western blot analysis
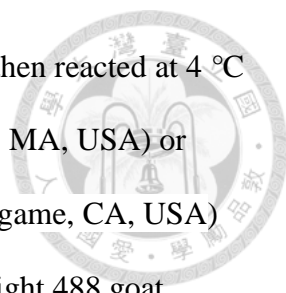
Western blot analyses were performed as described previously (Liang et al., 2013).

A549 cells were incubated with various concentrations (0.1, 0.3, 1, 3, or 10 ng/mL) of

TNF-α at different time intervals (4, 8, 16, or 24 h). Cell lysates were prepared by

incubating cells in a lysis buffer (20 mM Tris-HCl, 150 mM NaCl, 1 mM EDTA, 1 mM

EGTA, 1% Triton X-100, 1 mM phenylmethylsulfonyl fluoride, pH 7.4) for 1 h at 4 ℃.

The cell lysate was centrifuged at 4000 g for 30 min at 4 °C and the supernatant retained. Equal amounts of the supernatant (20 μg of protein) were separated on a 10% sodium dodecyl sulfate (SDS)-PAGE and blotted on to PVDF membranes. The membranes were blocked nonspecific binding of antibody in 3% nonfat milk in 0.1 M phosphate buffer for 1 h at room temperature (RT). Immunoreaction was performed with the following primary antibodies: rabbit antibodies against anti-ICAM-1(1:5000, Santa Cruz Biotechnology, Dallas, TX, USA), anti-phospho ERK1/2 (1:10000, Cell Signaling, Danvers, MA, USA), anti-phospho p38 (1:1000, Santa Cruz Biotechnology), anti-phospho JNK (1:1000, Cell Signaling), anti-phospho PI3K (1:1000, EnoGene Biotech, New York, NY, USA), anti-phospho AKT (1:1000, EnoGene Biotech), anti-phospho p65 (1:1000, Epitomics, Burlingame, CA, USA), anti-phospho IκB (1:1000, Cell Signaling), anti-total p65 (1:1000, Epitomics), anti-total ERK1/2 (1:10000, Cell signaling), and anti-total JNK (1:1000, OriGene, Rockville, MD, USA) at 4 °C for overnight. The membranes were then incubated for 1 h at room temperature with HRP-conjugated goat anti-rabbit IgG antibodies (1:2000, Santa Cruz Biotechnology). The immunoreactive bands were detected using the Chemiluminescence Reagent Plus (NEN, Boston, MA, USA). The intensity of each band was quantified using a densitometer. Antibodies against GAPDH (1:5000, Santa Cruz Biotechnology) or hnRNP (1:10000, Abcam, Cambridge, MA, USA) were designed as the internal standard.

2.4. Immunofluorescent staining of ICAM-1 and NF-κB p65

To examine ICAM-1 or NF-κB p65 expression in situ, confluent A549 cells (controls or cells treated for 24 h with eupafolin) on cover slips were incubated in the absence or presence of 3 ng/mL TNF-α for 4h at 37 °C and fixed in 4%

paraformaldehyde in PBS, pH 7.4, for 15 min at RT. The cells were then reacted at 4 °C

with rabbit anti-human ICAM-1 (1:100 dilution, Abcam, Cambridge, MA, USA) or

anti-human NF-κB p65 antibodies (1:100 dilution, Epitomics, Burlingame, CA, USA)

for overnight. After washes, the coverslips were incubated with DyLight 488 goat

anti-rabbit polyclonal antibody (1:200 dilution, Abcam) for 1 h at 37 °C and observed

by a fluorescence microscope.

2.5. siRNA knockdown of ERK, JNK, and p65

To perform the knockdown ERK, JNK, and p65 by siRNA, A549 cells were

transfected with siRNA specifically targeting ERK, JNK, p65, or scrambled gene

(ON-TARGET plus SMARTpool RNA duplexes; Thermo Scientific, Waltham, MA,

USA). For transfection, siRNA (1 nM) was transfected into A549 cells (10^6) for 48 h

according to the manufacturer's instruction. The siRNA results were evaluated by

Western blotting.

2.6. Preparation of nuclear extracts and electrophoretic mobility-shift assay (EMSA)

The nuclear protein extracts and the EMSA conditions were prepared as described

previously (Liang et al., 2013). Nuclear proteins were extracted using NE-PER reagent

(Pierce, Rockford, IL, USA) according to the manufacturer's protocol. The NF-κB

binding activity of equal amounts (10 μg) of nuclear protein was performed using the

LightShift chemiluminescence EMSA kit (Pierce). The synthetic double-stranded

oligonucleotides used as the probes in the gel-shift assay were

5′-AGTTGAGGGGACTTTCCCAGGC-3′ and

3′-TCAACTCCCCTGAAAGGGTCCG-5′.
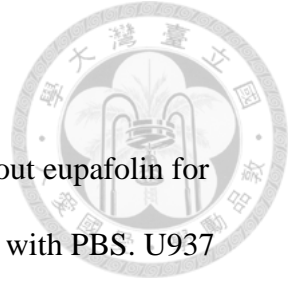
2.7.   Epithelial cell–leukocyte adhesion assay

A549 cells, grown in 24-well dish, were pretreated with or without eupafolin for 24h and treated with TNF-α for 4 h at 37℃, then washed three times with PBS. U937 cells, were labeled with 10 mM of BCECF-AM (2',7'-bis-(2-carboxyethyl)-5-(and-6)-carboxyfluorescein acetoxymethyl, Boehringer Mannheim, Mannheim, Germany) for 1 h at 37 °C. Labeled U937 cells (10^6) were added to A549 cells (10^6) and incubation continued for 1 h. Nonadherent cells were removed by gentle washes with PBS. The number of U937 cells adhering to A549 cells was counted in six randomly selected images captured by fluorescent microscope (Zeiss) for each experiment.

2.8.   Animal care and experimental procedures

All procedures involving experimental animals were performed in accordance with the guidelines for animal care of the National Taiwan University (No. 20130175) and complied with the *Guide for the Care and Use of Laboratory Animals,* NIH publication No. 86–23, revised 1985. Male 8-week-old C57BL6 mice, weighing between 25 and 35 g, were purchased from the National Taiwan University (Taipei, Taiwan). The mice were injected intraperitoneally (ip) with or without eupafolin (10 mg/2mL DMSO/Kg body weight/day) for 3 days and then were left untreated or were injected intratracheally with TNF-α (8 μg/Kg) for the next 1 day. Some mice were injected ip with an equivalent volume of the DMSO vehicle (2mL/Kg body weight) as the control. They were then anesthetized by ip injection of 30-40 mg/kg pentobarbital and sacrificed. A part of lung tissues was immersion-fixed with 4% buffered paraformaldehyde and paraffin-embedded for immunohistochemistry; the remaining larger portion was

immediately frozen in liquid nitrogen for protein isolation to detect the ICAM-1 level by Western blotting.
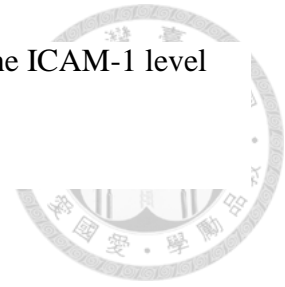
2.9. Immunohistochemistry

The sample size of lung is 5 x 5 x 5 mm. Sections (5 µm) were cut from the paraffin blocks. To determine the ICAM-1 expression in lung tissues, the sections were examined by immunostaining with ICAM-1 antibodies (1:100 dilution, Abcam). The sections were then incubated with biotin-conjugated goat anti-rabbit IgG (1:200 dilution, Vector lab, Cambridgeshire, UK) for 1h at room temperature (RT). Finally, the sections were stained with 3,3-diaminobenzidine tetrahydrochloride (DAB), counterstained with hematoxylin. To examine whether ICAM-1 was associated with type II alveolar epithelial cells, the section was examined by double immunofluorescent staining for, respectively, ICAM-1 (1:100, BioLegend, CA, USA) and SP-D (marker for type II alveolar epithelial cells, 1:100, Bioss, Beijing, China) for 1h at RT. After washed with PBS, the section was then incubated with Alexa Fluro 488 conjugated goat anti-rat IgG (1:500, BioLegend, green) for ICAM-1 and Dylight 594 conjugated donkey anti-rabbit IgG (1:500, BioLegend, red) for SP-D. Finally, the slides were counterstained with DAPI and examined by fluorescent microscope.

2.10. Statistical analysis

The data are expressed as a fold value compared to the control value and are the means ± SEM for five separate experiments unless other specified. All statistical analyses were performed with one-way ANOVA, and then followed with Duncan's Multiple range test. Analyses were done using SigmaPlot software (Systat Software, Inc., Chicago, IL, USA). *$P < 0.05$ compared to the untreated cells. [†]$P < 0.05$ compared

to the TNF-α-treated cells.

第三章 結果
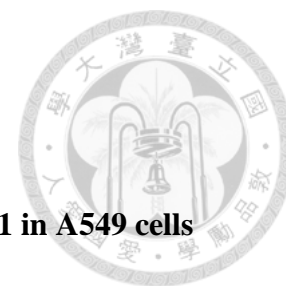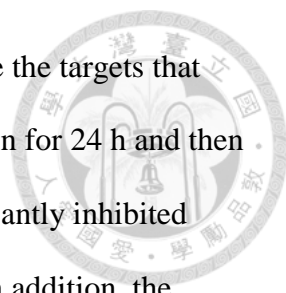
3.1. Eupafolin reduces TNF-α-induced upregulation of ICAM-1 in A549 cells

A549 cells were incubated with various concentrations of TNF-α at different time intervals. ICAM-1 expression was significantly upregulated with 1 ng/mL, 3 ng/mL or 10 ng/mL of TNF-α treatment for 4 h, 8 h, 16 h, and 24 h or with 0.3 ng/mL of TNF-α for 24 h (Fig. 2). We next analyzed the effect of eupafolin on ICAM-1 expression under inflammation. A549 cells were pretreated for 24 h with 1, 3, 10, 30, or 50 μM eupafolin before incubation with 3 ng/mL TNF-α for 4 h, TNF-α-induced ICAM-1 expression was reduced (2.3 ± 0.3, 2.1 ± 0.2, 1.6 ± 0.2, 0.9 ± 0.2, 0.6 ± 0.1 fold of control levels, respectively). The reductions caused by the three highest concentrations were significant ($P<0.05$, Fig. 3A). The effect of eupafolin on ICAM-1 expression was also confirmed by immunofluorescent staining (Fig. 3B). Cells treated for 4 h with 3 ng/mL TNF-α showed strong ICAM-1 expression (T) and this effect was inhibited by pretreatment with eupafolin (50 μM, ET). According to these results, 3 ng/mL TNF-α and 50 μM eupafolin were used in all subsequent experiments to evaluate the anti-inflammatory effects and molecular mechanisms of eupafolin treatment.

3.2. The inhibition of ERK1/2 and JNK phosphorylation mediates eupafolin-increased reduction in TNF-α-induced ICAM-1 expression
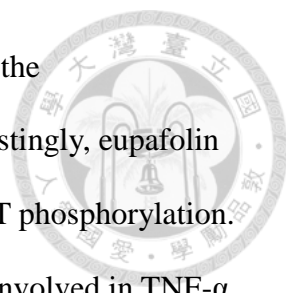
Previous studies have reported that TNF-α-induced inflammation includes the production of inflammatory cytokines via the MAPK pathways (Lee et al., 2011; Lee et al., 2013). We next investigated whether TNF-α-induced ICAM-1 expression was mediated through MAPKs phosphorylation. The phosphorylation of ERK1/2, p38, and JNK in A549 cells showed a significant increase at 15-30 min of TNF-α treatment and

followed by a decline within 60 min ($P<0.05$, Fig. 4A). To determine the targets that were affected by eupafolin, the cells were preincubated with eupafolin for 24 h and then incubated with TNF-α for 5, 15, 30, 45, or 60 min. Eupafolin significantly inhibited TNF-α-induced ERK1/2, p38, and JNK phosphorylation ($P<0.05$). In addition, the PD98059 (50μM, ERK1/2 inhibitor) or SP600125 (10μM, 30μM, 50μM, JNK inhibitor) inhibited the TNF-α-induced ICAM-1 expression (PD: 40±13% of inhibition; SP: 26±10 % for 10μM, 39±13% for 30μM, and 43±15% for 50μM, respectively, $P<0.05$). In contrast, SB203580 (p38 inhibitor) had no effects (Fig. 4B). To further confirm the involvement of ERK1/2 and JNK in the TNF-α-induced ICAM-1 expression, we used siRNA transfection to knockdown the ERK1/2 or JNK expression in A549 cells. As shown in Fig. 5A, the expression levels of ERK1/2 or JNK were significantly downregulated by siRNA transfection ($P<0.05$). Moreover, cells transfected with 1 nM ERK1/2- or with JNK-specific siRNA inhibited TNF-α-induced ICAM-1 expression (1.6±0.1 and 1.7±0.1 fold of control levels, respectively) ($P<0.05$, Fig. 5B). These results suggest that eupafolin inhibits TNF-α-induced ICAM-1 expression partly by inhibiting TNF-α-induced ERK1/2 and JNK phosphorylation.

3.3. The inhibition of AKT phosphorylation mediates eupafolin-increased reduction in TNF-α-induced ICAM-1 expression
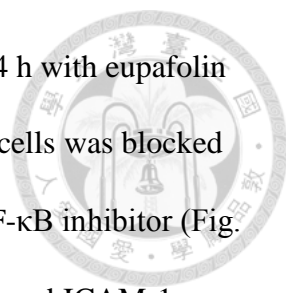
The phosphatidylinositol 3-kinase (PI3K)/AKT signaling pathway is reported to be involved in adhesion molecule expression in TNF-α-treated various cells (Choi et al., 2012; Jang et al., 2012; Oh and Kwon, 2009). To investigate whether eupafolin affects TNF-α-induced PI3K/AKT activation, we examined the effect of eupafolin on the TNF-α-induced PI3K/AKT in A549 cells using Western blot analysis. The expression levels of phosphorylated PI3K and AKT were gradually increased after TNF-α

stimulation, and pretreatment with eupafolin significantly attenuated the phosphorylation of PI3K and AKT (*P*<0.05, Figs. 6A and 6B). Interestingly, eupafolin pretreatment completely blocked the increase of TNF-α-induced AKT phosphorylation. Moreover, we determined whether the activation of PI3K/AKT was involved in TNF-α induced ICAM-1 expression. As shown in Fig. 6D, pretreatment with MK2206 (AKT inhibitor) caused a significant attenuation of ICAM-1 expression in TNF-α stimulated A549 cells (34±13% of inhibition, *P*<0.05). In contrast, pretreatment with LY294002 (PI3K inhibitor) did not reduce the ICAM-1 expression (*P*<0.05, Fig. 6C). These results suggest that eupafolin inhibits TNF-α-induced ICAM-1 expression partly by inhibiting TNF-α-induced AKT phosphorylation.

3.4. The inhibition of NF-κB activation and NF-κB p65 translocation mediates eupafolin-reduced ICAM-1 expression in TNF-α-treated A549 cells
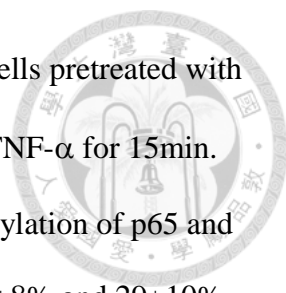
We investigated whether eupafolin reduced TNF-α-induced ICAM-1 expression via NF-κB signaling because the promoter of ICAM-1 gene contains consensus binding sites for the transcription factor (Rahman et al., 1999). At first, we examined the levels of phosphorylated NF-κB p65 in TNF-α-treated A549 cells by Western blotting and immunofluorescence staining. The phospho-p65 level was higher in TNF-α-treated A549 cells than in control cells and that eupafolin pretreatment significantly reduced the effect (*P*<0.05, Fig. 7A). The similar result was obtained for IκB phosphorylation (*P*<0.05, Fig. 7B), which is responsible for NF-κB activation (Choi et al., 2012). The results of immunofluorescent staining were consistent with the Western blot finding of NF-κB p65. Control A549 cells (C) or cells incubated only with eupafolin (E) showed no nuclear NF-κB p65 staining, but strong staining in the cytoplasm. In contrast, A549 cells stimulated with TNF-α for 1 h showed strong NF-κB p65 staining in the nucleus

(T), and this effect was significantly decreased by pretreatment for 24 h with eupafolin (Fig. 8). Furthermore, TNF-α-induced ICAM-1 expression by A549 cells was blocked by preincubation of the cells for 1 h with 5-50 μM Bay11-7082, a NF-κB inhibitor (Fig. 9A). To further confirm the involvement of NF-κB in the TNF-α-induced ICAM-1 expression, we used p65-specific siRNA transfection to knockdown the p65 expression in A549 cells. The expression level of NF-κB was markedly downregulated by siRNA transfection ($P<0.05$, Fig. 9B). Moreover, the level of TNF-α-induced ICAM-1 expression was also attenuated in the NF-κB p65-depleted A549 cells ($76\pm3\%$ of inhibition, $P<0.05$, Fig. 9C). Furthermore, we use Western blot analysis to determine the expression levels of NF-κB p65 in the nuclear portion of A549 cells. The expression level of p65 in the nuclear portion of TNF-α-treated A549 cells was reduced by eupafolin ($P<0.05$, Fig. 10A). Gel-shift assays were performed to determine the effect of eupafolin on NF-κB activation in TNF-α-treated A549 cells. As shown in Fig. 10B, low basal levels of NF-κB binding activity were detected in both untreated cells and cells treated only with eupafolin, but binding was increased by treatment with TNF-α for 1 h and further decreased by pretreatment with eupafolin. These results suggest that eupafolin-reduced ICAM-1 expression in TNF-α-treated A549 cells was mediated by the inhibition of NF-κB activation.

3.5. TNF-α-induced ICAM-1 expression was mediated by AKT/ERK1/2/JNK/NF-κB signaling pathway
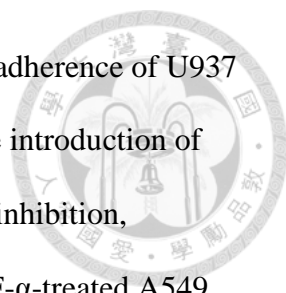
There are multiple cross-talk points between PI3K and MAPKs pathways, whose co-ordinated action determines the cell fate (Aksamitiene et al., 2012; Bölck et al., 2014). In addition, AKT activation has been shown to activate MAPK pathway (Binion et al., 2009). To further elucidate the detailed pathway, we examine the crosstalk among

AKT, MAPK, IκB, NF-κB p65 in TNF-α-treated A549 cells. A549 cells pretreated with

PD98059, SP600125 or MK2206 for 24h, and then stimulated with TNF-α for 15min.

As shown in Figs. 11A-11D, PD98059 had no effect on the phosphorylation of p65 and

AKT. In contrast, SP600125 reduced the phosphorylation of p65 ($21\pm8\%$ and $29\pm10\%$

of inhibition for 10 μM and 50 μM, respectively), but not AKT. In addition,

pretreatment with MK2206 significantly attenuated the phosphorylation of ERK1/2,

JNK and p65 ($70\pm3\%$, $48\pm1\%$, and $60\pm6\%$ of inhibition, respectively, $P<0.05$, Figs.

11E-11G). Moreover, to confirm whether MAPK/AKT was linked to IκB

phosphorylation, we performed that A549 cells pretreated with PD98059, SP600125 or

MK2206 for 24h, and then stimulated with TNF-α for 5min. PD98059 had no effect on

the expression of IκB phosphorylation. But both SP600125 and MK2206 reduced the

IκB phosphorylation ($59\pm17\%$ and $69\pm13\%$ of inhibition, respectively, $P<0.05$, Figs.

12A-12C). These data suggest that TNF-α-induced ICAM-1 expression in A549 cells

was mediated by AKT/IκB/ERK1/2, JNK/NF-κB signaling pathway.

3.6. Eupafolin suppressed the adhesion of monocytes to TNF-α-stimulated A549 cells

To evaluate the influence of eupafolin on the epithelial cell-leukocyte interaction,

we investigated the adhesion of U937 cells to TNF-α-stimulated A549 cells (Fig. 13A).

A549 cells pretreated with 3ng/mL TNF-α for 4 h (T) for 4 h substantially increased

monocyte adhesion than control cells (C). Pretreatment of A549 cells with eupafolin for

24 h (E/T) reduced the number of U937 cells adherent to TNF-α-treated A549 cells by

$52\pm6\%$ compared to TNF-α alone ($P<0.05$, Fig. 13B). As expected, A 549 cells

pretreated with 1 or 2 μg/mL anti-ICAM-1 antibody decreased the adhesion of U937

cells to TNF-α-treated A549 cells. This result showed that ICAM-1 plays the important

role in the adhesion of U937 cells to TNF-α-treated A549 cells. The adherence of U937 cells to TNF-α-treated A549 cells was also markedly inhibited by the introduction of PD98059, SB203580, or SP600125 (73±5%, 57±8%, and 71±4% of inhibition, respectively, $P<0.05$). Similarly, the adherence of U937 cells to TNF-α-treated A549 cells was also inhibited by Bay11-7082, MK2206, or LY294002 (69±7%, 67±6 %, and 45±12% of inhibition, respectively, $P<0.05$).

3.7. Eupafolin reduces ICAM-1 expression in lung tissues in TNF-α-treated mice
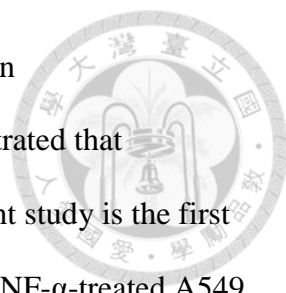
To detect the effect of eupafolin on ICAM-1 expression under inflammation in vivo, lung tissues of TNF-α-treated mice were examined by Western blotting and immunohistochemical staining. TNF-α significantly induced the ICAM-1 expression in lung tissues and pretreatment with eupafolin could downregulate the ICAM-1 level by Western blotting (53±15%, $P<0.05$, Fig. 14A). Fig. 14B shows that no ICAM-1 staining was seen on the lung tissues in the control (C) and eupafolin-treated (E) groups, whereas strong ICAM-1 staining was seen on the epithelial cells in the TNF-α-treated group (T) by the immunohistochemical staining. The stronger ICAM-1 expression was closely associated with type-II alveolar cells, which were identified by SP-D (Fig. 14C). In contrast, preadministration of eupafolin showed weak ICAM-1 staining in TNF-α-treated mice (ET).

第四章　討論

In the present study, our results showed that eupafolin significantly reduced ICAM-1 expression and monocytic cell line U937 adhesion in TNF-α-stimulated A549 cells *in vitro*. The influence was partly mediated through inhibition of AKT/ERK1/2/JNK phosphorylation and NF-κB activation. Furthermore, eupafolin attenuates ICAM-1 expression in lung tissues of TNF-α-treated mice *in vivo*.

P. nodiflora, an important ingredient of herbal tea, has long been used in traditional medicine to treat inflammatory diseases (Lai et al., 2011). The bioactive compounds isolated from *P. nodiflora* include flavonoids (Tom´as-Barber´an et al., 1987), essential oils, resin (Elakovich and Stevens., 1985), quinol (Siddiqui et al., 2009), cyclohexenone (Ravikanth et al., 2000), and steroids (Wang and Huang., 2005), which are responsible for its antiseptic, antitussive, antipyretic, antiurolithiatic, antidiabetic, antinociceptive, and anti-inflammatory effects (Balakrishnan et al., 2010; Forestieri et al., 1996). Eupafolin, a flavonoid isolated from *P. nodiflora,* was chosen for using in the present research, which possesses the anti-inflammatory action (Lai et al., 2011; Maas et al., 2011). Eupafolin promoted iron release from ferritin and donated electrons to the stable free radical DPPH (Dabaghi-Barbosa et al., 2005). Eupafolin protected cultured neurons against glutamate-induced oxidative stress (Kim et al., 2002) and inhibited xanthine oxidase activity (Sanz et al., 1994). The recent study has showed that eupafolin inhibited pro-inflammatory iNOS and COX-2 protein expressions in LPS-stimulated RAW264.7 macrophages (Lai et al., 2011). In addition, eupafolin exhibited anti-tumor effects on MK-1 (human gastric adenocarcinoma), B16-F10 (murine melanoma), HeLa (human cervical adenocarcinoma) cells, and prostate cancer cells (Abe et al., 2002; Chung et al., 2010; Ko et al., 2014; Liu et al., 2014). Eupafolin lessened virus-induced
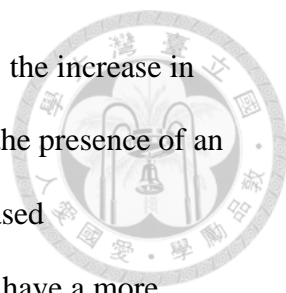
upregulation of IL-6 and RANTES in RD cells, derived from a human rhabdomyosarcoma (Wang et al., 2013). Our previous study demonstrated that eupafolin downregulated melanogenesis (Ko et al., 2014). The present study is the first to report that eupafolin strongly reduces the ICAM-1 expression in TNF-α-treated A549 cells and pulmonary tissues in TNF-α-treated mice. In addition, eupafolin treatment markedly inhibited leukocyte adhesion to these cells by the inhibiting ICAM-1 expression. The induced expression of adhesion molecules, especially ICAM-1, has been reported to be associated with airway inflammation and the migration and recruitment of lymphocytes (Lee and Yang, 2013; Qureshi et al., 2003), indicating that an additional mechanism by which eupafolin treatment may be important in preventing the progression of airway inflammation.

MAPK pathways, such as phosphorylation of ERK, JNK, and p38 play the important role in the expressions of proinflammatory mediators, which lead to the initiation and progression of lung inflammation (Lee et al., 2013). The present study demonstrated that TNF-α caused strong activation of three MAPK subtypes in human alveolar epithelial A549 cells, as reported in previous studies (Lee et al., 2013; Jang et al., 2012; Oh and Kwon, 2009). However, the involvement of their activation in the protective mechanism of eupafolin has not been detected. Our results showed that eupafolin decreased TNF-α-induced ERK1/2, JNK and p38 phosphorylation. The increase in ICAM-1 expression induced by TNF-α was markedly suppressed in the presence of an ERK1/2 inhibitor or a JNK inhibitor, but not a p38 inhibitor. ICAM-1 expression was also inhibited by ERK1/2 or JNK-specific siRNA. Based on the results, we suggest one of the signals by which eupafolin attenuates TNF-α-induced ICAM-1 expression involves a reduction in ERK1/2 and JNK activation. Consistent with our results, eupafolin specifically reduced virus-induced upregulation of IL-6 and RANTES

by inhibiting the ERK1/2 signaling pathway (Wang et al., 2013). Another study showed that nodiflora extract significantly inhibited the phosphorylation of ERK1/2 and JNK in LPS-treated RAW 264.7 macrophages (Balakrishnan et al., 2010). In contrast, eupafolin significantly induced the phosphorylation of ERK1/2 and p38 MAPK correlate well with the suppression of melanogenesis in B16F10 mouse melanoma cells (Ko et al., 2014). The differences between the above results in terms of the pathways involved may be related to differences in cell type, inducers, and cytokines.

The transcription factor NF-κB was served as the major activator in the regulation of inflammatory responses (Karin et al., 2002). MAPKs have been shown to phosphorylate NF-κB transcriptional activity. Our results demonstrated that the activation of NF-κB is necessary for TNF-α-induced ICAM-1 expression in A549 cells and that is in accordance with previous reports (Banerjee et al., 2002; Oh and Kwon, 2009; Wu et al., 2014). Our study further demonstrated that the eupafolin-decreased ICAM-1 expression in TNF-α-treated A549 cells was mediated through inactivation of NF-κB binding activity. The result is similar with a previous report that nodiflora extract inhibited LPS-induced TNF-α, IL-1β, and IL-6 production might be related the reduction of NF-κB activation in RAW 264.7 macrophages (Balakrishnan et al., 2010). NF-κB is activated by signals possibly involving of the IκB phosphorylation and its dissociation from the inactive cytoplasmic complex, followed by translocation of the active p50/p65 dimer to the nucleus and induced gene expression (Choi et al., 2012). We demonstrated that the eupafolin-induced decrease in ICAM-1 expression was mediated through inhibition of IκB phosphorylation and p65 translocation.

PI3K and AKT pathway have been implicated that they played the crucial role in activation of inflammatory mediators, inflammatory cell recruitment and immune cell function (Koyasu et al., 2003). This notion is confirmed by our observation that TNF-α

activated the phosphorylation of PI3K and AKT. In the present study, the increase in

ICAM-1 expression induced by TNF-α was markedly suppressed in the presence of an

AKT inhibitor, but not a PI3K inhibitor. In addition, eupafolin decreased

TNF-α-induced PI3K and AKT phosphorylation. Eupafolin seems to have a more

pronounced effect on AKT phosphorylation and subsequently reduced ICAM-1

expression. Thus, one of the mechanisms by which eupafolin reduces TNF-α-induced

ICAM-1 expression involves a reduction in AKT activation. Moreover, it has been

reported that there are multiple cross-talk points between PI3K and MAPKs pathways,

whose co-ordinated action determines the cell fate (Aksamitiene et al., 2012; Bölck et

al., 2014). In our study, the phosphylation of AKT was not affected by the inhibition of

ERK1/2 and JNK, but the phosphylation of ERK1/2 and JNK was affected by the

inhibition of AKT. These findings indicate that AKT is the upstream regulator of

IκB/ERK/JNK activation. Together these results suggest that eupafolin treatment

inactivates TNF-α-induced AKT phosphorylation, which in turn reduces the

phosphorylation of IκB/ERK1/2/JNK MAPK cascades and NF-κB pathways, and

subsequently suppressed ICAM-1 expression, resulting in the decreased binding of

leukocytes. Because the inflammation is involved in many kinds of chronic and acute

lung tissues and it is characterized by the production of proinflammtory cytokines, the

enhanced monocyte adhesion, and the accompanying inflmmatory signal (Lee and Yang,

2013), eupafolin may provide a new therapeutic approach for the prevention of

inflammation and lung diseases.

In summary, this study provides the first evidence that eupafolin reduces ICAM-1

expression under inflammatory conditions both *in vitro* and *in vivo* and also decreases

leukocyte adhesion to alveolar epithelial cells. Our results show that the eupafolin

inhibited ICAM-1 expression in A549 cells through blockade of AKT, ERK1/2, JNK,

and NF-κB phosphorylation (Fig. 15). Eupafolin, an active component of *P. nodiflora,* exerts the anti-inflammatory effect on pulmonary epithelial cells in the present study. Based on these findings, eupafolin should be considered as a novel therapeutic agent targeting epithelial activation in pulmonary inflammation.
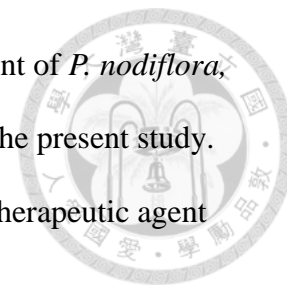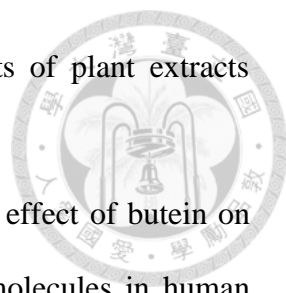
參考資料

Abe, F., Nagao, T., Okabe, H., 2002. Antiproliferative constituents in plants 9. Aerial parts of *Lippia dulcis* and *Lippia canescens*. Biological and Pharmaceutical Bulletin 25, 920-922.

Aksamitiene, E., Kiyatkin, A., Kholodenko, B. N., 2012. Cross-talk between mitogenic Ras/MAPK and survival PI3K/Akt pathways: a fine balance. Biochemical Society Transactions 40, 139-146.

Balakrishnan, G., Janakarajan, L., Balakrishnan, A., 2010. Lakshmi, B. S., Molecular basis of the anti-inflammatory property exhibited by cyclo-pentano phenanthrenol isolated from Lippia nodiflora. Immunological Investigations 39, 713-739.

Banerjee, T., Valacchi, G., Ziboh, V. A., van der Vliet, A., 2002. Inhibition of TNFα-induced cyclooxygenase-2 expression by amentoflavone through suppression of NF-κB activation in A549 cells. Molecular and Cellular Biochemistry 238, 105-110.

Barnes, P.J., 2011. Similarities and differences in inflammatory mechanisms of asthma and COPD. Breathe 7, 229-238.

Binion, D. G., Heidemann, J., Li, M. S., Nelson, V. M., Otterson, M. F., Rafiee, P., 2009. Vascular cell adhesion molecule-1 expression in human intestinal microvascular endothelial cells is regulated by PI 3-kinase/Akt/MAPK/NF-κB: inhibitory role of curcumin. American Journal of physiology-Gastrointestinal and Liver Physiology 297, G259-G268.

Bölck, B., Ibrahim, M., Steinritz, D., Morguet, C. Dühr, S., Suhr, F., Lu-Hesselmann, J., Bloch, W., 2014. Detection of key enzymes, free radical reaction products and activated signaling molecules as biomarkers of cell damage induced by benzo [a]

pyrene in human keratinocytes. Toxicology in Vitro 28, 875-884.

Chen, C. C., Chou, C. Y., Sun, Y. T., Huang, W. C., 2001. Tumor necrosis factor α-induced activation of downstream NF-κB site of the promoter mediates epithelial ICAM-1 expression and monocyte adhesion: Involvement of PKCα, tyrosine kinase, and IKK2, but not MAPKs, pathway. Cellular Signalling 13, 543-553.

Choi, K. W., Um, S. H., Kwak, J. H., Park, H. J. Kim, K. H., Moon, E. Y., Kwon, S. T., Pyo, S., 2012. Suppression of adhesion molecule expression by phenanthrene-containing extract of bulbils of Chinese Yam in vascular smooth muscle cells through inhibition of MAPK, Akt and NF-κB. Food and Chemical Toxicology 50, 2792-2804.

Chung, K. S., Choi, J. H., Back, N. I., Choi, M. S. Kang, E. K., Chung, H. G., Jeong, T. S., Lee, K. T., 2010. Eupafolin, a flavonoid isolated from *Artemisia princeps*, induced apoptosis in human cervical adenocarcinoma HeLa cells. Molecular Nutrition & Food Research 54, 1318-1328.

Dabaghi-Barbosa, P., Rocha, A. M., Da Cruz Lima, A.F., De Oliveira, B. H., Martinelli De Oliveira, M. B., Skare Carnieri, E. G., Cadena, S. M., Merlin Rocha, M. E., 2005. Hispidulin: Antioxidant properties and effect on mitochondrial energy metabolism. Free Radical Research 39, 1305-1315.

Demir, T., Yalcinoz, C., Keskinel, I., Demiröz, F., Yildirim, N., 2002. sICAM-1 as a serum marker in the diagnosis and follow-up of treatment of pulmonary tuberculosis. The International Journal of Tuberculosis and Lung Disease 6, 155-159.

Elakovich, S. D., Stevens, K. L., 1985. Volatile constituents of *Lippia nodiflora*. Journal of Natural Products 48, 504-506.

Forestieri, A. M., Monforte, M. T., Ragusa, S., Trovato, A., Iauk, L., 1996.

Antiinflammatory, analgesic and antipyretic activity in rodents of plant extracts used in African medicine. Phytotherapy Research 10, 100–106.

Jang, J. H., Yang, E. S., Min, K. J., Kwon, T. K., 2012. Inhibitory effect of butein on tumor necrosis factor-α-induced expression of cell adhesion molecules in human lung epithelial cells via inhibition of reactive oxygen species generation, NF-κB activation and Akt phosphorylation. International Journal of molecular and cellular medicine 30, 1357-1364.

Karin, M., Cao, Y., Greten, F. R., Li, Z. W., 2002. NF-κB in cancer: from innocent bystander to major culprit. Nature Reviews Cancer 2, 301-310.

Kim, H., Hwang, J. S., Woo, C. H., Kim, E. Y., Kim, T. H., Cho, K. J., Seo, J. M., Lee, S. S., Kim, J. H., 2008. TNF-α-induced up-regulation of intercellular adhesion molecule-1 is regulated by a Rac-ROS-dependent cascade in human airway epithelial cells. Experimental & Molecular Medicine 40, 167-175.

Kim, S. R., Park, M. J., Lee, M. K., Sung, S. H., Park, E. J., Kim, J., Kim, S. Y., Oh, T. H., Markelonis, G. J., Kim, Y. C., 2002. Flavonoids of *Inula Britannica* protect cultured cortical cells from necrotic cell death induced by glutamate. Free Radical Biology and Medicine 32, 596-604.

Ko, H. H., Chiang, Y. C., Tsai, M. H., Liang, C. J., Hsu, L. F., Li, S. Y., Wang, M. C., Yen, F. L., Lee, C. W., 2014. Eupafolin, a skin whitening flavonoid isolated from *Phyla nodiflora*, downregulated melanogenesis: Role of MAPK and Akt pathways. Journal of Ethnopharmacology 151, 386–393.

Koyasu, S., The role of PI3K in immune cells, 2003. Nature Immunology 4, 313-319.

Lai, Z. R., Ho, Y. L., Huang, S. C., Huang, T. H., Lai, S. C., Tsai, J. C., Wang, C. Y., Huang, G. J., Chang, Y. S., 2011. Antioxidant, anti-inflammatory and antiproliferative activities of *Kalanchoe gracilis* (L.) DC stem. The American

Journal of Chinese Medicine 39, 1275-1290.

Lee, C. W., Lin, C. C., Lee, I. T., Lee, H. C., Yang, C. M., 2011. Activation and induction of cytosolic phospholipase A2 by TNF-α mediated through Nox2, MAPKs, NF-κB, and p300 in human tracheal smooth muscle cells. Journal of Cellular Physiology 226, 2103-2114.

Lee, I. T., Lin, C. C., Lee, C. Y., Hsieh, P. W., Yang, C. M., 2013. Protective effects of (−)-epigallocatechin-3-gallate against TNF-α-induced lung inflammation via ROS-dependent ICAM-1 inhibition. The Journal of Nutritional Biochemistry 24, 124-136.
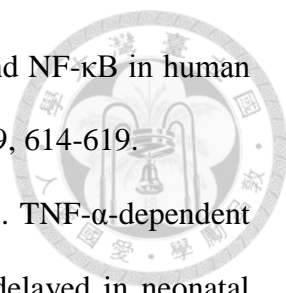
Lee, I. T., Yang, C.M., 2013. Inflammatory signalings involved in airway and pulmonary diseases. Mediators of Inflammation ID 791231.
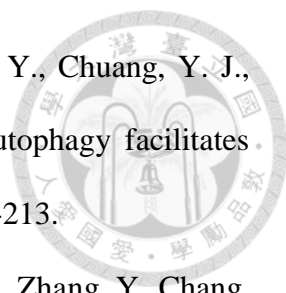
Liang, C. J., Yen, Y. H., Hung, L. Y., Wang, S. H., Pu, C. M., Chien, H. F., Tsai, J. S., Lee, C. W., Yen, F. L., Chen, Y. L., 2013. Thalidomide inhibits fibronectin production in TGF-β1-treated normal and keloid fibroblasts via inhibition of the p38/Smad3 pathway. Biochemical Pharmacology 85, 1594-1602.

Liu, K., Park, C., Chen, H., Hwang, J., Thimmegowda, N. R., Bae, E. Y., Lee, K. W., Kim, H. G., Liu, H., Soung, N. K., Peng, C., Jang, J. H., Kim, K. E., Ahn, J. S., Bode, A. M., Dong, Z., Kim, B. Y., Dong, Z., 2014. Eupafolin suppresses prostate cancer by targeting phosphatidylinositol 3 - kinase - mediated Akt signaling. Molecular Carcinogensis DOI 10.1002/mc.22139.

Maas, M., Deters, A. M., Hensel, A., 2011. Anti-inflammatory activity of *Eupatorium perfoliatum* L. extracts, eupafolin, and dimeric guaianolide via iNOS inhibitory activity and modulation of inflammation-related cytokines and chemokines. Journal of Ethnopharmacology 137, 371-381.

Oh, J. H., Kwon, T. K., 2009. Withaferin A inhibits tumor necrosis factor-α-induced

expression of cell adhesion molecules by inactivation of Akt and NF-κB in human pulmonary epithelial cells. International Immunopharmacology 9, 614-619.

Qureshi, M. H., Cook-Mills, J., Doherty, D. E., Garvy, B. A., 2003. TNF-α-dependent ICAM-1-and VCAM-1-mediated inflammatory responses are delayed in neonatal mice infected with *Pneumocystis carinii*. Journal of Immunology 171, 4700-4707.

Rahman, A., Anwar, K. N., True, A. L., Malik, A. B., 1999. Thrombin-induced p65 homodimer binding to downstream NF-κB site of the promoter mediates endothelial ICAM-1 expression and neutrophil adhesion. Journal of Immunology 162, 5466-5476.

Ravikanth, V., Ramesh, P., Diwan, P. V., Venkateswarlu, Y., 2000. Halleridone and Hallerone from *Phyla nodiflora* as taxonomic markers. Biochemical Systematics and Ecology 28, 905-906.

Rosseau, S., Selhorst, J., Wiechmann, K., Leissner, K., Maus U., Mayer K., Grimminger F., Seeger W., Lohmeyer J., 2000. Monocyte migration through the alveolar epithelial barrier: adhesion molecule mechanisms and impact of chemokines. Journal of Immunology 164, 427-435.

Sanz, M. J., Ferrandiz, M. L., Cejudo, M., Terencio, M. C., Gil, B., Bustos, G., Ubeda, A., Gunasegaran, R., Alcaraz, M. J., 1994. Influence of a series of natural flavonoids on free radical generating systems and oxidative stress. Xenobiotica 24, 689-699.

Siddiqui, B. S., Ahmed, F., Ali, S. K., Perwaiz, S., Begum, S., 2009. Steroidal constituents from the aerial parts of *Lippia nodiflora* Linn. Natural Product Research 23, 436-441.

Tomás-Barberán, F. A., Harborne, J. B., Self, R., 1987. Twelve 6-oxygenated flavone sulphates from *Lippia nodiflora* and *L. canescens*. Phytochemistry 26, 2281-2284.

Wang, C. Y., Chiang, T. H., Chen, C. L., Tseng, P. C., Chien, S. Y., Chuang, Y. J., Yang, T. T., Hsieh, C. Y., Choi, P. C., Lin, C. F., 2014. Autophagy facilitates cytokine-induced ICAM-1 expression. Innate Immunity 20, 200-213.

Wang, C.Y., Huang, S. C., Lai, Z. R., Ho, Y. L. Jou, Y. J., Kung S. H., Zhang, Y., Chang, Y. S., Lin, C. W., 2013. Eupafolin and ethyl acetate fraction of *Kalanchoe gracilis* stem extract show potent antiviral activities against enterovirus 71 and coxsackievirus A16. Evidence-based Complementary and Alternative Medicine, ID 591354.

Wang, Y. C., Huang, T. L., 2005. Screening of anti-*Helicobacter pylori* herbs deriving from Taiwanese folk medicinal plants. FEMS Immunology and Medical Microbiology 43, 295-300.

Wu, C., Wang, H., Xu, J., Huang, J., Chen, X., Liu, G., 2014. Magnolol inhibits tumor necrosis factor-α-induced ICAM-1 expression via suppressing NF-κB And MAPK Signaling pathways in human lung epithelial cells. Inflammation 37, 1957-1967.

Yang, Y. P., Lu, S. Y., Chen, T. T., 1998. Verbenaceae. Flora of Taiwan 127, 421.

附圖

Figure 1
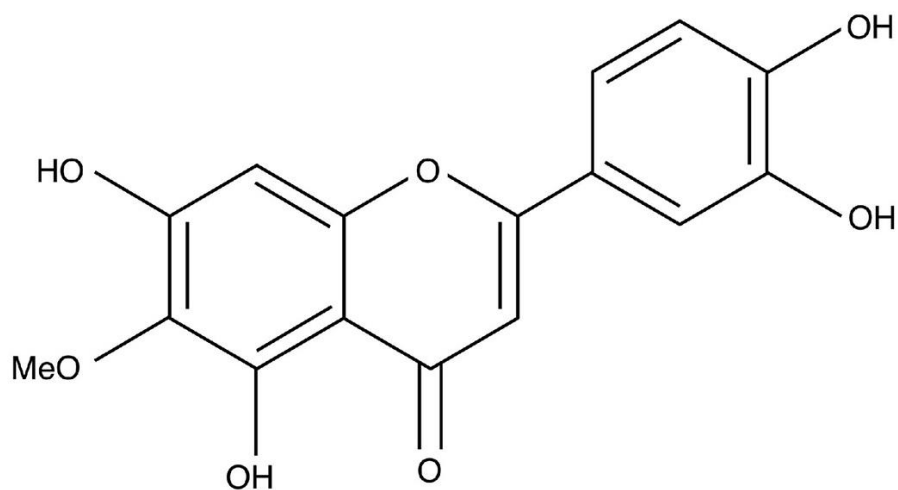
Figure 1: Chemical structure of eupafolin.

Figure 2
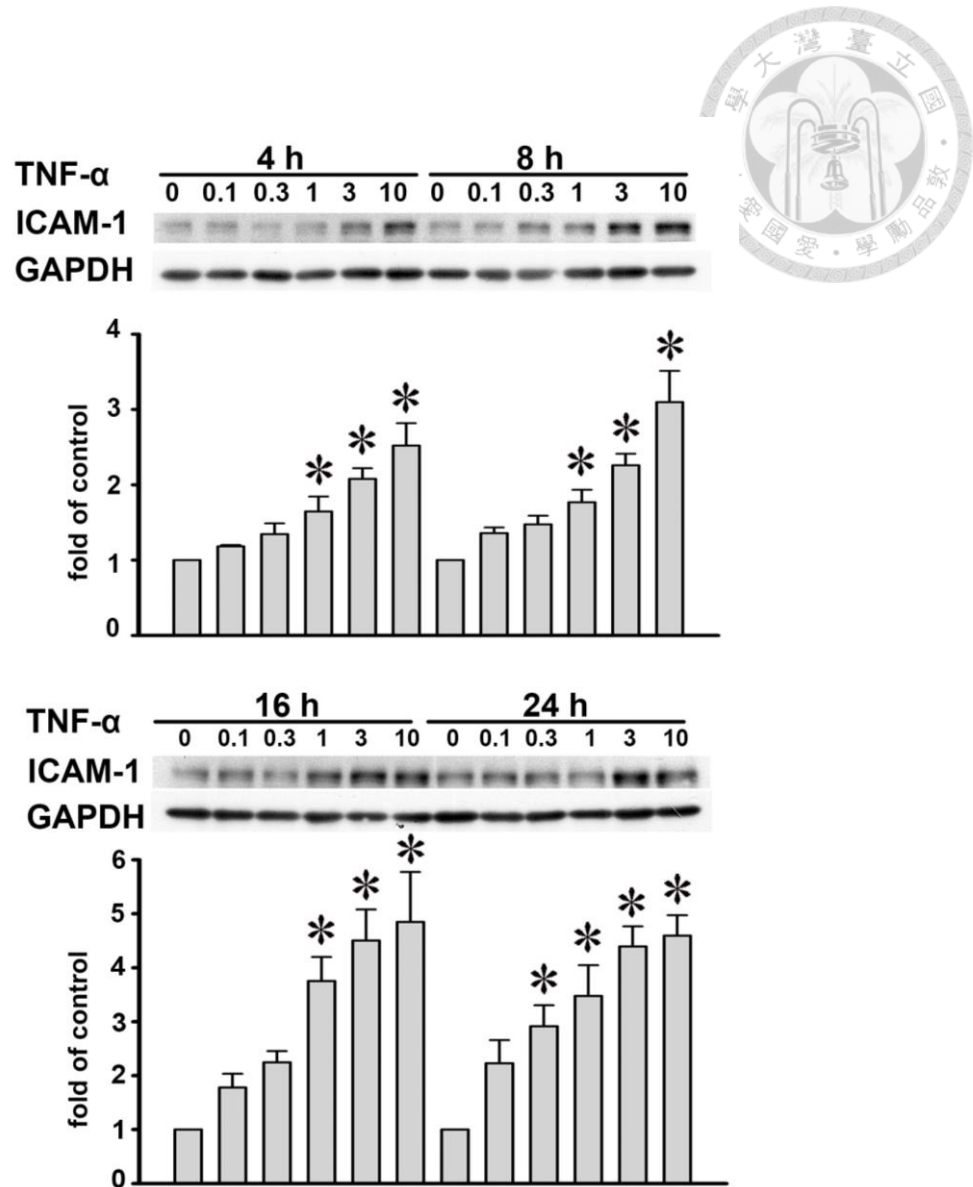
Figure 2: The effects of TNF-α-induced ICAM-1 expression in A549 cells.

A549 cells were treated with TNF-α (0.1-10 ng/mL) for the indicated times, then the

ICAM-1 level in the cell lysates was measured by Western blots. GAPDH was used as

the loading control. The data are expressed as a fold value compared to the control value

and are the means ± SEM for five separate experiments. $*P < 0.05$ compared to the

untreated cells.

Figure 3

Figure 3: The effects of eupafolin on ICAM-1 expression in TNF-α-treated A549 cells.

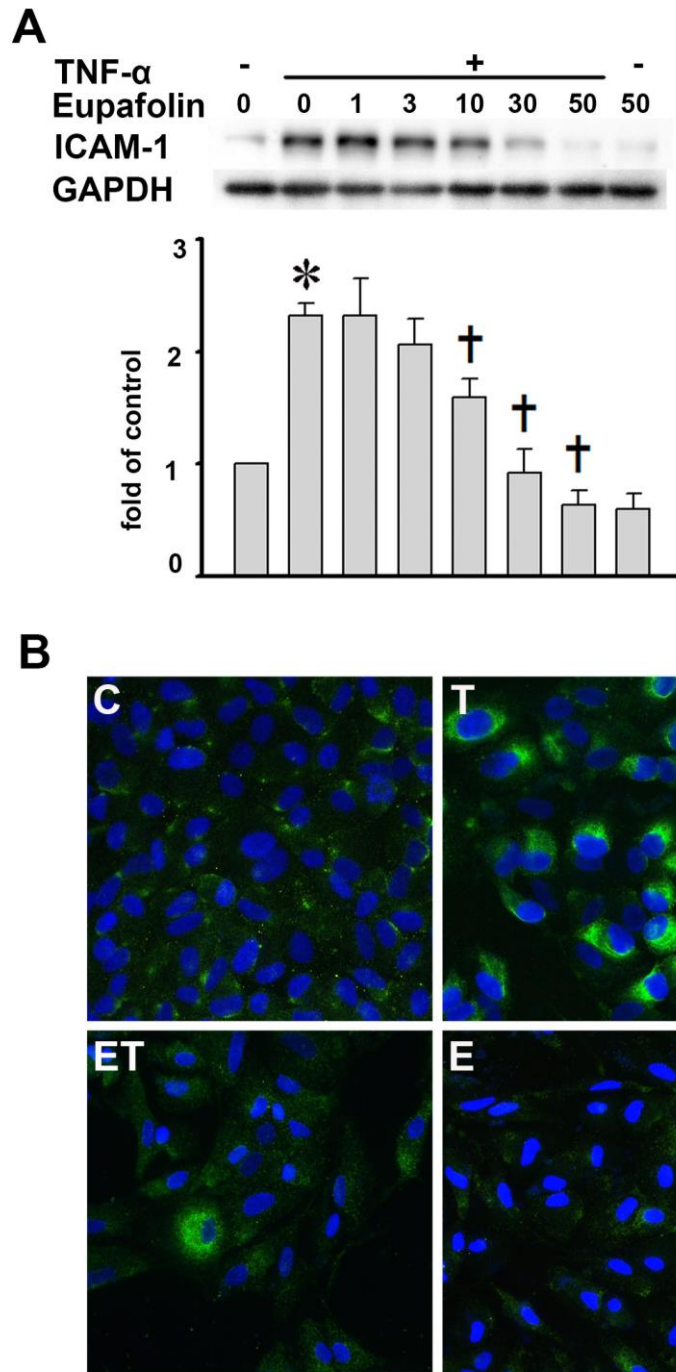(A) A549 cells were incubated with the indicated concentration of eupafolin (1-50μM) for 24 h and then with 3 ng/mL TNF-α for 4 h in the continued presence of the same

concentration of eupafolin, and the ICAM-1 expression was measured by Western blot. GAPDH was used as the loading control. The data are expressed as a fold value compared to the control value and are 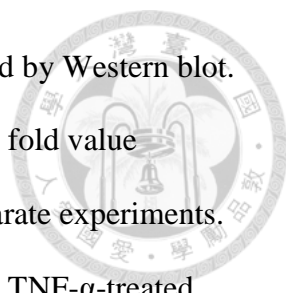the means $\pm$ SEM for five separate experiments. *$P < 0.05$ compared to the untreated cells. [†]$P < 0.05$ compared to the TNF-α-treated cells. (ANOVA followed with Duncan's Multiple range test). (B) The distribution of ICAM-1 was analyzed by immunofluorescent staining. ICAM-1 expression is indicated by green fluorescence (FITC) and nuclei by blue fluorescence (DAPI). C: control ; T: treated with TNF-α alone; ET: pretreated with eupafolin and then stimulated with TNF-α; E: treated with eupafolin alone. Bar=50 μm.
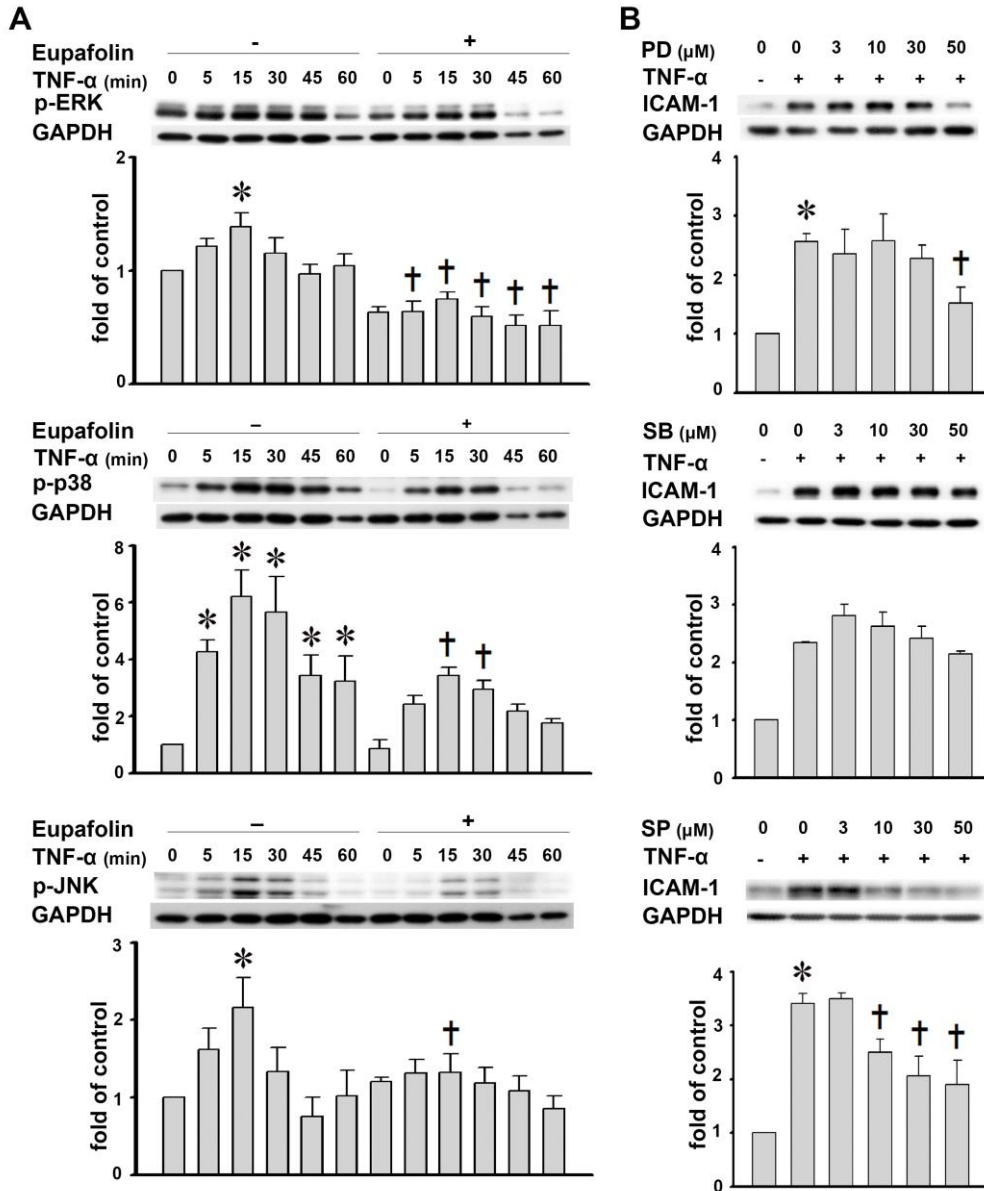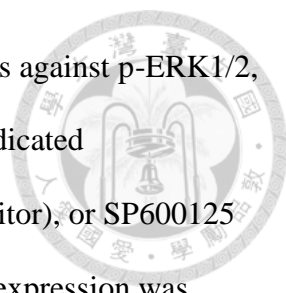
Figure 4

Figure 4: The role of MAPKs activation on eupafolin-reduced ICAM-1 expression in TNF-α-treated A549 cells.

(A) Western blot analysis showed the effects of eupafolin treatment on the phosphorylation of ERK1/2, JNK, or p38 in TNF-α-treated A549 cells. A549cells were incubated for 24 h with or without 50 μM eupafolin, and then the cells were incubated with 3 ng/mL of TNF-α for the indicated time and equal amounts of protein aliquots in

cell lysates subjected to immunoblotting with the indicated antibodies against p-ERK1/2,

p-p38, or p-JNK. (B) The cells were preincubated for 1 h with the indicated

concentration of PD98059 (ERK1/2 inhibitor), SB203580 (p38 inhibitor), or SP600125

(JNK inhibitor), and then were treated with TNF-α for 4 h. ICAM-1 expression was

analyze by Western blot. GAPDH was used as the loading control. The data are

expressed as a fold value compared to the control value and are the means ± SEM for

five separate experiments. $*P < 0.05$ compared to the untreated cells. $^{\dagger}P < 0.05$

compared to the TNF-α-treated cells.
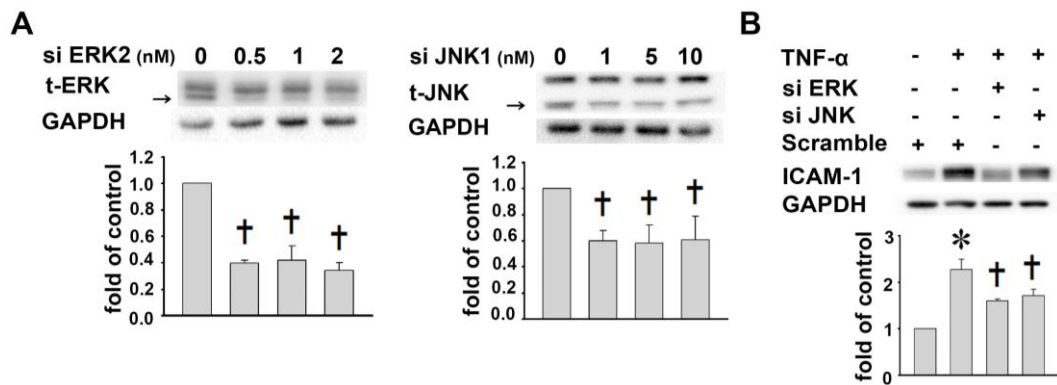
Figure 5

Figure 5: The effects of MAPKs phosphorylation on ICAM-1 expression in TNF-α-treated A549 cells.

(A) A549 cells were transfected with the various concentrations of siRNA of ERK or JNK for 48 h. Expression levels of ERK1/2 or JNK were determined by Western blot. (B) After transfected with ERK or JNK siRNA, A549 cells were then stimulated with 3 ng/mL TNF-α for 4h. Expression of ICAM-1 was determined by Western blot. GAPDH was used as the loading control. The data are expressed as a fold value compared to the control value and are the means ± SEM for five separate experiments. $*P < 0.05$ compared to the untreated cells. $^{†}P < 0.05$ compared to the TNF-α-treated cells.

Figure 6

Figure 6: The roles of AKT/PI3K activation on eupafolin-reduced ICAM-1 expression in TNF-α-treated A549 cells.

(A, B) The effect of eupafolin on the phosphorylation of PI3K and AKT in TNF-α-treated A549 cells was evaluated by Western blot. A549 cells were pretreated with or without 50 μM eupafolin for 24h and then stimulated with 3 ng/mL TNF-α at different time intervals (5, 15, 30, 45, 60 min). (C, D) A549 cells were pretreated with the various concentrations of LY294002 (PI3K inhibitor) or MK2206 (AKT inhibitor)

for 1 h, and then stimulated with 3ng/mL TNF-α for 4h. The ICAM-1 expression was determined by Western blot. The data are expressed as a fold value compared to the control value and are the means ± SEM for five separate experiments. $*P < 0.05$ compared to the untreated cells. $^{†}P < 0.05$ compared to the TNF-α-treated cells.

Figure 7

**Figure 7: The effects of eupafolin on NF-κB and IκB phosphorylation in TNF-α-treated A549 cells.**

A549 cell were pretreated with or without 50 μM eupafolin and then incubated with 3ng/mL TNF-α for 5, 15, 30, 45, 60 min. The phosphorylation of p65 (A) and IκB (B) were determined by Western blot. The expression of GAPDH was shown as the loading control. The data are expressed as a fold value compared to the control value and are the means ± SEM for five separate experiments. *$P < 0.05$ compared to the untreated cells. †$P < 0.05$ compared to the TNF-α-treated cells.
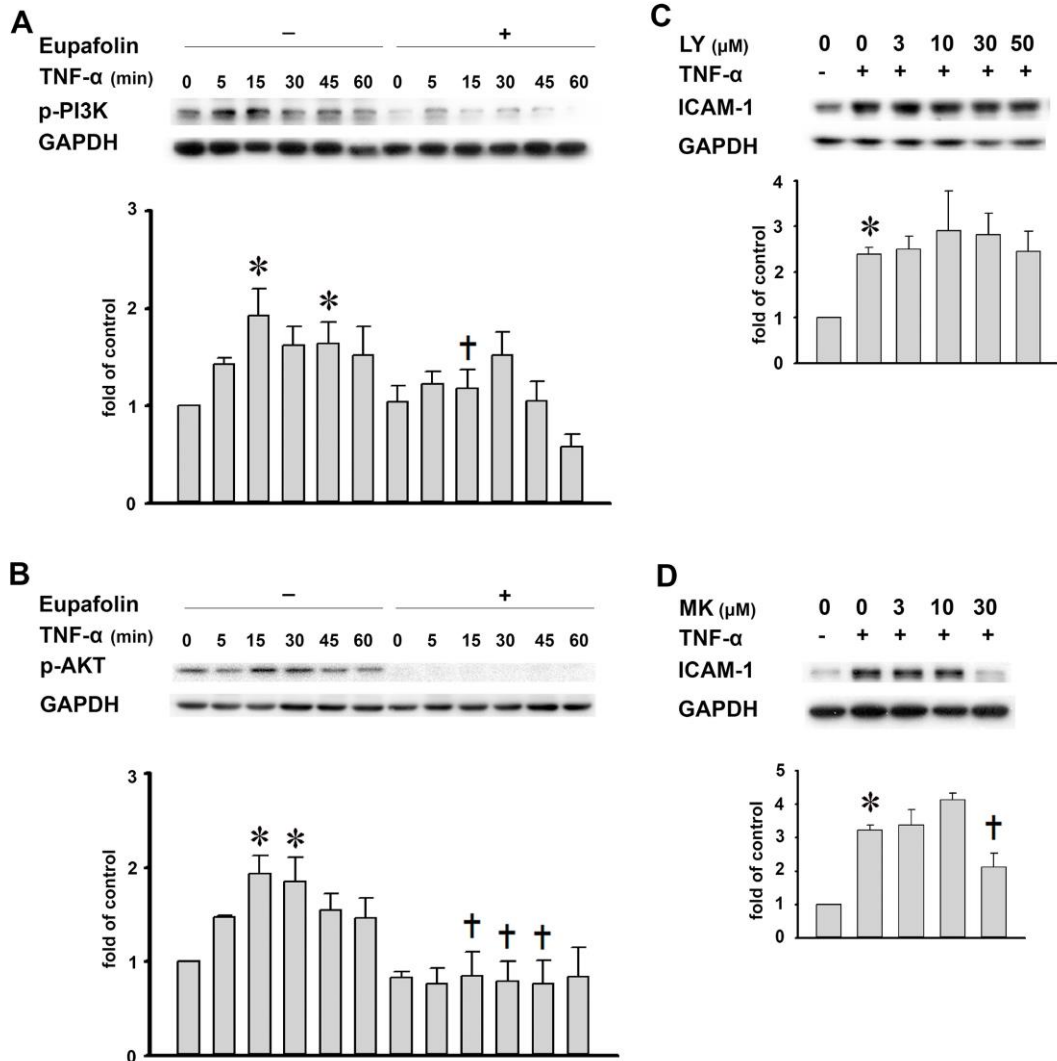
Figure 8

Figure 8: The effects of eupafolin on NF-κB expression in TNF-α-stimulated A549 cells.

Immunofluorescent staining for NF-κB p65. A549 cells were preincubated for 24 h with or without 50 μM eupafolin and then were treated with 3 ng/mL TNF-α for 4 h. C: control ; T: treated with TNF-α alone; ET: pretreated with eupafolin and then stimulated with TNF-α; E: treated with eupafolin alone. Bar, 50 μm.
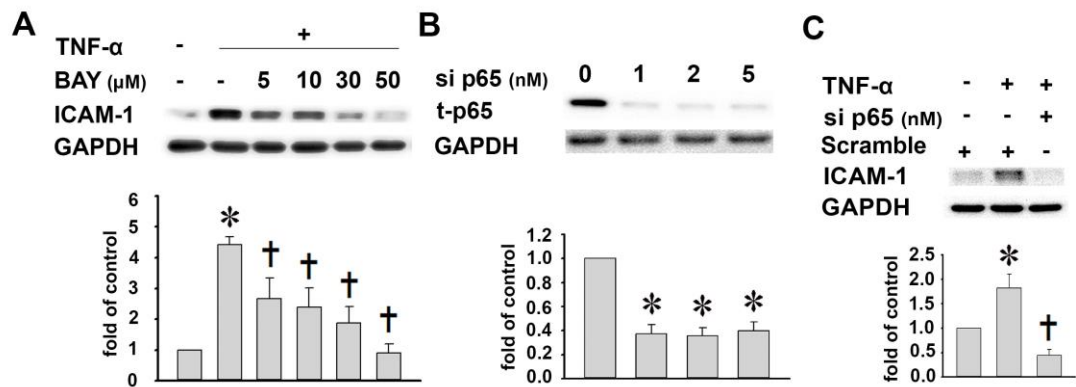
Figure 9

Figure 9: The effects of NF-κB on ICAM-1 expression in TNF-α-stimulated A549 cells.

(A) A549 cells were pretreated with the various concentrations of BAY (NF-κB inhibitor) for 1 h, and then stimulated with 3 ng/mL TNF-α for 4h. The levels of ICAM-1 protein were assayed by Western blot. (B) A549 cells were transfected with various concentrations of siRNA of p65 for 48 h. Expression levels of p65 were determined by Western blot. (C) After transfected with NF-κB siRNA, A549 cells were then stimulated with 3 ng/mL TNF-α for 4h. The ICAM-1 expression was determined by Western blot. GAPDH was used as the loading control. The data are expressed as a fold value compared to the control value and are the means ± SEM for five separate experiments. *$P < 0.05$ compared to the untreated cells. †$P < 0.05$ compared to the TNF-α-treated cells.
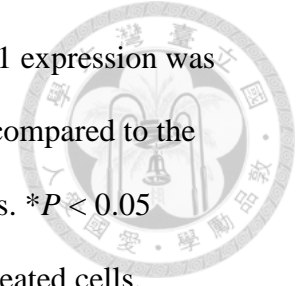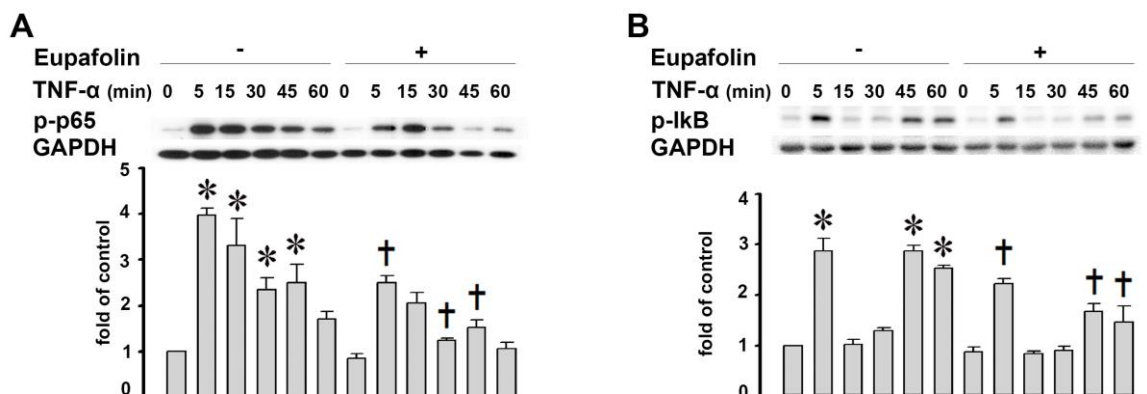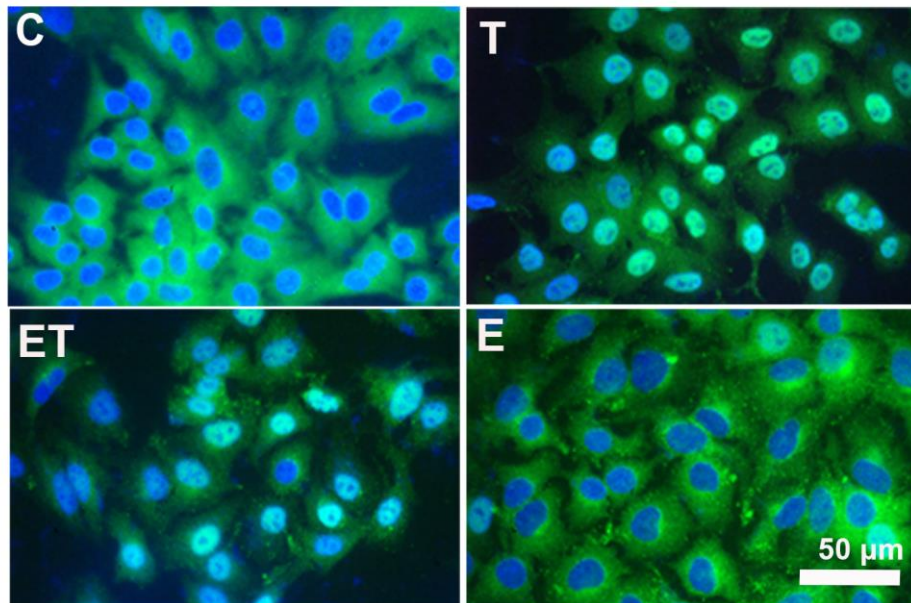
Figure 10

Figure 10: The effects of eupafolin on the nuclear activation of NF-κB in TNF-α-stimulated A549 cells.

(A) A549 cell were pretreated with or without 50 μM eupafolin and incubated with or without 3 ng/mL TNF-α for 1h. The level of p65 expression in the nuclear portion of A549 cells was determined by Western blot. The expression of hnRNP was shown as the loading control. The data are expressed as a fold value compared to the control value and are the means ± SEM for five separate experiments. $*P < 0.05$ compared to the untreated cells. $^{\dagger}P < 0.05$ compared to the TNF-α-treated cells. (ANOVA followed with Duncan's Multiple range test). (B) Nuclear extracts prepared from untreated cells or from cells with or without 24 h pretreatment with 50 μM eupafolin and then incubated with 3 ng/mL TNF-α for 1h were tested for NF-κB DNA binding activity by EMSA.

Figure 11
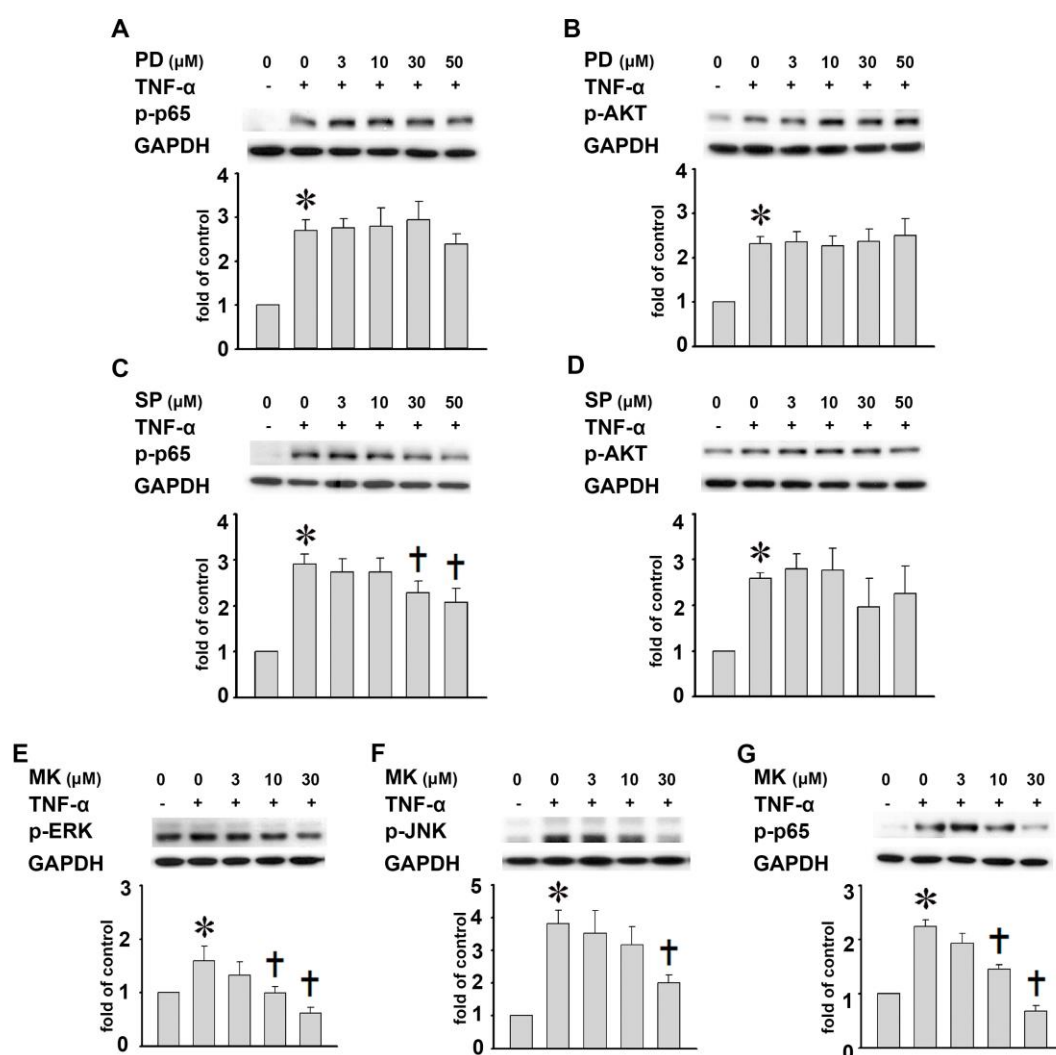
Figure 11: The crosstalk among AKT, ERK1/2, JNK and NF-κB signaling pathways in TNF-α-treated A549 cells.

A549 cells were pretreated with the various concentrations of PD98059 (ERK1/2 inhibitor), SP600125 (JNK inhibitor) or MK2206 (AKT inhibitor) for 1 h, and then stimulated with 3 ng/mL TNF-α for 15 min. The phosphorylation of p65 (A, C, G), AKT (B, D), ERK1/2 (E), and JNK (F) were determined by Western blot. GAPDH was used as the loading control. The data are expressed as a fold value compared to the control

value and are the means ± SEM for five separate experiments. *$P < 0.05$ compared to the untreated cells. †$P < 0.05$ compared to the TNF-α-treated cells.
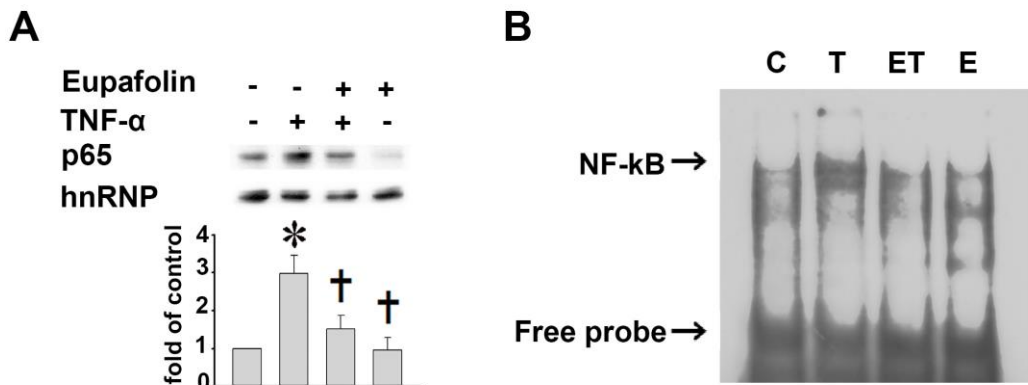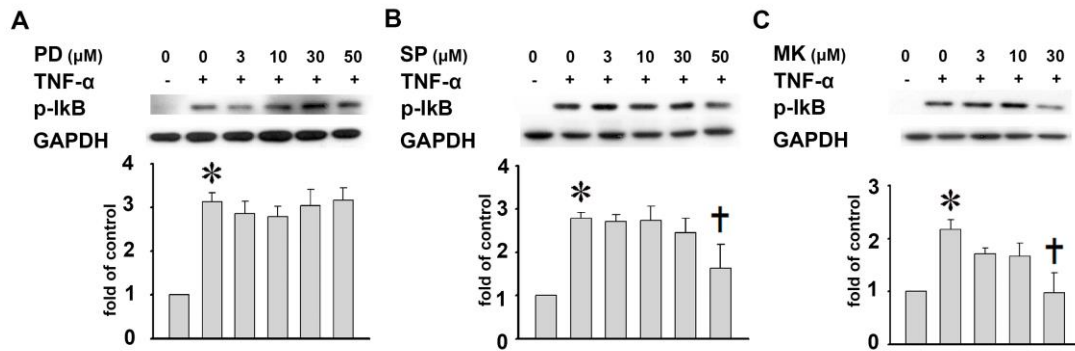
Figure 12

Figure 12: The effects of AKT/ERK1/2/JNK signaling pathways on IκB phosphorylation in TNF-α-treated A549 cells.

(A-C) A549 cells were pretreated with the various concentrations of PD98059 (ERK1/2 inhibitor), SP600125 (JNK inhibitor) or MK2206 (AKT inhibitor) for 1 h, and then stimulated with 3ng/mL TNF-α for 5 min. The phosphorylation of IκB protein was determined by Western blot. The data are expressed as a fold value compared to the control value and are the means ± SEM for five separate experiments. $*P < 0.05$ compared to the untreated cells. $^{\dagger}P < 0.05$ compared to the TNF-α-treated cells.
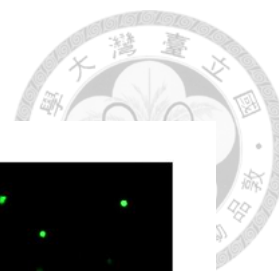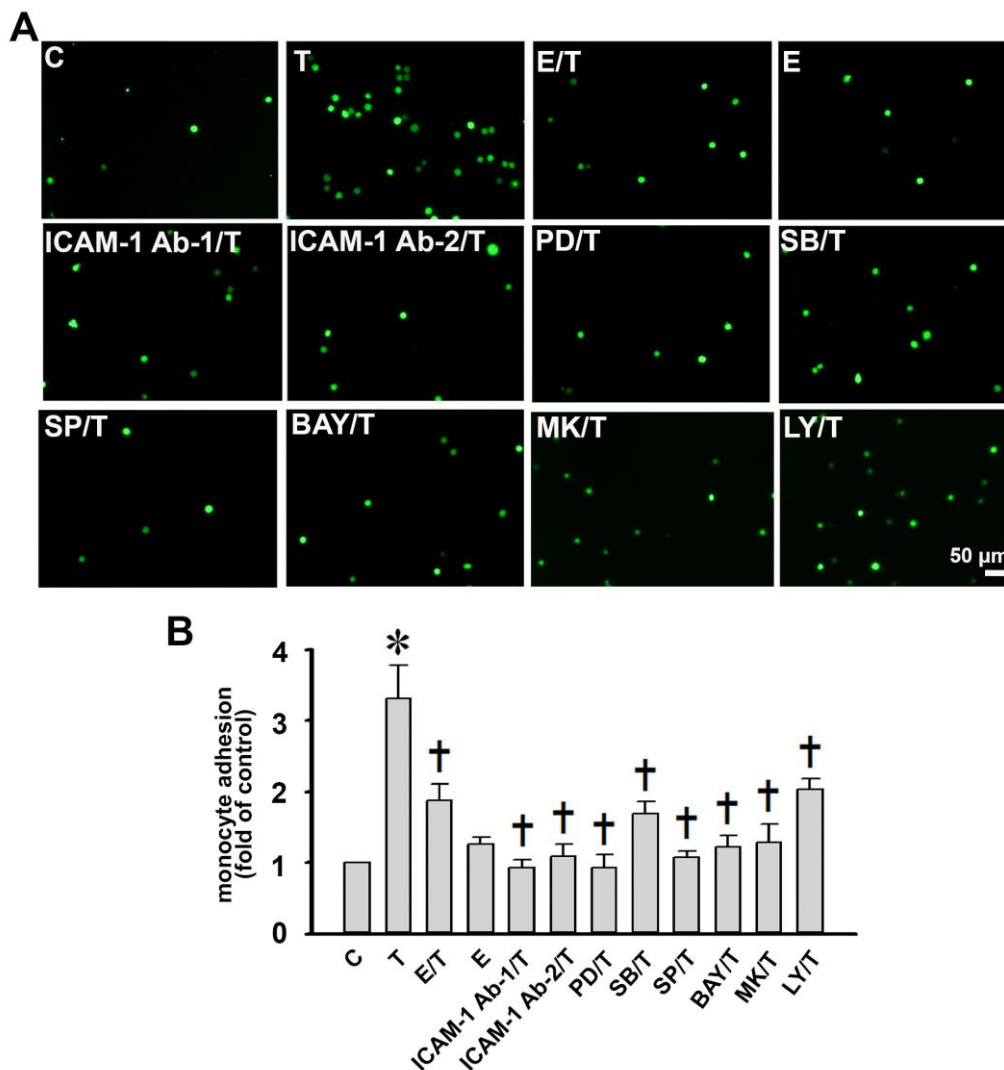
Figure 13

Figure 13: The effects of eupafolin on the adhesion of U937 cells to TNF-α-treated A549 cells.

A549 cells were left untreated or were pretreated for 24 h with 50 μM eupafolin; or for 1 or 2 μg/mL anti-ICAM-1 antibodies; or for 1 h with 50μM PD98059 (ERK1/2 inhibitor), 50μM SB203580 (p38 inhibitor), 10μM SP600125 (JNK inhibitor), 30μM BAY-11-7082 (NF-κB inhibitor), 30μM MK 2206 (AKT inhibitor) or 50μM LY294002 (PI3K inhibitor) for 1 h. Then they were incubated with 3 ng/mL TNF-α for 1 h in the continued presence of the inhibitor. BCECF-AM-labeled U937 cells were added to

A549 cells and incubated at 37℃ for 45 min. The adherent cells were photographed

with a fluorescent microscope. Bar, 50 μm. (B) The number of U937 cells bound per

high power field in six randomly selected images was counted. The data are expressed

as a fold value compared to the control value and are the means ± SEM for five separate

experiments. *$P < 0.05$ compared to the untreated cells. [†]$P < 0.05$ compared to the

TNF-α-treated cells.
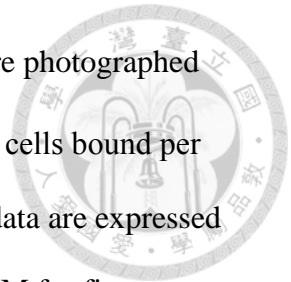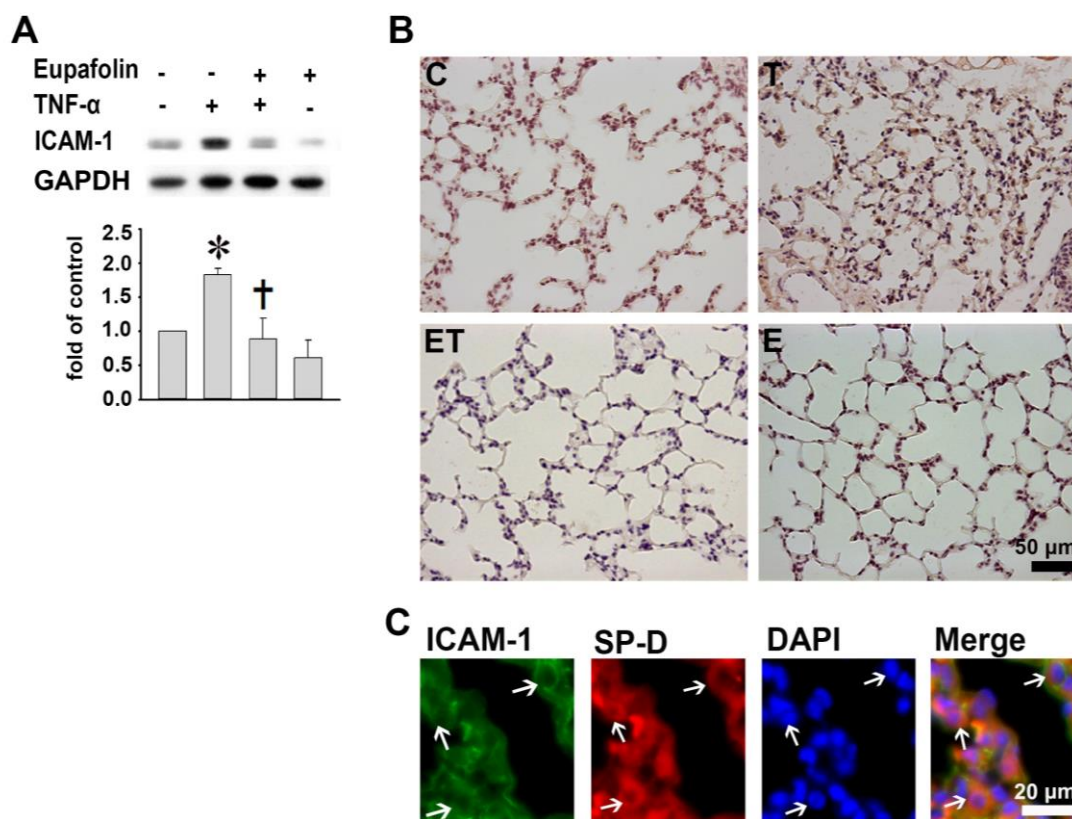
Figure 14

Figure 14: The effects of eupafolin on the TNF-α-induced ICAM-1 expression in lung tissues.

C57BL/6J mice were given intraperitoneally eupafolin (10 mg/Kg/day) for 3days, and then stimulated with TNF-α (8 μg/Kg) intratracheally administered and sacrificed after 24h. (A) The level of ICAM-1 expression in lung tissues of the C, T, ET, and E groups was determined by Western blot. GAPDH was used as the loading control. The data are expressed as a fold value compared to the control value and are the means ± SEM for five separate experiments. *$P < 0.05$ compared to the untreated cells. [†]$P < 0.05$ compared to the TNF-α-treated cells. (ANOVA followed with Duncan's Multiple range test). (B, C) The location of ICAM-1 expression was examined in lung tissues by immunostaining. The sections were stained for ICAM-1 (green) and SP-D (typeII

alveolar cell marker, red) antibodies by double immunofluorescent staining. C: control mice, T: treated with TNF-α alone, ET: pretreated with eupafolin and then stimulated with TNF-α, E: treated with eupafolin alone.
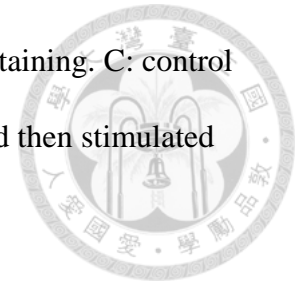
Figure 15
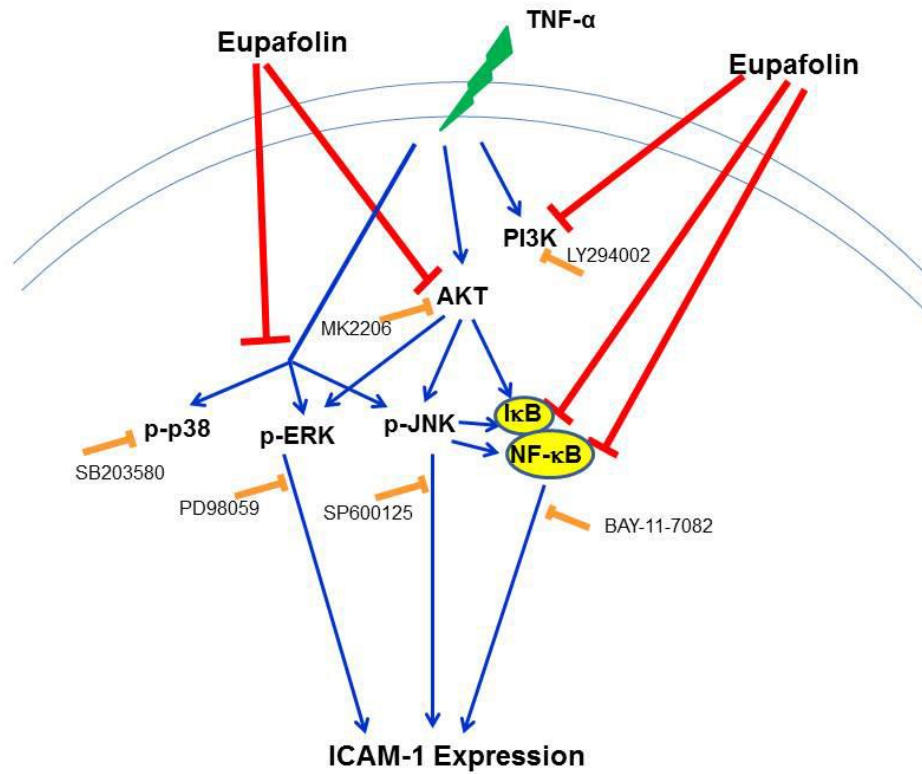
Figure 15: A summary diagram showing that eupafolin reduced ICAM-1 expression in TNF-α-treated A549 cells through the inhibition of the phosphorylation of AKT, ERK, and JNK as well as the inactivation of transcription factor NF-κB.

PART II

中文摘要

　　山苦瓜在亞洲是常見的食用蔬菜，也常被當作傳統中藥來使用。山苦瓜具有許多的藥理功能。然而，山苦瓜在肺臟疾病中的抗發炎反應機轉中所扮演的角色目前並不清楚。因此，我們主要研究山苦瓜萃取物對 TNF-α 刺激或不刺激 A549 細胞、C57BL/6 小鼠以及 miRNA-221/222 基因剔除小鼠後 ICAM-1 表現的影響。動物實驗中，C57BL/6 小鼠以及 miRNA-221/222 基因剔除小鼠分為 4 組，分別為控制組、TNF-α 刺激組、投予山苦瓜及 TNF-α 刺激組、山苦瓜組。接著利用西方點墨法、免疫螢光染色及組織免疫染色法觀察山苦瓜萃取物對 A549 細胞、C57BL/6 小鼠以及 miRNA-221/222 基因剔除小鼠之 ICAM-1 表現及相關蛋白的影響。細胞實驗結果顯示，山苦瓜萃取物確實可減緩因 TNF-α 引起的 A549 細胞表現 ICAM-1，而此作用是經過抑制 PI3K/AKT/NF-κB/IκB 的磷酸化作用以及白血球之黏附作用。除此之外，山苦瓜萃取物也會降低內生性的 ICAM-1 表現，並且會增加 miRNA -221/-222 的表現量。讓細胞過度表現 miRNA 222 也可降低 PI3K/AKT/NF-κB/IκB 的磷酸化及 ICAM-1 表現以及白血球的黏附作用。另外，在小鼠肺臟組織中，山苦瓜萃取物可抑制 TNF-α 刺激或沒刺激而表現的 ICAM-1 以及增加 miRNA -221/-222 的表現。山苦瓜萃取物不影響 miRNA-221/222 基因剔除小鼠之 miRNA-221/-222 但些微影響 ICAM-1 的表現。本實驗結果顯示，山苦瓜萃取物在動物及細胞實驗中，可降低因 TNF-α 引起的 ICAM-1 表現；而此保護機制是部分經由 miR-221/-222/PI3K/AKT/NF-κB 這條路徑來控制。

關鍵字: 山苦瓜; 發炎; 細胞黏附因子-1; miR-221/-222; PI3K/AKT; NF-κB

英文摘要

Wild bitter gourd (WBG, *Momordica charantia* L.) is consumed as a vegetable and has been used as traditional herbal medicine in Asia. The extracts from wild bitter gourd fruit (WBGE) were reported to possess numerous pharmacological activities. However, the anti-inflammatory effects of WBGE on human lung epithelial cells and the underlying mechanisms have not been determined. To evaluate the molecular basis of the effects of WBGE on intercellular adhesion molecule-1 (ICAM-1) expression in alveolar epithelial (A549) cells, C57BL/6 wild-type (WT) mice and microRNA (miR)-221/222 knockout (KO) mice with or without tumor necrosis factor (TNF-α; 3 ng/mL) treatment. WT mice and miR-221/-222 KO mice were fed a control diet and divided into four groups (C: control mice; T: treated with TNF-α alone; WBGE/T: pretreated with WBGE and then stimulated with TNF-α; WBGE: treated with WBGE alone). The effects of WBGE on ICAM-1 expression and the related signals in A549 cells and mice with or without TNF-α treatment were examined by Western blot and immunofluorescent staining. WBGE significantly decreased the TNF-α-induced ICAM-1 expression in A549 cells through the inhibition of phosphoinositide 3-kinase (PI3K)/ protein kinase B (AKT)/ nuclear factor- kappa B (NF-κB)/ inhibitor of NF-κB (IκB) phosphorylation and decreased leukocyte adhesion. In addition, WBGE reduced endogenous ICAM-1 expression and upregulated miR-221/-222 expression. The overexpression of miR-222 decreased PI3K/AKT/NF-κB/IκB and ICAM-1 expression, which resulted in reducing monocyte adhesion. Moreover, WBGE reduced ICAM-1 expression in lung tissues of WT mice with or without TNF-α treatment and upregulated miR-221/222. WBGE did not affect the miR-221/-222 level and had little effect on ICAM-1 expression in miR-221/-222 KO mice. These results suggest that WBGE

reduced ICAM-1 expression both under *in vitro* and *in vivo* conditions. The protective effects were mediated partly through the miR-221/-222/PI3K/AKT/NF-κB pathway.
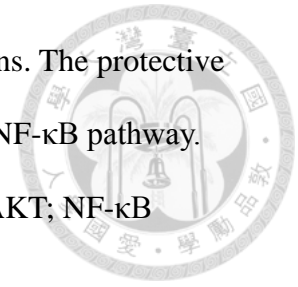
第一章　簡介

Wild bitter gourds (WBG, *Momordica charantia* L.) are consumed as a vegetable and have been used as a traditional herbal medicine in Asia (Chao et al., 2014). The noticeable pharmacological properties of WBG fruit extract (WBGE) are anti-diabetic (Chaturvedi, 2012), anti-inflammatory (Chao et al., 2014, Lii et al., 2009), anti-tumor (Bai et al., 2016; Somasagara et al., 2015) and anti-oxidative actions (Lu et al., 2014). WBG is known to contain several phytochemicals, including glycosides (charantin, momordin), alkaloids (momordicin), phenolics, and lysophosphatidylcholines (Chaturvedi, 2012). Charantin, which is a bioactive compound in WBG, has been reported to possess potential hypoglycemic activity (Desai and Tatke., 2015), anti-bacterial activity (Patel et al., 2010), antidiabetic activity and anti-cancer activity (Dandawate et al., 2016). However, the anti-inflammatory effects of WBGE on human lung epithelial cells and the underlying mechanisms have not been investigated.

Lung inflammation is a pivotal event in the initiation and development of respiratory disorders, such as chronic obstructive pulmonary disease (COPD) and asthma (Lee and Yang, 2013). These inflammatory responses are mediated by complex interactions between circulating polymononuclear cells and the component cells in lung tissues. The expression of adhesion molecules on airway epithelial cells was important for selective recruitment of effector cells onto epithelial cells (Chen et al., 2001). Intercellular adhesion molecule-1 (ICAM-1) which is an adhesion molecule, has long been known for its importance in mediating cell-cell interactions. Its expression is increased by the stimulation of inflammatory cytokines and enhances adhered leukocytes that migrated across the vascular endothelial cells and then interacted with epithelial cells at sites of inflammatory airways (Lee and Yang, 2013). The clinical study also showed that the sICAM-1 levels in plasma of patients with pulmonary

diseases were significantly higher than in healthy subjects (Demir et al., 2002). Currently available therapies for inflammation include corticosteroids and CXC chemokine receptor antagonists (Durham et al., 2015). However, many of these agents have a number of serious adverse effects. Therefore, the search for more effective and safer antiinflammatory agents has continued to be an important area of investigation. Thus, attenuating ICAM-1 production with or without TNF-α stimulation in lung epithelial cells was recognized as new potential therapeutic approach for the management of respiratory diseases.

The intracellular signaling pathways through which TNF-α promotes ICAM-1 expression are generally not well understood, but certain mechanisms have been proposed, including mitogen-activated protein kinases (MAPKs), PI3K/AKT, and transcription factors (Lee and Yang, 2013; Chen et al., 2001). Little is known about the effects of WBGE on ICAM-1 expression and the mechanisms of these effects, and a better understanding of these processes might provide important insights into the prevention of airway inflammation. In addition, evidence also suggested that miRNA was involved in lung inflammation (Alipoor et al., 2016). MiRNAs, which are a new class of non-coding small RNAs, are 19-25 nucleotides in length (Alipoor et al.2016). They target mRNAs through complementarity between the miRNAs and the 3'-untranslated regions (3'UTRs) of target mRNAs, which causes either mRNA cleavage or translational suppression and results in gene silencing (Hu et al., 2010). Additionally, recent studies have shown that miR-221 or miR-222 can suppress ICAM-1 translation and regulate ICAM-1 expression (Hu et al., 2010; Gong et al., 2011; Jansen et al., 2015). However, the relationship between miRNAs and ICAM-1 in lung inflammation is still unclear. Accordingly, this study is the initial study to demonstrate that WBGE represses ICAM-1 expression in A549 cells and mice with or without

TNF-α treatment. The protective effects were mediated in part through the miR-221/-222 /PI3K/AKT/NF-κB/IκB pathway.

第二章　材料與方法

2.1　Extraction of WBG (WBGE)

Crude dry Taiwanese WBG fruit (Hualien No. 4) was obtained from the Aquavan Technology Company (Taiwan). Then, 20 g of WBG was soaked in 400 mL methanol, boiled with a microwave at 400 W for 10 min, and then filtered through an Adventec filter (No. 5, 55 mm). The fractions were concentrated in 20-25 mL under a rotary evaporator (R-2000V, Panchun, Taiwan) for 3 h. Then, the methanol extract of WBG was sonicated with an ultrasonic oscillator (LEO-2003S, Leo, Taiwan) and freeze-dried with a Freeze Dryer (FD3-12P, Kingmech, Taiwan) for 3-5 days. The extracts of wild bitter gourd (WBGE) were stored at 4 ℃ until analysis. WBGE was dissolved in dimethylsulfoxide (DMSO) with a stock concentration of 40 mg/mL before dilution with the medium.

2.2　Analysis of WBGE by HPLC

We measured the charantin content in WBGE using the Thermo UltiMate 3000 HPLC system. The HPLC system consisted of an UltiMate 3000 RS pump, an UltiMate 3000 RS autosampler, an UltiMate 3000 RS column compartment, a variable wavelength detector (Thermo, MA, USA) and a reversed-phase column (Inertsil ODS-3V, 4.6 Å, 150 mm, GL Science, Tokyo, Japan). The mobile phase was 98:2 (v/v) water-methanol and was delivered at a flow rate of 1 mL/min. The injection volume was 20 mL and UV wavelength detection was carried out at 204 nm. The retention time of charantin was approximately 6-8 min. The data were collected and analyzed in the Chromelion software from Thermo Corporation.

2.3 Cell culture

A549 (human lung epithelial alveolar cells) and U937 cells (human monocytic leukemia cells) were purchased from American Type Culture Collection (VA, USA). A549 cells were cultured in Dulbecco's Modified Eagle Medium (DMEM) (Life Technology, NY, USA) supplemented with 10% fetal bovine serum (FBS, Life Technology) and 1% penicillin/streptomycin. U937 cells were cultured in RPMI 1640 medium (Life Technology) supplemented with 10% FBS and 1% penicillin/streptomycin. The cells were grown in a humidified atmosphere of 95% air and 5% CO_2 at 37 ℃. The 3-(4,5-dimethylthiazol-2-yl)-2,5-diphenyl tetrazolium bromide (MTT) assay was used to measure cell viability. The cells were grown in 48-well plates and incubated with various concentrations of WBGE (10-100 μg/mL) or charantin (0.5-10 μg/mL) for 24 h, then 100 μL of MTT (0.5 mg/mL) was added to each well and incubated at 37 ℃ for an additional 2 h. The absorbance of the solubilized blue formazan was detected with a DIAS Microplate Reader (Dynex Technologies, USA).

2.4 Preparation of cell lysates and Western blot analysis

A Western blot was performed as described previously (Sung et al., 2015). The following primary rabbit antibodies against ICAM-1(1:5000, Santa Cruz Biotechnology, TX, USA), phospho-ERK1/2 (1:10000, Cell Signaling, MA, USA), phospho-p38 (1:1000, Santa Cruz Biotechnology), phospho-JNK (1:1000, Cell Signaling), phospho-PI3K (1:1000, EnoGene Biotech, NY, USA), phospho-AKT (1:1000, EnoGene Biotech), phospho-p65 (1:1000, Epitomics, CA, USA), and phospho-IκB (1:1000, Cell Signaling) were used at 4 ℃ and incubated overnight. The membranes were then incubated for 1 h at RT with HRP-conjugated goat anti-rabbit IgG secondary antibodies (1:5000, Santa Cruz Biotechnology) or HRP-conjugated goat anti-mouse IgG antibodies

57 *doi:10.6342/NTU201701930*

(1:5000, Santa Cruz Biotechnology). The immunoreactive bands were detected using the Chemiluminescence Reagent Plus (NEN, MA, USA), and the intensity was quantified with a densitometer. Antibodies against GAPDH (1:5000, Santa Cruz Biotechnology) or β-actin (1:5000, GeneTex, TX, USA) were used as an internal control.
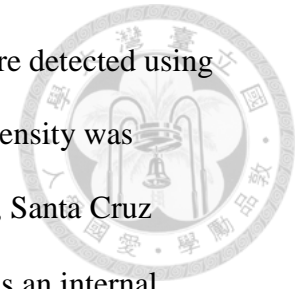
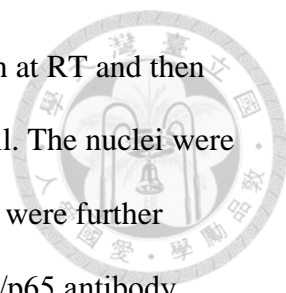## 2.5 Immunocytochemical localization of ICAM-1 and NF-κB p65

To localize ICAM-1 and NF-κB p65 expression *in situ*, A549 cells on coverslips were pretreated with or without WBGE for 24 h, and then treated with or without 3 ng/mL TNF-α for 4 h at 37 °C. The cells were fixed in 4% paraformaldehyde in PBS for 15 min at RT, and then the samples were incubated with rabbit anti-human ICAM-1 (1:100 dilution, Abcam, MA, USA) or anti-human NF-κB p65 antibodies (1:100 dilution, Epitomics) at 4 °C overnight. After the samples were washed, the coverslips were incubated with a DyLight 488 goat anti-rabbit polyclonal antibody (1:200 dilution, Abcam) for 1 h at RT and observed using a fluorescence microscope.

2.6 Preparation of cytoplasmic and nuclear extracts for Western blotting

The method for cytoplasmic and nuclear extract conditions were described previously (Sung et al., 2015). The cytoplasmic and nuclear proteins were extracted using NE-PER reagent (Pierce, Rockford, IL, USA) according to the manufacturer's protocol.

2.7 Chromatin immunoprecipitation assay

ChIP assays were performed using an EZ-Magna ChIP™ A/G Kit (17-10086, Millipore, Watford, UK) according to the manufacturer's instructions.

Briefly, the cells were cross-linked with 1% formaldehyde for 10 min at RT and then were harvested with lysis buffer containing protease inhibitor cocktail. The nuclei were isolated and sonicated to generate 200-500 bp DNA fragments. They were further diluted with dilution buffer and immunopricipitated with anti-NF-κB/p65 antibody (17-10060, Millipore). The immune complexes bound to protein A/G magnetic beads overnight at 4 ℃ with rotation. The beads were then washed sequentially in low-salt, high salt, LiCl, and Tris-EDTA buffers subsequently, and the immune complexes were extracted with ChIP elution buffer. Cross-linking was reversed by heating at 62 ℃ for 2 h. The DNA was purified and subjected to PCR using primers covering the NF-κB binding site of the ICAM-1 promoter. The primers used for amplification of the NF-κB binding elements were 5′-ACCTTAGCGCGGTGTAGACC-3′ and 5′-CTCCGGAACAAATGCTGC-3′. The PCR conditions included an initial denaturation step at 94 ℃ for 5 min, followed by 40 cycles of denaturation at 94 ℃ for 30 sec, primer annealing at 55 ℃ for 30 sec, and extension at 72 ℃ for 45 sec. The PCR products were analyzed by electrophoresis on 2% agarose gels stained with ethidium bromide. Input samples were amplified simultaneously as internal controls.

2.8   RNA preparation and real-time PCR

Total RNA was isolated from cells using TRIzol reagent (Thermo) according to the manufacturer's instructions. For analysis of miR-221/-222 expression, real-time PCR was performed by using the TaqMan Universal PCR Master Mix (Applied Biosystems, CA, USA). TaqMan microRNA assay kits for miR-221 (000524), -222 (002276) and RNU6B (001973) were obtained from Applied Biosystems. All reactions were run in triplicate. The amount of miR-221/-222 was obtained by normalizing the samples to RNU6B.
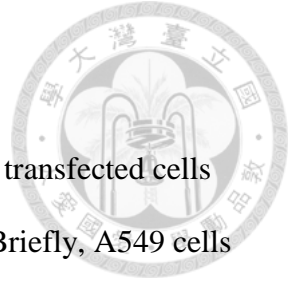
2.9 Overexpression of miR-221/-222

To manipulate the functions of miR-221/-222 in A549 cells, we transfected cells with miR-221/-222 precursor to increase miR-221/-222 expression. Briefly, A549 cells were grown to 70% confluency and transfected with the miR-221or with the miR-222 mimic (Dharmacon, CO, USA) at a concentration of 100 nM/well using the Lipofectamine 3000 reagent (Invitrogen, CA, USA) followed by analysis of ICAM-1 expression and monocyte adhesion.

2.10 Cell adhesion assay

The fluorescence labelling approach was used to assess epithelial cell-mediated adhesion of monocytes as previously reported (Sung et al., 2015). Briefly, U937 cells were labelled with the fluorescent dye, 1 μg/mL of BCECF-AM (2',7'-bis-(2-carboxyethyl)-5-(and-6)-carboxyfluorescein acetoxymethyl, Boehringer Mannheim, Mannheim, Germany), for 1 h at 37 °C. A549 cells were grown in a 24-well dish and then pretreated with or without WBGE for 24 h or for 1 h with MK2206 (30 μM, AKT inhibitor, BioVision, CA, USA), LY294002 (50μM, PI3K inhibitor, Cayman Chemical, MI, USA), or Bay11-7082 (30μM, NF-κB inhibitor, Cayman Chemical). After treatment with TNF-α for 4 h at 37°C, the cells were washed three times with PBS. Labeled U937 cells (10^6) were then added and incubated with A549 cells for 1 h at 37 °C. Representative images were taken using a Zeiss fluorescence microscope, and the number of U937 cells adhering to A549 cells was counted in six randomly selected images for each experiment. The data are expressed as a fold value compared to the control value and are the means ± SEM for five separate experiments.

2.11 Luciferase reporter assay

A549 cells were transfected with 1 µg of the ICAM-1 luciferase reporter construct (pIC339) with TurboFect(Thermo). The pIC339 was a gift obtained from the Medical Microbiota Center of the First Core Laboratory, National Taiwan University. After 20 h of transfection, the cells were pretreated with or without WBGE for 24 h, and then the cells were treated with or without 3 ng/mL TNF-α for 4 h. Luciferase activity was measured by a Reporter Assay Kit (Promega Corp., WI, USA).

2.12 Mouse model, diets, and experimental procedures

C57BL/6 wild-type (WT) mice and miR-221/-222 knockout (KO) mice (weight: 25-30 gm; age: 9-12 weeks) were used in this study. We generated miR-221/-222 KO mice by deleting the X-linked miR-221/222 gene and bred them for 10 generations on a C57BL/6 background. These mice were viable and fertile. All mice were maintained in the Laboratory Animal Center of the Department of Bioscience Technology of Chung Yuan Christian University (CYCU). All procedures involving experimental animals were performed according to the guidelines for animal care at National Taiwan University (No. 20150502) and complied with the *Guide for the Care and Use of Laboratory Animals,* NIH publication No. 86–23, revised 1985. All mice were fed a commercial diet (containing 2900 IU/100 g vitamin A, 650 IU/100 g vitamin D3, 21.2 IU/100 g vitamin E, 4.4 mg/100 g vitamin B1, 3.01 mg/100 g vitamin B2, 1.05 mg/100 g vitamin B6, 7.9% moisture, 22.9% crude protein, 5.4% crude fat, 6.2% ash, 3.4% crude fiber, 54.2% nitrogen free extract and 357 Kcal/100 g, Biolasco Industry). The mice were then randomly divided into four groups that were treated with DMSO, TNF-α, TNF-α plus WBGE, or WBGE only. The mice were orally treated with WBGE (1000 mg/kg/day in 50 µL of DMSO) or DMSO (50 µL) for 5 days, and then the mice

were left untreated or were injected intratracheally with TNF-α (10 μg/kg) for 1 day. The mice were then anesthetized by intraperitoneal injection of Zoletil/Xylazine (2 mg/kg+5 mg/kg) and sacrificed, and the lung tissues were removed. Some of the lung tissues were immersion-fixed with 4% buffered paraformaldehyde and paraffin-embedded for immunohistochemistry, and the remaining larger portion was immediately frozen in liquid nitrogen for RNA and protein isolation.
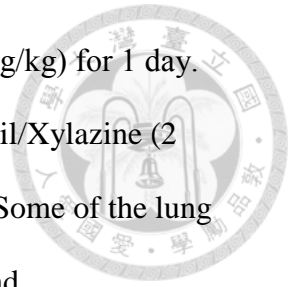
2.13 Immunohistochemistry

To determine the level of ICAM-1 expression in lung tissues, the 5 μm-thick sections were treated with ICAM-1 antibodies (1:100 dilution, Abcam) at 4℃ overnight. The sections were then incubated with biotin-conjugated goat anti-rabbit IgG (1:200 dilution, Vector lab, Cambridgeshire, UK) for 1 h at RT. Finally, the sections were stained with 3,3-diaminobenzidine tetrahydrochloride (DAB) and counterstained with hematoxylin.

2.14 Statistical analysis

The data are expressed as the means ± SEM for five separate experiments unless otherwise specified. Statistical analyses were performed with a one-way ANOVA or a two-way ANOVA, and followed by Duncan's Multiple range test. Analyses were conducted using SigmaPlot software (Systat Software, Inc.*, IL, USA*).

第三章 結果

3.1 Characterization of WBGE

The chemical structure of Charantin is a mixture of Stigmasta-5,25-dien-3β-yl,
β-D-glucopyranoside and β-Sitosteryl glucoside (Upadhyay et al., 2015, Fig. 1A).
WBGE showed two peaks along with the chromatogram of charantin, which is a
standard, in HPLC chromatograms (Fig. 1 B). The retention times of charantin for
Stigmasta-5,25-dien-3β-yl,β-D-glucopyranoside and β-Sitosteryl glucoside were 6.8
min and 7.5 min, respectively. The levels of
Stigmasta-5,25-dien-3β-yl,β-D-glucopyranoside and β-Sitosteryl glucoside in WBGE
were calculated to be 9.23±0.11 μg/mg and 0.61±0.03 μg/mg, respectively. The total
amount of charantin in WBGE was 9.85±0.13 mg/g.

3.2 WBGE decreased the TNF-α-induced ICAM-1 expression in A549 cells

A549 cells treated with 10-100 μg/mL WBGE or with 10-100 μg/mL charantin for
24 h did not cause cytotoxicity in the MTT assay (Fig. 2A). To analyze the effects of
WBGE and charantin on ICAM-1 expression under inflammation, A549 cells were
preincubated with WBGE for 24 h with 10, 30, 50, or 80 μg/mL or charantin with 0.5, 1,
3, 5 μg/mL and then followed by stimulation with 3 ng/mL TNF-α for 4 h. TNF-α
treatment significantly increased ICAM-1 expression in A549 cells (Fig. 2B). This
effect was inhibited by pretreatment with WBGE or charantin. WBGE significantly
reduced ICAM-1 expression in a concentration-dependent manner. Consistently,
fluorescence microscopy images showed that ICAM-1 was strongly present in the
cytosol of TNFα-treated A549 cells (T) (Fig. 3). In contrast, ICAM-1 expression was
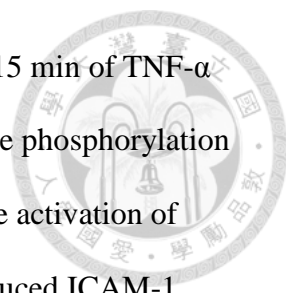weaker in TNF-α-stimulated A549 cells pretreated with WBGE (WBGE/T) or charantin

(CH/T). Luciferase activity of ICAM-1 promoter was significantly induced with TNF-α and was significantly reduced by WBGE (Fig. 4). Based on these results, 80 µg/mL WBGE was used in the present study to evaluate the anti-inflammatory effects and molecular mechanisms of WBGE treatment.
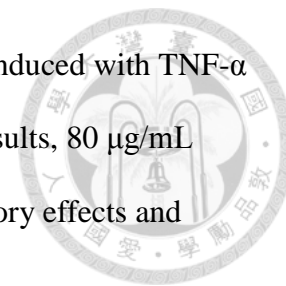
Since cell adhesion molecules are critical for monocyte adhesion, the next step was to examine the effects of WBGE on monocyte adhesion. As shown in Fig. 5, minimal binding of monocytes to confluent control cells was observed, but adhesion was substantially increased when the cells were treated with TNF-α. In contrast, WBGE-pretreated cells significantly reduced the binding of monocytes to TNF-α-treated cells. In addition, pretreatment of the A549 cells with a neutralizing antibody against ICAM-1 led the number of monocytes binding to TNF-α-treated cells to be significantly reduced. The present study demonstrated that ICAM-1 played an important role in monocyte adhesion to TNF-α-treated A549 cells.

3.3 The inhibition of PI3K/AKT phosphorylation mediates the reduction in ICAM-1 expression by WBGE in TNF-α-treated A549 cells
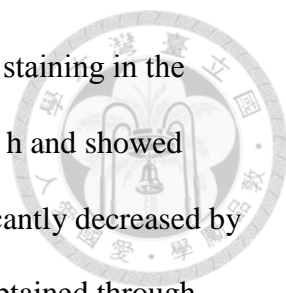
Previous studies have demonstrated that MAPKs (Lee et al., 2013) and the PI3K/AKT signaling pathway (Choi et al., 2012; Oh and Kwon, 2009) were involved in TNF-α-induced inflammation. We next investigated whether TNF-α-induced ICAM-1 expression was mediated through MAPKs or PI3K/AKT phosphorylation. The phosphorylation of ERK1/2, p38, and JNK in A549 cells showed a significant increase at 15-30 min of TNF-α treatment and was followed by a decline at 60 min (Fig. 6). To determine the effects of WBGE, the cells were pretreated with WBGE for 24 h and then stimulated with TNF-α for 5, 15, 30, 45, or 60 min. WBGE had no effect on TNF-α-induced ERK1/2, p38, and JNK phosphorylation (Fig. 6). The expression levels

of phosphorylated PI3K and AKT were significantly increased after 15 min of TNF-α stimulation, and pretreatment with WBGE significantly attenuated the phosphorylation of PI3K and AKT (Fig. 7A). Additionally, we determined whether the activation of PI3K/AKT was involved in the suppression of WBGE on TNF-α-induced ICAM-1 expression. As shown in Fig. 7B, pretreatment with MK2206 (AKT inhibitor) and LY294002 (PI3K inhibitor) caused significant attenuation of ICAM-1 expression in TNF-α-treated A549 cells. In addition, pretreatment with WBGE and inhibitors enhanced the decrease in ICAM-1 expression. According to these results, WBGE suppressed TNF-α-induced ICAM-1 expression through PI3K/AKT phosphorylation and an undetermined pathway. In addition, inhibitors specific for PI3K and AKT blocked TNF-α-induced monocyte adhesion (Fig. 8), which further supported the notion that sequential activation of the PI3K/AKT pathway resulted in upregulation of ICAM-1 and subsequent monocyte adhesion.

3.4 The inhibition of NF-κB p65 activation and translocation mediates WBGE-reduced ICAM-1 expression in TNF-α-treated A549 cells
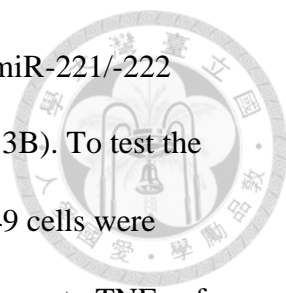
We investigated whether WBGE reduced TNF-α-induced ICAM-1 expression via NF-κB signaling because the promoter of the ICAM-1 gene contains consensus binding sites for the transcription factor (Rahman et al., 1999). First, we examined the levels of phosphorylated NF-κB p65 in TNF-α-treated A549 cells through Western blotting. The phospho-p65 level was higher in TNF-α-treated A549 cells than in control cells, and WBGE pretreatment significantly reduced that effect (Fig. 9A). A similar result was obtained for IκB phosphorylation (Fig. 9B), which is responsible for NF-κB activation (Choi et al., 2012). The results of immunofluorescent staining were consistent with the Western blot findings of NF-κB p65. Control A549 cells or cells incubated only with

WBGE showed no nuclear NF-κB p65 staining, but there was strong staining in the cytoplasm. In contrast, A549 cells were stimulated with TNF-α for 1 h and showed strong NF-κB p65 staining in the nucleus, and this effect was significantly decreased by pretreatment for 24 h with WBGE (Fig. 10A). A similar result was obtained through Western blotting (Fig. 10B). The binding of NF-κB/p65 to the ICAM-1 promoter was further examined by ChIP-PCR. TNF-α significantly increased the binding of p65 to the ICAM-1 promoter, whereas WBGE reduced the binding activity (Fig. 11A). Furthermore, TNF-α-induced ICAM-1 expression in A549 cells was blocked by preincubation of the cells for 1 h with 30 μM Bay11-7082, which is an NF-κB inhibitor (Fig. 11B). Moreover, pretreatment of cells with Bay 11-7082 blocked TNF-α-induced monocyte adhesion (Fig. 12), which further supported the notion that sequential activation of the NF-kB pathway leads to upregulation of ICAM-1 and subsequent monocyte adhesion to TNF-α-treated A549 cells. These results suggested that WBGE-reduced ICAM-1 expression in TNF-α-treated A549 cells was mediated by inhibition of NF-κB activation.

3.5 WBGE reductions in endogenous ICAM-1 expression in A549 cells involves miR-222 upregulation

Recent studies suggest that ICAM-1 is a target of miR-221/-222, and both miRNAs regulate ICAM-1 expression (Duan et al., 2013). miR-221 and miR-222 are encoded in tandem on X chromosomes and are conserved miRNAs with significant homology between them. According to TargetScan.org (http://www.targetscan.org), miR-221 and miR-222 are complementary to the ICAM-1 3'UTR and extend between 413 and 419 (Fig. 13A). Furthermore, we examined whether posttranscriptional regulation by miR-221/-222 was critical for the ICAM-1 expression in A549 cells treated with TNF-α

and WBGE. There were no significant changes in the levels of both miR-221/-222 expression in A549 cells following TNF-α stimulation for 4 h (Fig. 13B). To test the role of miR-221/-222 in TNF-α-mediated induction of ICAM-1, A549 cells were transfected with miR-221/-222 precursors for 44 h, followed by exposure to TNF-α for 4 h with subsequent assessment of ICAM-1 protein expression via Western blot. Transfection of cells with a precursor miR-221 or miR-222 sequence, however, did not affect TNF-α-induced ICAM-1 (Fig. 14A), p-p65, p-PI3K and p-IκB expression (Fig. 14B). We also found that miR-221 or miR-222 precursors had no effect on adhesion of U937 cells to TNF-treated A549 cells (Fig. 15).

Interestingly, we found that WBGE treatment significantly increased miR-221/-222 expression (Fig. 13B). In addition, WBGE treatment significantly reduced endogenous ICAM-1 expression (Fig. 2B). Additionally, the phosphorylation of PI3K, AKT, p65, and IκB decreased after WBGE treatment compared to the control group (Figs. 7A, 9A, 9B). Therefore, we investigated whether miR-221/-222 was involved in the effects of WBGE on endogenous ICAM-1 expression in A549 cells. As shown in Fig. 16, the precursor of miR-222 significantly attenuated endogenous ICAM-1 expression in A549 cells. An increase in the phosphorylation of AKT, p65, and IκB was detected in A549 cells, which was significantly ameliorated in cells transfected with a miR-222 precursor (Fig. 16). To determine the functional relevance of miR-221/-222-regulated expression of ICAM-1 in A549 cells, monocyte adhesion assays were performed in the presence of A549 cells transfected with miR-221 or miR-222 precursors. As shown in Fig. 17, there was a significant reduction of monocyte adhesion in cells transfected with either of the precursors. We also found that ICAM-1 expression was downregulated by AKT, PI3K and p-65 inhibitors (Fig. 18). These data further corroborate the fact that WBGE-mediated upregulation of miR-222 is involved

in endogenous expression of ICAM-1 in A549 cells and influences monocyte adhesion.
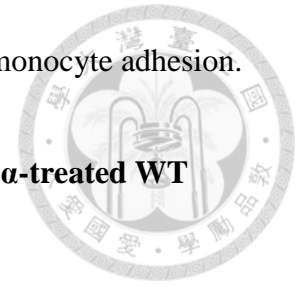
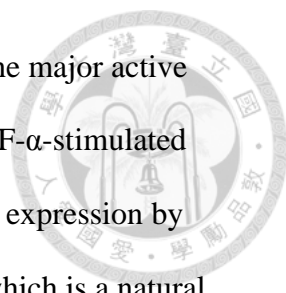## 3.6 WBGE reduces ICAM-1 expression in lung tissues of TNF-α-treated WT mice

To determine the effects of WBGE on ICAM-1 expression *in vivo*, WT mice and miR-221/-222 KO mice were fed WBGE for 5 days followed by an either an injection of TNF-α for 1 day or no injection; then, RT-PCR, Western blot and immunohistochemical staining were performed to detect the expression of miRNA-221/-222, ICAM-1 protein, and ICAM-1 in sections of lung tissues. As shown in Fig. 19, TNF-α treatment significantly reduced the levels of miRNA-222 expression. WBGE significantly increased miRNA-221/-222 expression in lung tissues with or without TNF-α treatment. The levels of miRNA-221/-222 were very low for lung tissues of four groups in miRNA-221/-222 KO mice. As shown in Fig. 20A, TNF-α treatment significantly induced ICAM-1 expression, whereas WBGE decreased ICAM-1 expression in lung tissues of WT mice. Furthermore, TNF-α induced higher ICAM-1 expression in miRNA-221/-222 KO mice compared to wild-type mice. WBGE had little effect on ICAM-1 expression. As shown in Fig. 20B, in the control and WBGE-treated groups, weak ICAM-1 staining was seen in the lung tissues, whereas in the TNF-α-treated group, strong ICAM-1 staining was seen in the lung tissues after immunohistochemical staining. In contrast, preadministration of WBGE resulted in weak ICAM-1 staining in the TNF-α-treated animals (WBGE /T). ICAM-1 expression was stronger in TNF-α-treated miR-221/-222 KO mice compared with the TNF-α-treated WT animals. Additionally, WBGE mildly decrease ICAM-1 expression in miR-221/-222 KO mice. These beneficial effects of WBGE were lost in miR-221/-222 KO mice.

第四章　討論

In this study, we demonstrated that WBGE treatment significantly decreased ICAM-1 expression and adhesion of monocyte U937 to TNF-α-stimulated A549 cells. The influence was partially mediated through inhibition of the phosphorylation of PI3K/AKT/NF-κB/IκB. Moreover, WBGE treatment significantly reduced endogenous ICAM-1 expression in A549 cells without TNF-α treatment. The effect was mediated through upregulation of miR-222 expression as well as decreased phosphorylation of PI3K/AKT/p65/IκB. Furthermore, WBGE attenuated ICAM-1 expression and upregulated miR-221/-222 expression in the lung tissues of mice with or without TNF-α treatment but had little effect in miR-221/-222 KO mice. The protection of lung cells by WBGE is due to the inhibition of PI3K/AKT/p65/IκB and ICAM-1 by miR-221/-222.

Inflammation is a central feature of respiratory disorders. Substantial evidence has demonstrated that WBG is not only a functional food but also has anti-diabetic, anti-inflammatory, and anti-tumor activities (Chao et al., 2014; Bai et al., 2016; Wu et al., 2009). The ethanol extract of WBG reduced iNOS and IL-1β expression in LPS-treated RAW264.7 macrophages (Lii et al., 2009). Addition of WBG lyophilized powder reduced the inflammation biochemical markers IL-1, IL-6 and TNF-α in LPS-treated mice (Chao et al., 2014). A triterpenoid isolated from WBG exhibited an antiproliferative effect on breast cancer cells (Bai et al., 2016). The triglycerides and dicarboxylic acids in bitter gourd inhibited PGE_2 production, which is a proinflammatory mediator, in LPS-treated RAW264.7 macrophages (Wu et al., 2009). This study is the first to report that WBGE reduced ICAM-1 expression in TNF-α-stimulated A549 cells and lung tissues in mice. In addition, WBGE inhibited leukocyte adhesion to TNF-α-stimulated A549 cells. We also showed that the

phytoconstituent from WBGE contained charantin, which is one of the major active

compounds in WBGE. Charantin reduced ICAM-1 expression in TNF-α-stimulated

A549 cells. These data indicated that the downregulation of ICAM-1 expression by

WBGE may be partially attributed to the rich fraction of charantin, which is a natural

steroidal glycoside. Because ICAM-1 has been reported as an important modulator of

inflammation in epithelial cells of the respiratory airway and leukocyte adhesion (Lee et

al., 2013), our experiments provide evidence that WBGE has the capability to reduce

ICAM-1 expression and monocyte adhesion and may serve as a therapeutic reagent in
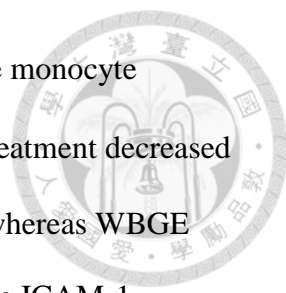
lung inflammation.

MAPK and PI3K/AKT pathways played an important role in the expression of

proinflammatory mediators and inflammatory cell recruitment, which led to the

initiation and progression of lung inflammation (Lee et al., 2013). The present study

demonstrated that TNF-α caused strong phosphorylation of three MAPK subtypes and

PI3K/AKT in A549 cells, as reported in previous studies (Lee et al., 2013; Oh and

Kwon, 2009). However, the involvement of their activation in the protective mechanism

of WBGE has yet to be determined. Our results showed that WBGE significantly

decreased TNF-α-induced PI3K and AKT phosphorylation, whereas WBGE had no

effects on TNF-α-induced MAPK phosphorylation. The increase in ICAM-1 expression

induced by TNF-α was markedly suppressed in the presence of PI3K inhibitor or AKT

inhibitor. Thus, one of the mechanisms through which WBGE reduces TNF-α-induced

ICAM-1 expression involves a reduction in PI3K/AKT activation. Consistent with our

results, bitter melon juice was effective at decreasing AKT/PI3K phosphorylation and

viability of pancreatic cancer cells (Somasagara et al., 2015). A triterpenoid isolated

from WBG induced breast cancer cell apoptosis through the downregulation of AKT

signaling (Bai et al., 2016). However, our findings do not agree with several reports.

The butanol fraction of bitter gourd suppressed phosphorylation of p38, JNK, and ERK in LPS-treated RAW 264.7 cells (Kobori et al., 2008). The preventive effects of bitter melon against insulin resistance and diabetes are associated with the inhibition of JNK pathway in the livers of rats fed a high-fat diet (Yang et al., 2015). The differences between these results in terms of the pathways involved may be related to differences in the cell type, inducers, and cytokines.

PI3K/AKT has been shown to phosphorylate NF-κB transcription activity, which is the major activator in the regulation of inflammatory responses (Lee and Yang, 2013). Our results demonstrated that activation of NF-κB is necessary for TNF-α-induced ICAM-1 expression in A549 cells and that this activation is similar to results from previous reports (Oh and Kwon, 2009). Our study further demonstrated that the WBGE-decreased ICAM-1 expression in TNF-α-treated A549 cells was mediated through inactivation of NF-κB binding activity. The result was similar to the previous reports. Bitter melon preventive effects against insulin resistance and diabetes are associated with the modulation of NF-κB pathway in high-fat-fed rats (Yang et al., 2015). *Momordica charantia* fruit extract protects cardiomyocytes from TNF-α-induced apoptosis partially through inhibition of the NF-κB pathway (Hu et al., 2016). Wild bitter gourd lyophilized powder significantly inhibited the expression levels of NF-κB, iNOS, and COX-2 in LPS-treated mice (Chao et al., 2014). Furthermore, inducible NF-κB activation is controlled by signals involved in IκB phosphorylation and its dissociation from the inactive cytoplasmic complex, followed by translocation of the active p50/p65 dimer to the nucleus and induced gene expression (Choi et al., 2012). We demonstrated that the WBGE-induced decrease in ICAM-1 expression was mediated through inhibition of IκB phosphorylation and p65 translocation. Together these results suggest that WBGE treatment inactivates TNF-α-induced PI3K/AKT

phosphorylation and NF-κB /IκB pathways as well as subsequently suppresses ICAM-1

expression, which results in decreased binding of leukocytes. Because the inflammation

is involved in many kinds of chronic and acute lung tissues and it is characterized by the

production of proinflammatory cytokines, the enhanced monocyte adhesion as well as

the accompanying inflammatory signal (Lee and Yang, 2013), WBGE may provide a

new natural therapeutic approach for the prevention of inflammation and lung diseases.

MicroRNAs have been reported to play a key role in mediating cellular responses

under various stress conditions in lung diseases (Alipoor et al., 2016). COPD patients

have lower miRNA-222 expression (Ikari et al., 2015). Recent reports indicated that

ICAM-1 expression was controlled by a number of miRNA species, such as miR-221

and miR-222 (Hu et al., 2010; Duan et al., 2013). These miRNAs are complementary to

the ICAM-1 3'UTR region and modulate ICAM-1 expression at the posttranscriptional

level by binding to the untranslated region (Marques-Rocha, 2015). The increased

ICAM-1 expression in human immunodeficiency virus-1 (HIV-1) Tat-treated

endothelial cells was concomitant with a reduction in miR-221/-222 expression (Duan et

al., 2013). IFN-γ suppressed miR-221 and resulted in increased ICAM-1 expression in

cholangiocytes (Hu et al, 2010). Another study demonstrated that the upregulation of

ICAM-1 protein in human intrahepatic biliary epithelial cells following the parasite

infection involves downregulation of miRNA-221 (Gong et al., 2011). Endothelial

microparticles promote an anti-inflammatory effect by reducing endothelial ICAM-1

expression through higher amounts of miR-222 (Jansen et al., 2015). In the present

study, we showed that A549 cells treated with TNF-α or with the TNF-α+WBGE

treatment did not alter the miRNA-221/-222 levels. Interestingly, only WBGE treatment

can increase miRNA-221/-222 levels and decrease endogenous ICAM-1 expression in

A549 cells. Furthermore, the overexpressed miRNA-222 levels significantly reduced

the phosphorylation of PI3K/AKT and IκB /NFκB-p65 as well as the monocyte adhesion. Furthermore, the *in vivo* study demonstrated that TNF-α treatment decreased the miRNA-221/-222 levels and increased the ICAM-1 expression, whereas WBGE pretreatment increased the miRNA-221/-222 levels and attenuated the ICAM-1 expression in lung tissues. In contrast, WBGE treatment showed little effect on ICAM expression in lung tissues of miR-221/-222 KO mice with or without TNF-α treatment. These different results between *in vivo* and *in vitro* studies suggest that the effects of WBGE and miR-221/-222 expression probably did not depend on only one cell type. The result in the *in vivo* study may be due to the component cells of lung tissues, including type I cells, endothelial cell, smooth muscle cells, and macrophages. Further investigations are needed to better understand the role of WBGE plays in the prevention and treatment of inflammatory lung diseases.

In summary, this study provides the first evidence that WBGE reduces ICAM-1 expression under inflammatory conditions both *in vitro* and *in vivo* and decreases leukocyte adhesion to alveolar epithelial cells. We also showed that WBGE inhibited endogenous ICAM-1 expression in A549 cells through blockade of PI3K/AKT/NF-κB/IκB phosphorylation and regulation of miRNA-222 expression. Based on these findings, WBGE should be considered a novel therapeutic agent for targeting epithelial activation in pulmonary inflammation. Taken together, the pleiotropic mechanism against inflammation highlights the usefulness of WBGE as a healthy food.

參考資料

Alipoor, S.D., Adcock, I.M., Garssen, J., Mortaz, E., Varahram, M., Mirsaeidi, M., Velayati, A., 2016. The roles of miRNAs as potential biomarkers in lung diseases. Eur. J. Pharmacol. 791, 395-404.

Bai, L. Y., Chiu, C.F., Chu, P.C., Lin, W.Y., Chiu, S.J., Weng, J.R., 2016. A triterpenoid from wild bitter gourd inhibits breast cancer cells. Sci. Rep. 6, 22419.

Chao, C.Y., Sung, P.J. Wan, W.H., Kuo, Y.H., 2014. Anti-inflammatory effect of momordica charantia in sepsis M\mice. Molecules. 19, 12777-12788.

Chaturvedi, P., 2012. Antidiabetic potentials of momordica charantia: multiple mechanisms behind the effects. J. Med. Food 15, 101-107.

Chen, C.C., Chou, C.Y., Sun, Y.T., Huang, W.C., 2001. Tumor necrosis factor α-induced activation of downstream NF-κB site of the promoter mediates epithelial ICAM-1 expression and monocyte adhesion: Involvement of PKCα, tyrosine kinase, and IKK2, but not MAPKs, pathway. Signal. 13, 543-553.

Choi, K.W., Um, S.H., Kwak, J.H., Park, H.J., Kim, K.H., Moon, E.Y., Kwon, S.T., Pyo, S., 2012. Suppression of adhesion molecule expression by phenanthrene-containing extract of bulbils of Chinese Yam in vascular smooth muscle cells through inhibition of MAPK, Akt and NF-κB. Food Chem. Toxicol. 50:2792–804.

Demir, T., Yalcinoz, C., Keskinel, I., Demiröz, F., Yildirim, N., 2002. sICAM-1 as a serum marker in the diagnosis and follow-up of treatment of pulmonary tuberculosis. Int. J. Tuberc. Lung Dis. 6,155-159.

Desai, S., Tatke, P., 2015. Charantin: An important lead compound from Momordica charantia for the treatment of diabetes. J. Pharmacogn. Phytochem. 3, 163-166.

Dandawate, P.R., Subramaniam, D., Padhye, S.B., Anant, S., 2016. Bitter melon: a

panacea for inflammation and cancer. Chin. J. Nat. Med. 2016, 14, 0081-0100.
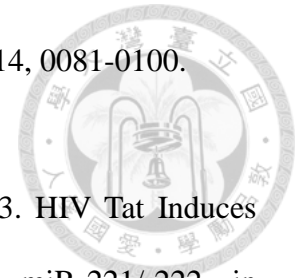
Duan, M., Yao, H., Hu, G., Chen, X., Lund, A.K., Buch, S., 2013. HIV Tat Induces Expression of ICAM-1 in HUVECs: Implications for miR-221/-222 in HIV-Associated Cardiomyopathy. PLoS. One 8, 1-11.

Duirham, A.L., Caramori, G., Chung, K.F., Adcock, I. M., 2015. Targeted anti-inflammatory therapeutica astham and chronic obstructive luing disease. Transl. Res. 67, 192-203.
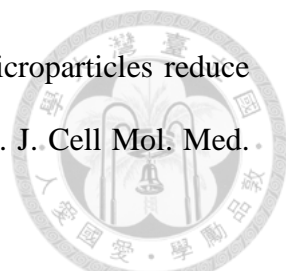
Gong, A.Y., Hu, G., Zhou, R. Liu, J., Feng, Y., Soukup, G.A. , Chen ,X.M., 2011. MicroRNA-221 controls expression of intercellular adhesion molecule-1 in epithelial cells in response to Cryptosporidium parvum infection. Int. J. Parasit. 41, 397-403.

Hu, G., Gong, A. Y., Liu, J., Zhou, R., Deng, C., Chen, X. M., 2010. miR-221 suppresses ICAM-1 translation and regulates interferon-γ-induced ICAM-1 expression in human cholangiocytes. Am. J. Physiol. Gastroint. Liver 298, G542–G550.

Hu, H., Liu, Y., Kong, B., Fan, Y., Wang, Z., Peng, J., Xiong, X., Mei, Y., Liu, W., Huang, H., 2016. Protective effect of momordica charantia fruit extract on TNF α-induced NF-κB activation and cardiomyocyte apoptosis. Int. J. Clin. Exp. Med. 9, 5951-5959.

Ikari, J., Smith, L.M., Nelson, A.J., Iwasawa, S., Gunji, Y., Farid, M., Wang, X., Basma, H., Feghali-Bostwick, C., Liu, X., DeMeo, D.L., Rennard, S. I., 2015. Effect of culture conditions on microRNA expression in primary adult control and COPD lung fibroblasts in vitro. In Vitro Cell Dev. Biol. Anim. 51, 390-399.

Jansen, F., Yang, X., Baumann, K., Przybilla, D, Schmitz, T., Flender, A., Paul, K.,

Alhusseiny, A., Nickenig, G., Werner, N., 2015. Endothelial microparticles reduce ICAM-1 expression in a microRNA-222-dependent mechanism. J. Cell Mol. Med. 19, 2202-2214.

Lee, I.T., Lin, C.C., Lee, C.Y., Hsieh, P.W., Yang, C.M., 2013. Pertective effects of (一)-epigallocatechin-3-gallate against TNF-α-induced lung inflammation via ROS-dependent ICAM-1 inhibition. J. Nutr. Biochem. 24, 124-36.

Lee, I.T., Yang, C.M., 2013. Inflammatory signalings involved in airway and pulmonary disease. Mediat. Inflamm. 791231.

Lii, C.K., Chen, H.W., Yun, W.T., Liu, K.L., 2009. Suppressive effects of wild bitter gourd (Momordica charantia Linn. var. abbreviate ser.) fruit extracts on inflammatory responses in RAW264.7 macrophages. J. Ethnopharmacol. 122, 227-233.

Lu, K.H., Tseng, H.C., Liu, C.T., Huang, C.J., Chyuan, J.H., Sheen, L.Y., 2014. Wild bitter gourd protects against alchoholic fatty liver in mice by attenuating oxidative stress and inflammatory responses. Food Funct. 5, 10271037.

Marques-Rocha, JL, Samblas, M, Milagro, FI, Bressan, J, Martínez, JA, Marti, A. Noncoding RNAs, cytokine, and inflammation-related diseases. F.A.S.E.B. J. 2015;29:3595-611.

Oh, J.H., Kwon, T.K., 2009. Withaferin A inhibits tumor necrosis factor-α-induced expression of cell adhesion molecules by inactivation of Akt and NF-κB in human pulmonary epithelial cells. Int. Immunopharmacol. 9, 614–619.

Patel, S., Patel, T., Parmar, K., Bhatt, Y., Patel, Y, Patel, N.M., 2010. Isolation, characterization and antimicrobial activity of charantin from momordica charantialinn. Fruit. Int. J. Drug Dev. & Res. 2, 629-634.

Rahman, A., Anwar, K.N., True, A.L., Malik, A.B.. 1999. Thrombin-induced p65

homodimer binding to downstream NF-κB site of the promoter mediates endothelial ICAM-1 expression and neutrophil adhesion. J. Immunol. 162:5466-76.
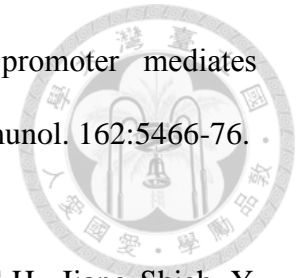
Sung, H.C., Liang, C.J., Lee, C.W., Yen, F.L., Hsiao, C.Y., Wang, S.H., Jiang-Shieh, Y. F., Tsai, J. S., Chen, Y.L., 2015. The protective effect of eupafolin against TNF-α-induced lung inflammation via the reduction of intercellular cell adhesion molecule-1 expression. J. Ethnopharmacol. 170, 136–147.

Somasagara, R.R., Deep, G., Shrotriya, S., Patel, M., Agarwal, C., Agarwal, R., 2015. Bitter melon juice targets molecular mechanisms underlying gemcitabine resistance in pancreatic cancer cells. Int. J. Oncol. 46: 1849-1857.

Upadhyay, A., Agrahari, P., Singh, D.K., 2015. A Review on Salient Pharmacological Features of Momordica charantia. Int. J. Pharmacol. 11, 405-413.

Wu, W.H., Lin, B.Y., Kuo, Y.H., Huang, C.J., 2009. Triglycerides constituted of short and medium chain fatty acids and dicarboxylic acids in Momordica charantia, as well as capric acid, inhibit PGE2 production in RAW264.7. macrophages. Food Chem. 117, 306-311.

Yang, S.J., Choi, J. M., Park, S.E., Rhee, E.J., Lee, W.Y., Oh, K.W., Park, S.W., Park, C.Y., 2015. Preventive effects of bitter melon (Momordica charantia) against insulin resistance and diabetes are associated with the inhibition of NF-κB and JNK pathways in high-fat-fed OLETF rats. The Journal of Nutritional Biochemistry. 26,234–240.
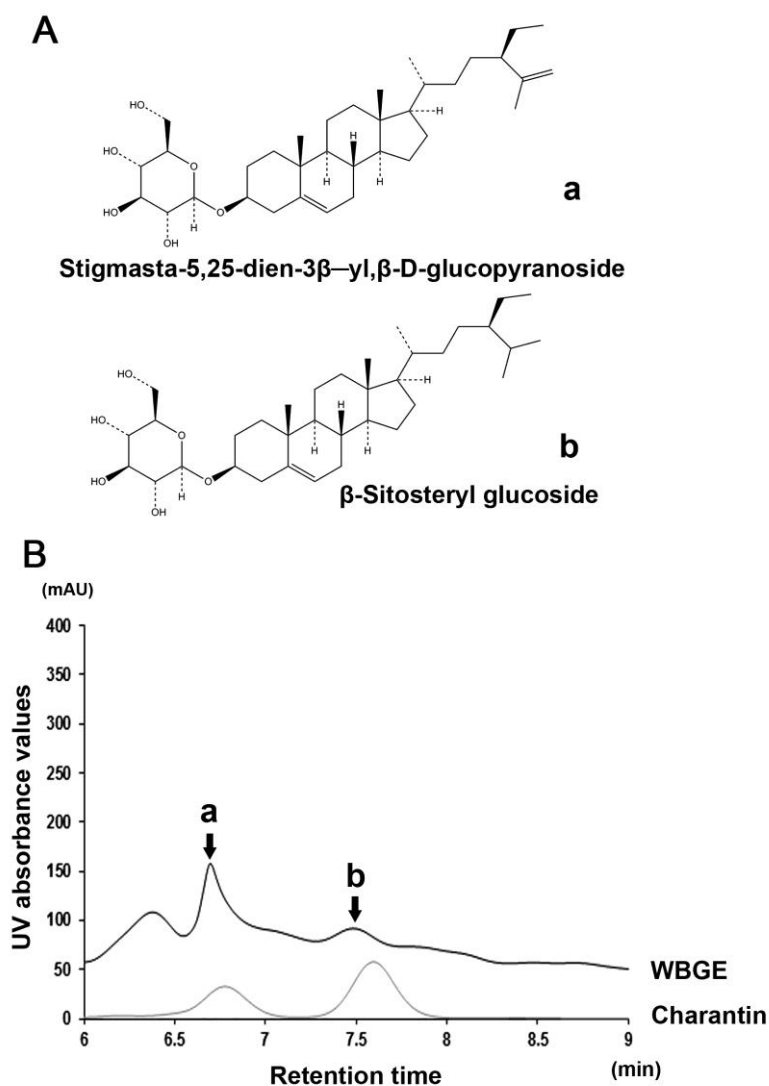
Figure 1

Figure 1: Characterization of WBGE

(A) The chemical structure of charantin contains

Stigmasta-5,25-dien-3β-yl,β-D-glucopyranoside and β-Sitosteryl glucoside. (B) HPLC

chromatogram of WBGE and charantin. The vertical and horizontal axes represent the

intensity of the UV absorbance values (mAU) and the retention time (min),
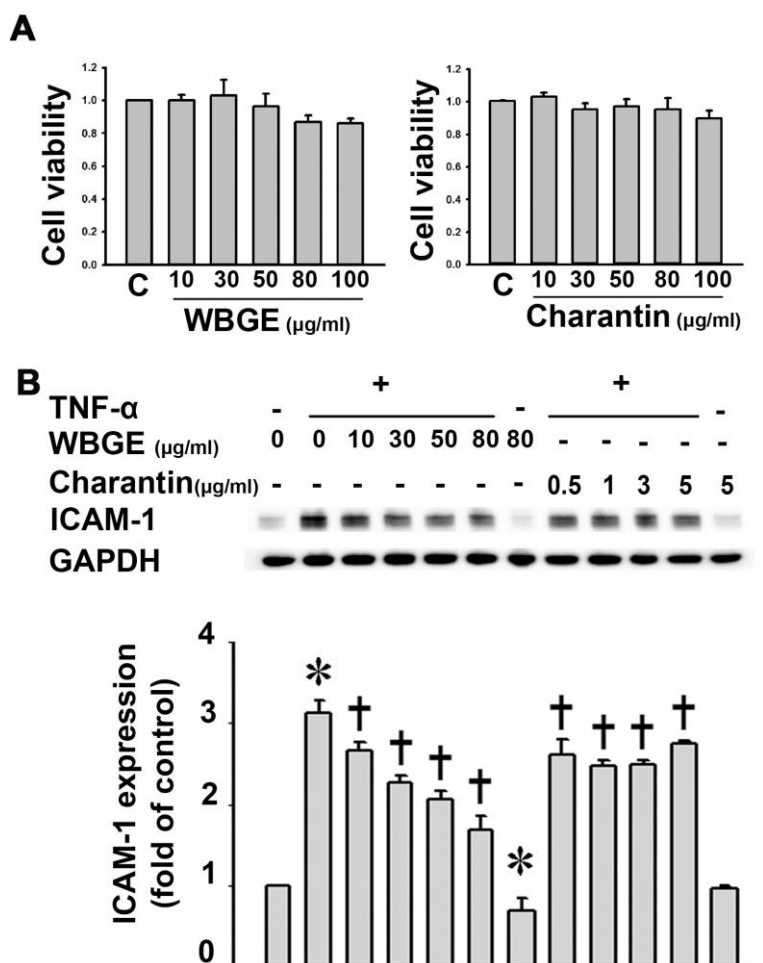
respectively.

Figure 2

Figure 2: The effects of WBGE and charantin on ICAM-1 expression in TNF-α-treated A549 cells

(A) The effects of WBGE and charantin on cell viability were examined by MTT assay.

(B) A549 cells were incubated with the indicated concentration of WBGE (10-80μg/mL) or charantin (0.5-5 μg/mL) for 24 h and then with 3 ng/mL TNF-α for 4 h. The ICAM-1 protein expression levels were measured by Western blot. GAPDH was used as the loading control. The data are expressed as a fold value compared to the control value and are the means ± SEM for five separate experiments. $*P < 0.05$ compared to the untreated cells. $^{†}P < 0.05$ compared to the TNF-α-treated cells.
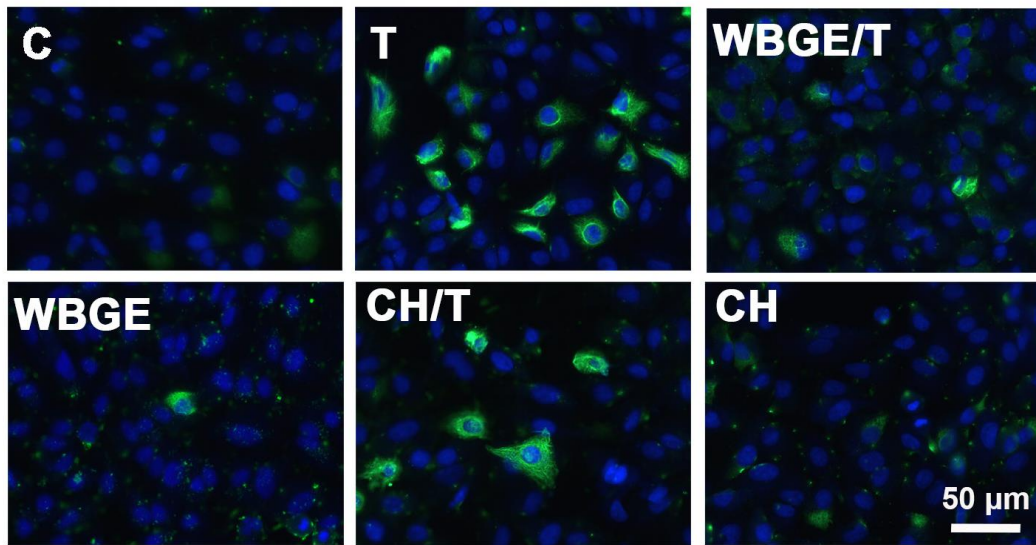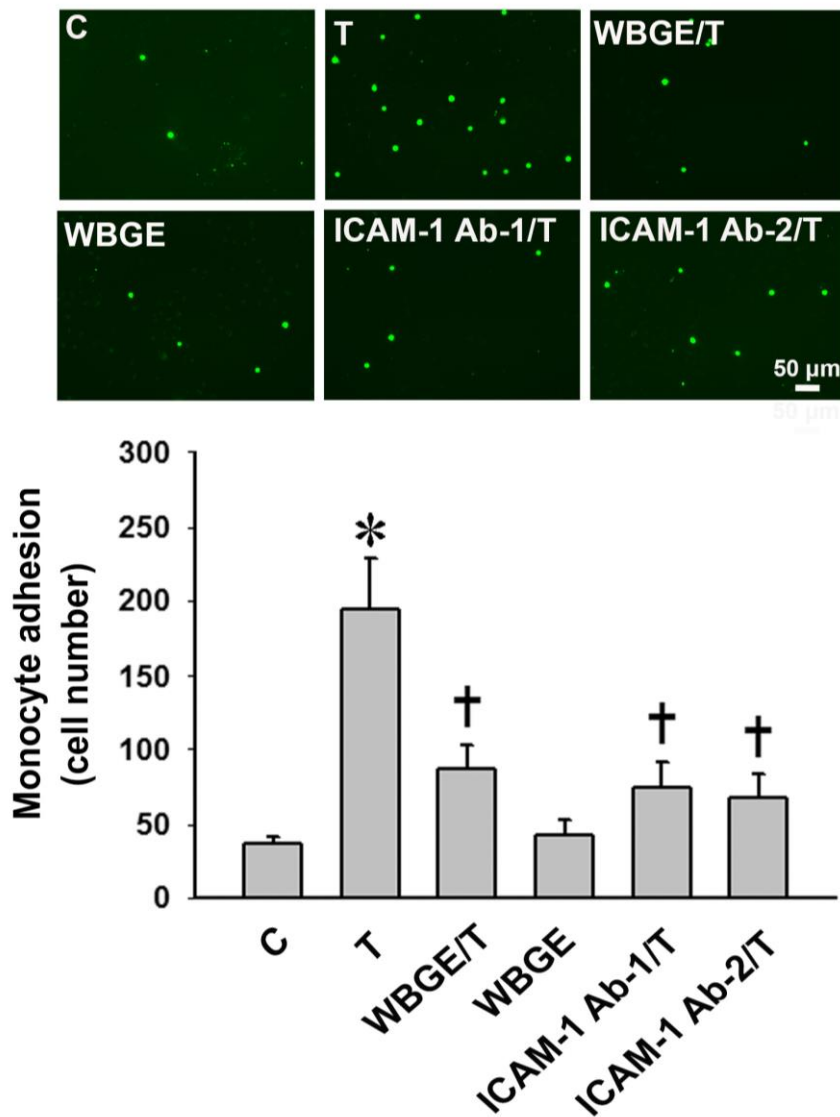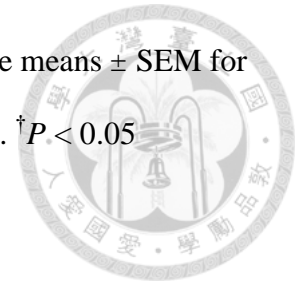
Figure 3

Figure 3: The effects of WBGE and charantin on ICAM-1 expression patterns in A549 cells

A549 cells were incubated for 24 h with or without WBGE (80 μg/mL) or charantin (CH, 5 μg/mL) and then were incubated with or without TNF-α (T). ICAM-1 expression was examined by immunofluorescence staining. The nuclei were stained with DAPI. C: control ; T: treated with TNF-α alone; WBGE/T: pretreated with WBGE and then stimulated with TNF-α; WBGE: treated with WBGE alone; CH/T: pretreated with charantin and then stimulated with TNF-α; CH: treated with charantin alone.Bar = 50 μm.
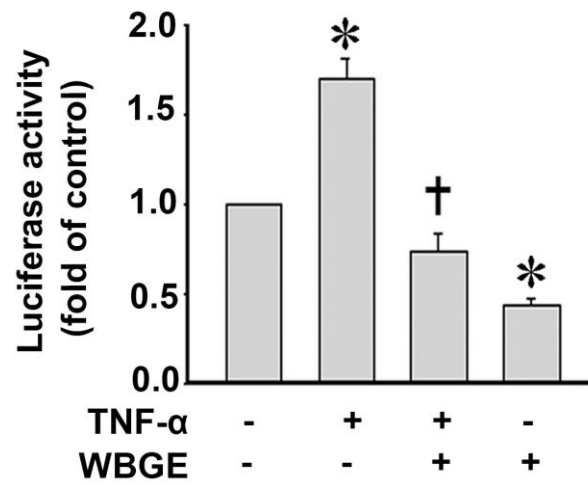
Figure 4

Figure 4: The effects of WBGE on ICAM-1 promoter activity in A549 cells.

A549 cells were transfected with the ICAM-1 promoter plasmid for 44h and then with 3 ng/mL TNF-α for 4 h. ICAM-1 promoter activity was examined by Luciferase assay. The data are expressed as a fold value compared to the control value and are the means ± SEM for five separate experiments. *$P < 0.05$ compared to the untreated cells. [†]$P < 0.05$ compared to the TNF-α-treated cells.
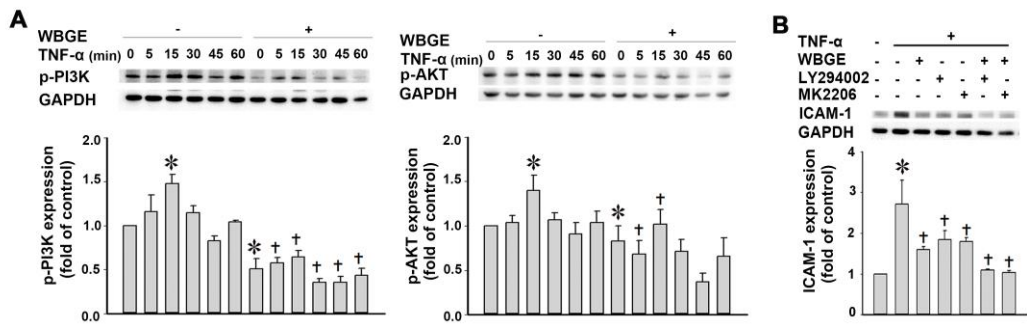
Figure 5

Figure 5: The effects of WBGE on the adhesion of U937 cells to TNF-α-treated A549 cells

A549 cells were left untreated or pretreated for 24 h with WBGE (80 μg/mL) or anti-ICAM-1 antibodies (1 or 2 μg/mL) for 1 h, and then incubated with 3 ng/mL TNF-α for 4 h. BCECF-AM-labeled U937 cells were added to A549 cells and incubated at 37℃ for 45 min. The adherent cells were photographed with a fluorescent microscope. Bar = 50 μm. The number of U937 cells bound per high power field in six

randomly selected images was counted. The data are expressed as the means $\pm$ SEM for five separate experiments. $*P < 0.05$ compared to the untreated cells. $^{\dagger}P < 0.05$ compared to the TNF-α-treated cells.
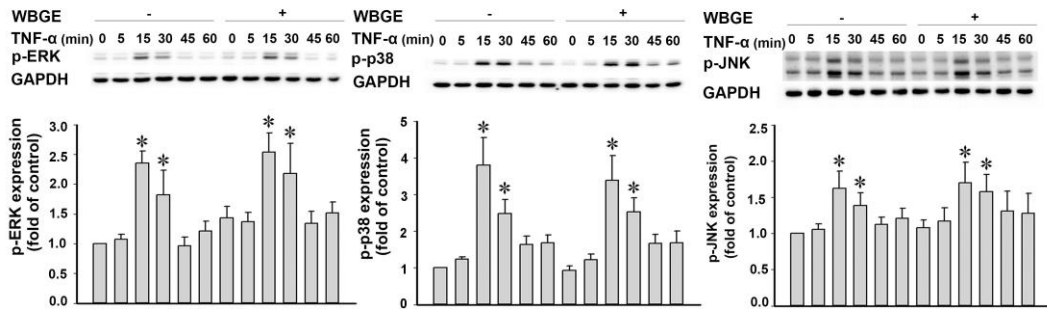
Figure 6

Figure 6: The effects of WBGE on MAPKs phosphorylation in TNF-α-treated A549 cells.

A549 cells were incubated for 24 h with or without 80 μg/mL WBGE, and then incubated with 3 ng/mL of TNF-α for the indicated time. GAPDH was used as the loading control. The data are expressed as a fold value compared to the control value and are the means ± SEM for five separate experiments. $*P < 0.05$ compared to the untreated cells.
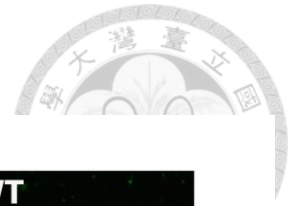
Figure 7

Figure 7: The effects of PI3K/AKT phosphorylation on WBGE-reduced ICAM-1 expression in TNF-α-treated A549 cells

(A) A549 cells were incubated for 24 h with or without 80 μg/mL WBGE, and then incubated with 3 ng/mL of TNF-α for the indicated time. (B) These cells were left untreated or treated with WBGE for 24 h, preincubated with 50 μM LY294002 (a PI3K inhibitor) or 30 μM MK2206 (an AKT inhibitor) for additional 1 h, and then stimulated with TNF-α. ICAM-1 expression was analyzed by Western blot. GAPDH was used as the loading control. The data are expressed as a fold value compared to the control value and are the means ± SEM for five separate experiments. *$P < 0.05$ compared to the untreated cells. [†]$P < 0.05$ compared to the TNF-α-treated cells.
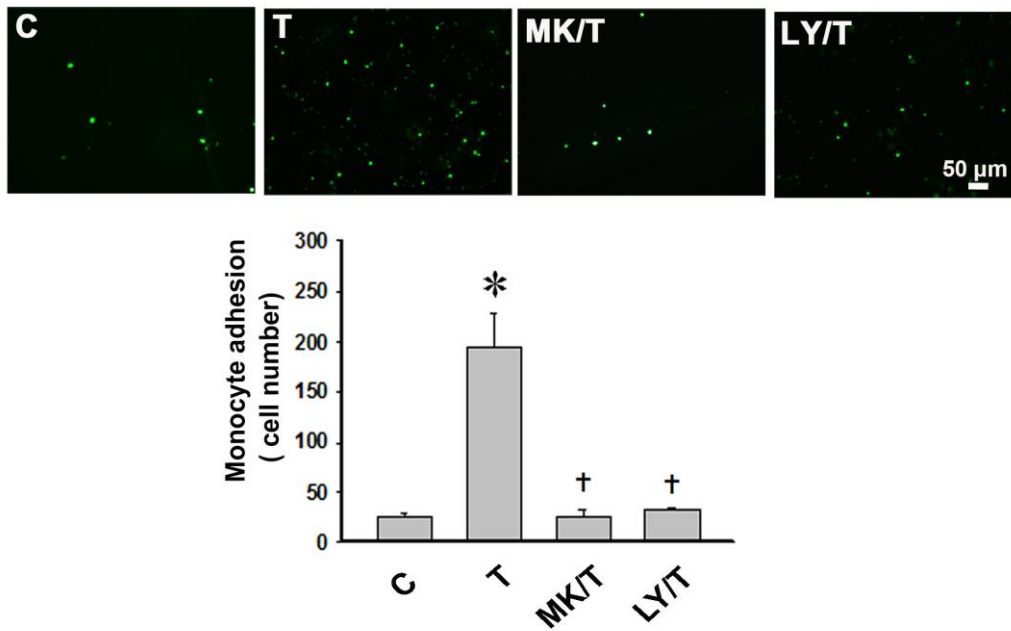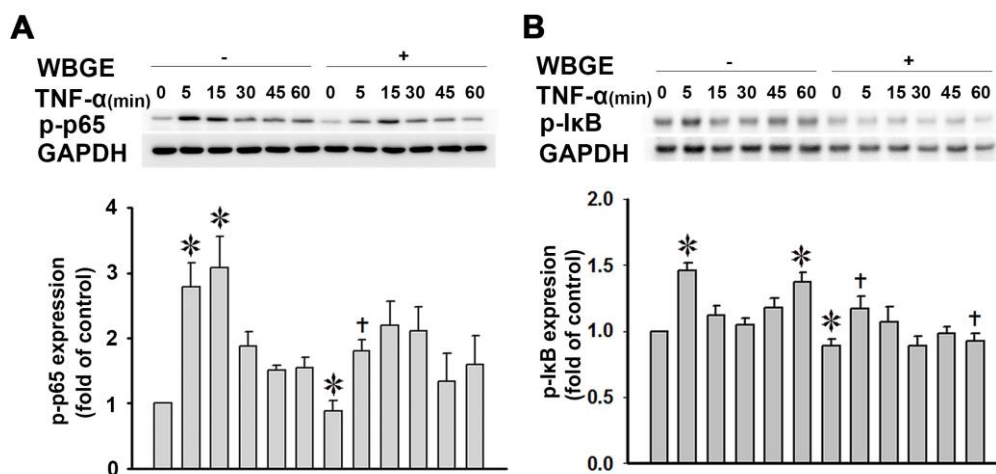
Figure 8

Figure 8: The effects of PI3K/AKT on the adhesion of U937 cells to TNF-α-treated A549 cells

Cells were left untreated or were pretreated for 1 h with MK (an AKT inhibitor) or LY (a PI3K inhibitor), and then treated with TNF-α (3 ng/mL) in the continued presence of the inhibitor. BCECF-AM-labeled U937 cells were added to A549 cells and incubated at 37℃ for 45 min. The adherent cells were photographed with a fluorescent microscope. Bar = 50 μm. The number of U937 cells bound per high power field in six randomly selected images was counted. The data are expressed as the means ± SEM for five separate experiments. *$P < 0.05$ compared to the untreated cells. $^{\dagger}P < 0.05$ compared to the TNF-α-treated cells.
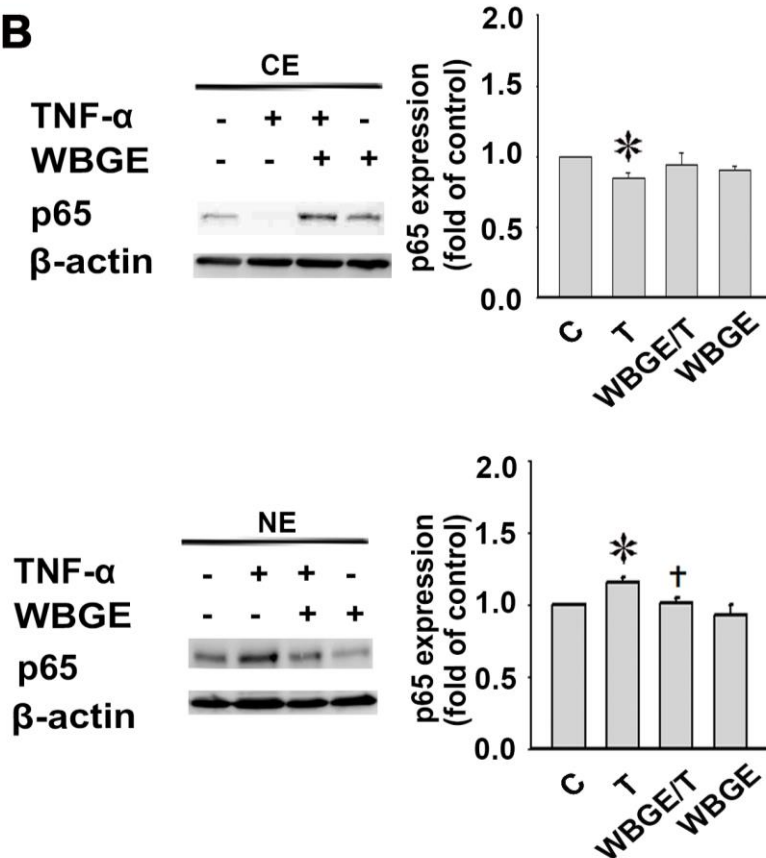
Figure 9

Figure 9: The effects of WBGE on NF-κB and IκB phosphorylation in TNF-α-treated A549 cells.

A549 cells were preincubated with WBGE (80 μg/mL) and then treated with TNF-α (3 ng/mL) for the indicated time. GAPDH was used as the loading control. The data are expressed as a fold value compared to the control value and are the means ± SEM for five separate experiments. $*P < 0.05$ compared to the untreated cells. $^{\dagger}P < 0.05$ compared to the TNF-α-treated cells.
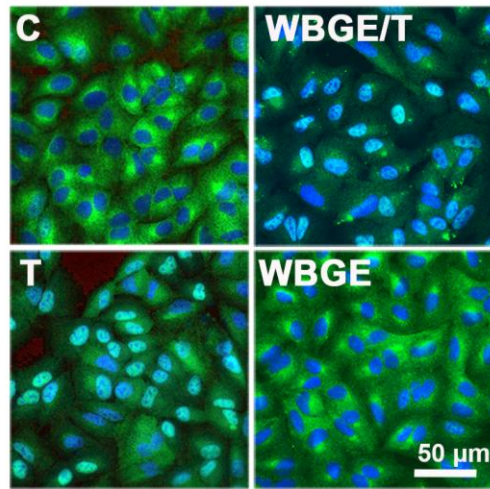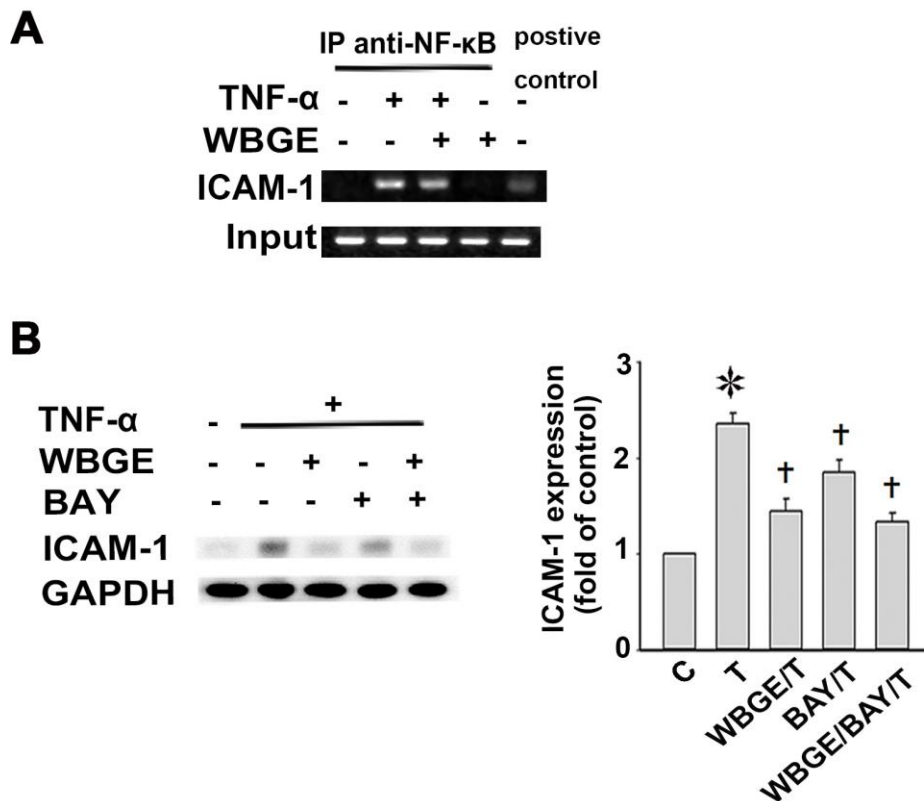
Figure 10

Figure 10: The effects of WBGE on NF-κB activation in TNF-α-treated A549 cells

(A) Immunofluorescence staining for NF-κB p65. The nuclei were stained with DAPI.

C: control ; T: treated with TNF-α alone; WBGE/T: pretreated with WBGE and then

stimulated with TNF-α; WBGE: treated with WBGE alone. Bar = 50 μm. (B) Western

blot for NF-κB p65 expression in cytoplasmic and nuclear extracts. The data are

expressed as a fold value compared to the control value and are the means ± SEM for

five separate experiments. *$P < 0.05$ compared to the untreated cells. †$P < 0.05$

compared to the TNF-α-treated cells.

Figure 11

Figure 11: The effects of NF-κB on WBGE-reduced ICAM-1 expression in TNF-α-treated A549 cells

(A) The association of NFκB p65 with the NFκB binding region of the ICAM-1 promoter was examined by the CHIP-PCR analysis. (B) These cells were left untreated or treated with WBGE for 24 h, preincubated with 30μM Bay117082 (a NF-κB inhibitor) for additional 1 h, and then stimulated with TNF-α. ICAM-1 expression was analyzed by Western blot. The data are expressed as a fold value compared to the control value and are the means ± SEM for five separate experiments. *$P < 0.05$ compared to the untreated cells. †$P < 0.05$ compared to the TNF-α-treated cells.
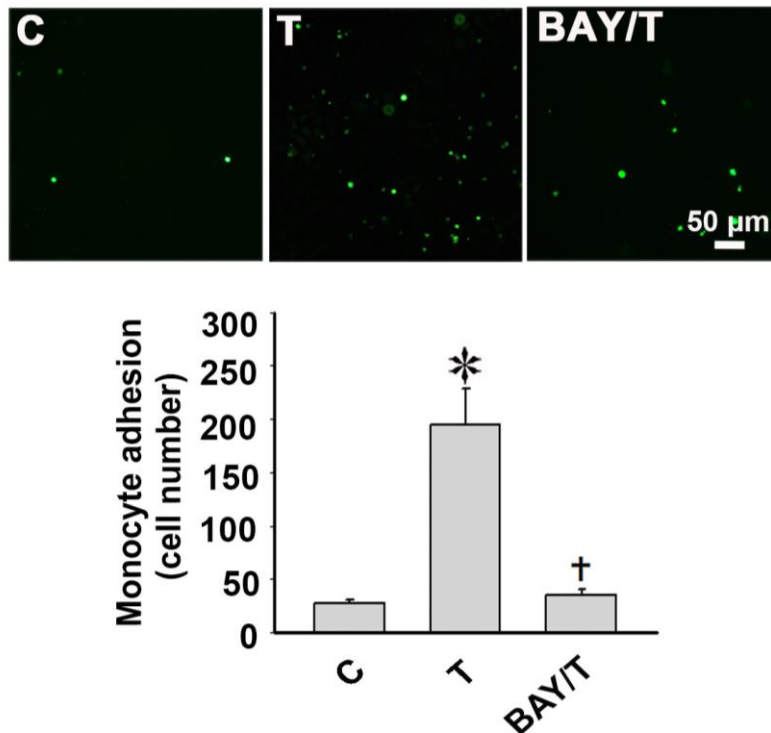
Figure 12

Figure 12: The effects of NF-κB on the adhesion of U937 cells to TNF-α-treated A549 cells

Cells were left untreated or were pretreated for 1 h with Bay117082 (a NF-κB inhibitor), and then treated with TNF-α (3 ng/mL) in the continued presence of the inhibitor. BCECF-AM-labeled U937 cells were added to A549 cells and incubated at 37℃ for 45 min. The adherent cells w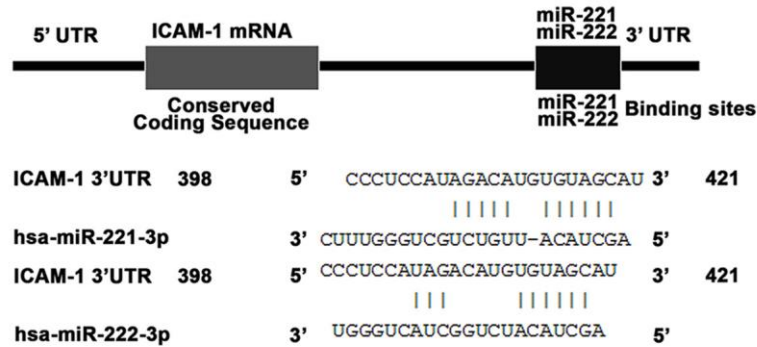ere photographed with a fluorescent microscope. Bar = 50 μm. The number of U937 cells bound per high power field in six randomly selected images was counted. The data are expressed as the means ± SEM for five separate experiments. $*P < 0.05$ compared to the untreated cells. $^{†}P < 0.05$ compared to the TNF-α-treated cells.
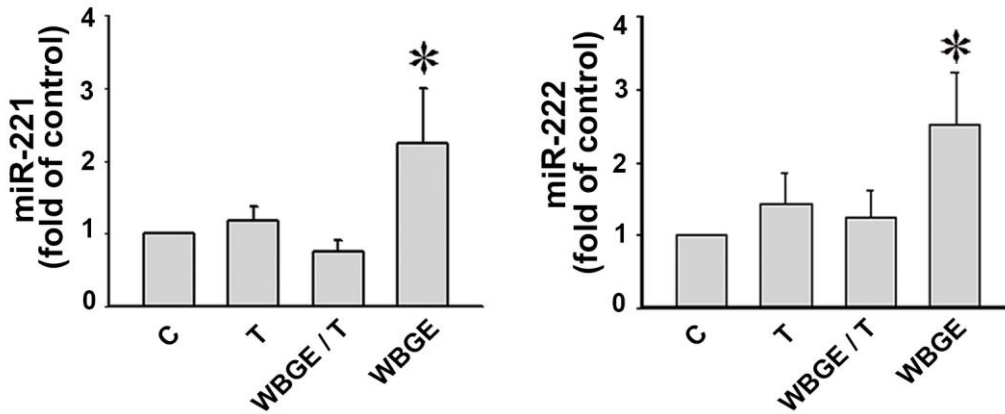
Figure 13

Figure 13: The levels of miRNA-221 and -222 expression in TNF-α-treated A549 cells

(A) The bioinformatics analysis of the potential target sites in the ICAM-1 3' untranslated region (UTR) for miR-221 or miR-222. (B) The levels of miRNA-221 and -222 expression were analyzed by real time-PCR. RUN6B (U6) was used as the control. The data are expressed as a fold value compared to the control value and are the means ± SEM for five separate experiments. *$P < 0.05$ compared to the untreated cells.
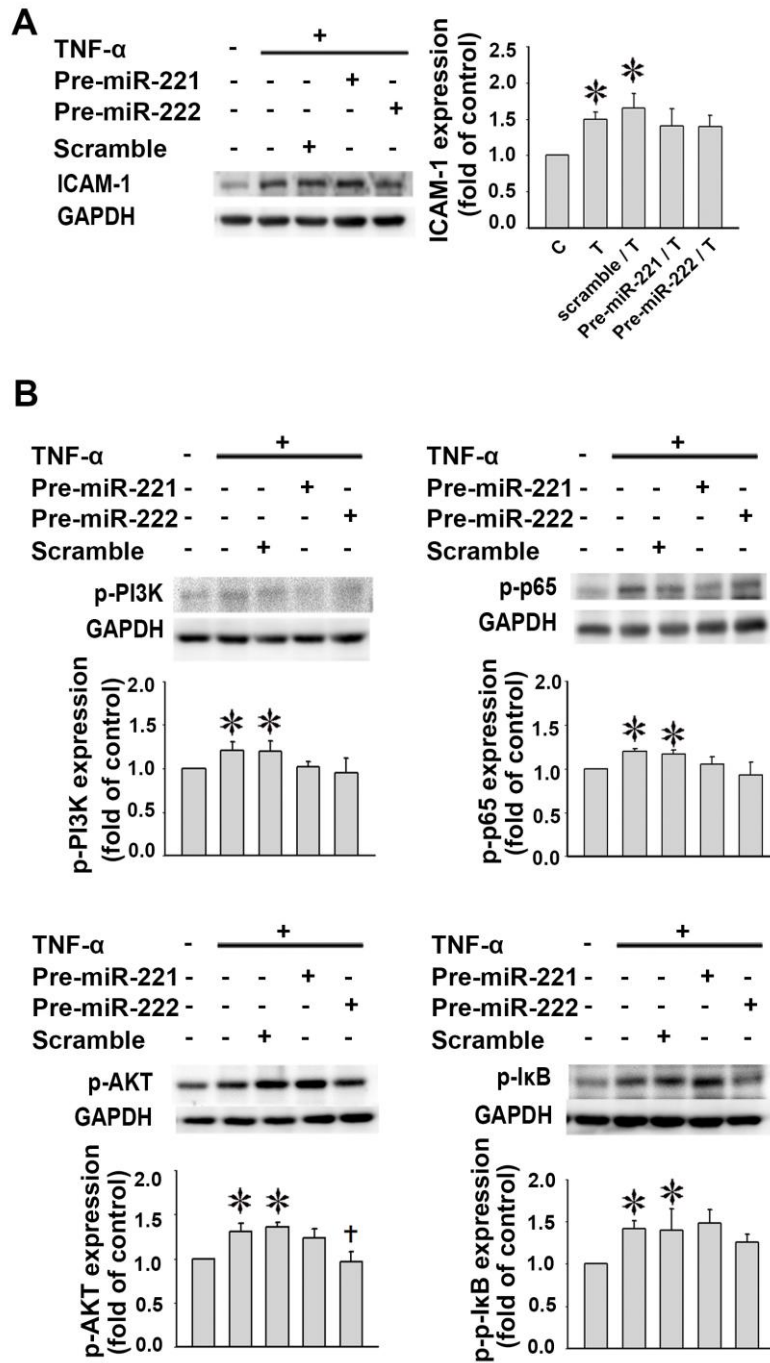
Figure 14

Figure 14: The effects of pre-miRNA-221/-222 on the TNF-α-treated A549 cells.

A549 cells were transfected with miR-221 or miR-222 precursors and then exposed to

TNF-α (3ng/mL), followed by Western blot analysis for ICAM-1, p-AKT, p-PI3K,

p-p65, and p-IκB expression. GAPDH was used as the loading control. The data are

doi:10.6342/NTU201701930

expressed as a fold value compared to the control value and are the means ± SEM for five separate experiments. *$P < 0.05$ compared to the untreated cells. †$P < 0.05$ compared to the TNF-α-treated cells.
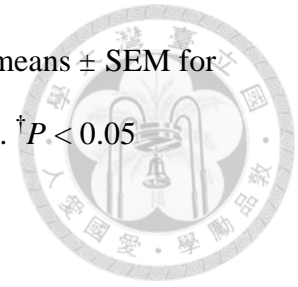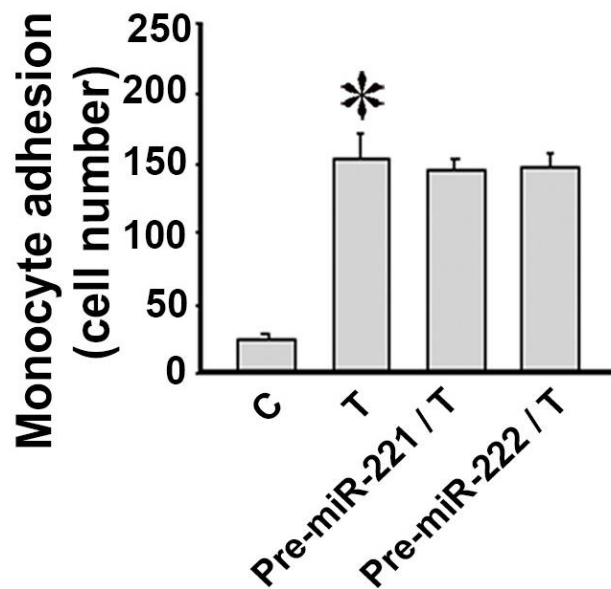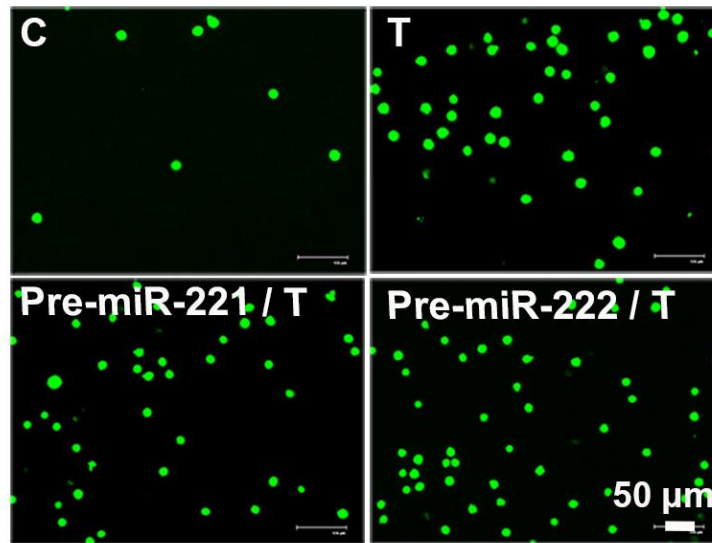
Figure 15

Figure 15: The effects of pre-miRNA-221/-222 on the adhesion of U937 cells to the TNF-α-treated A549 cells

A549 cells were transfected with miR-221 or miR-222 precursors for 44 h, and then incubated with 3 ng/mL TNF-α for 4 h. BCECF-AM-labeled U937 cells were added to A549 cells and incubated at 37℃ for 45 min. The adherent cells were photographed with a fluorescent microscope. Bar = 50 μm. The number of U937 cells bound per high

power field in six randomly selected images was counted. The data are expressed as the

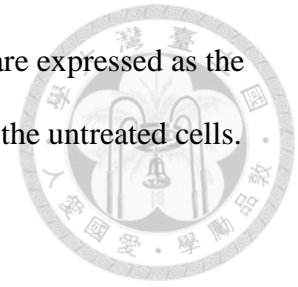means ± SEM for five separate experiments. *$P < 0.05$ compared to the untreated cells.
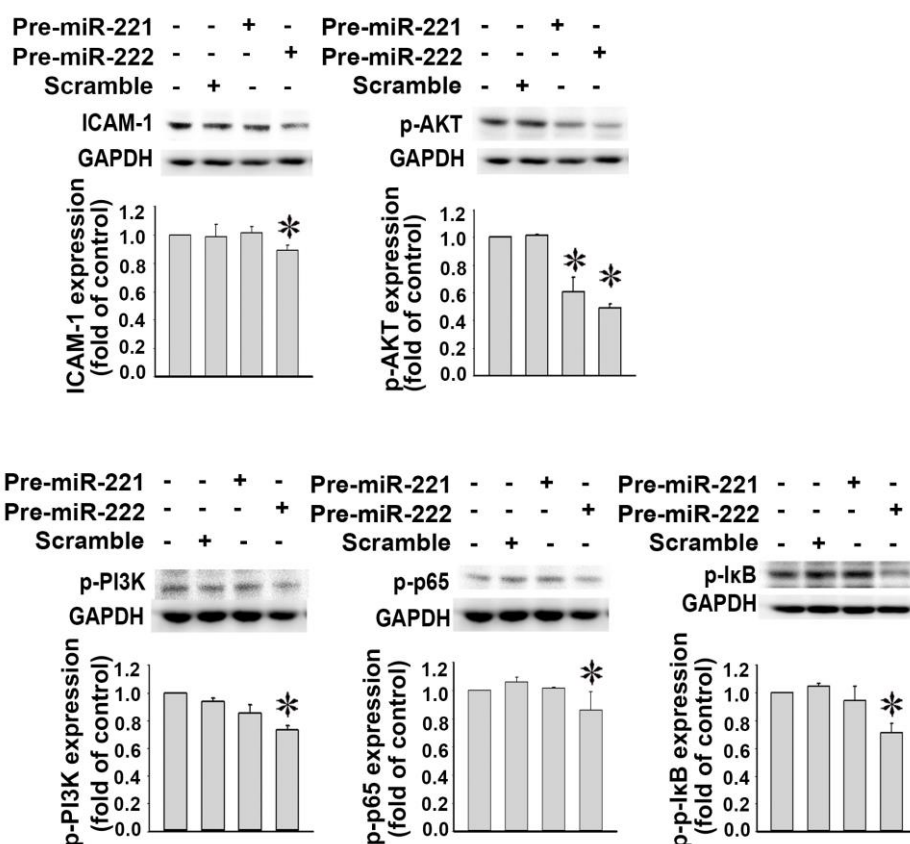
Figure 16

Figure 16: The effects of pre-miRNA-221/-222 on the A549 cells

A549 cells were transfected with miR-221 or miR-222 precursors followed by Western blot analysis for ICAM-1, p-AKT, p-PI3K, p-p65, and p-IκB expression. GAPDH was used as the loading control. The data are expressed as a fold value compared to the control value and are the means ± SEM for five separate experiments. *$P < 0.05$ compared to the untreated cells.
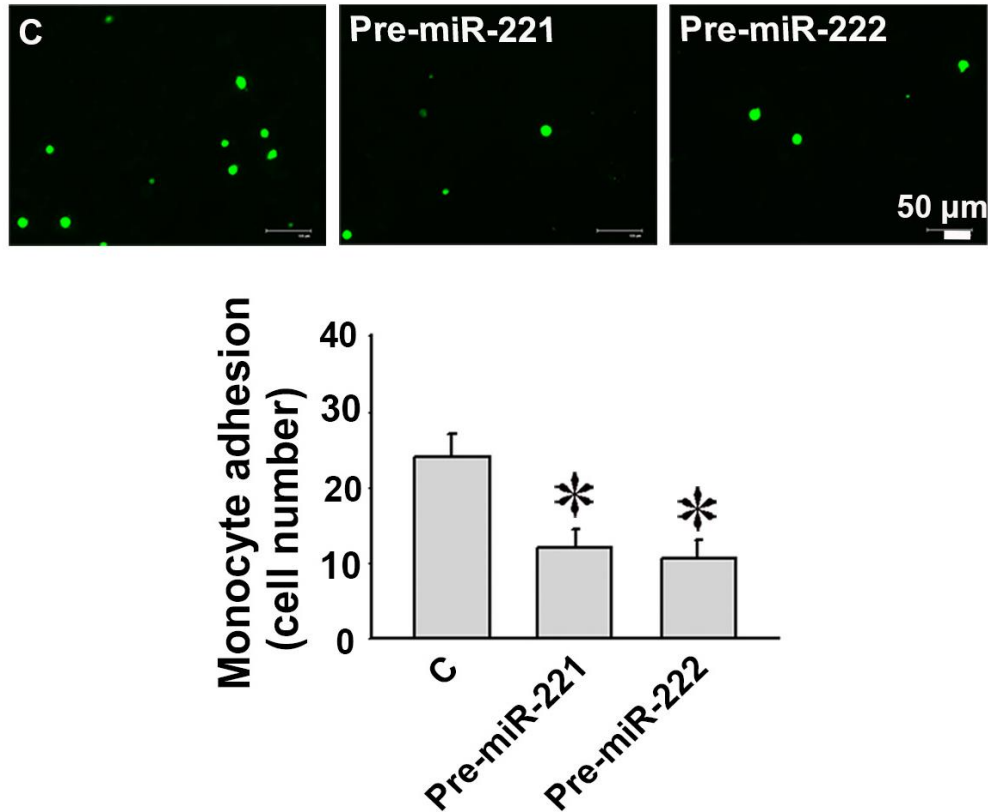
Figure 17

Figure 17: The effects of pre-miRNA-221/-222 on the adhesion of U937 cells to the A549 cells

A549 cells were transfected with miR-221 or miR-222 precursors for 48 h. BCECF-AM-labeled U937 cells were added to A549 cells and incubated at 37℃ for 45 min. The adherent cells were photographed with a fluorescent microscope. Bar = 50 μm. The number of U937 cells bound per high power field in six randomly selected images was counted. The data are expressed as the means ± SEM for five separate experiments. *$P < 0.05$ compared to the untreated cells.
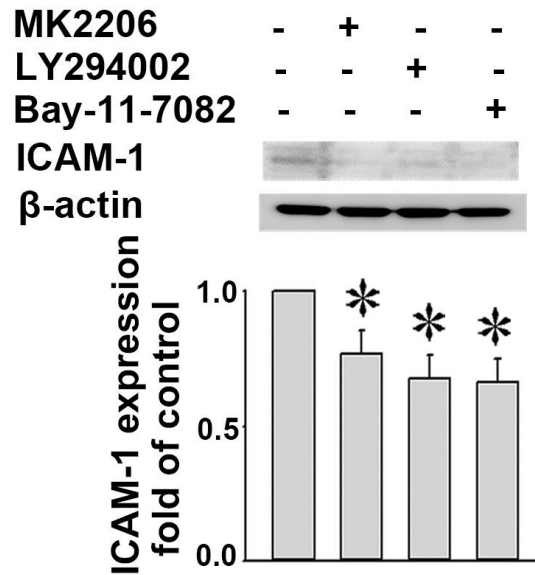
Figure 18

Figure 18: The effects of p-AKT, p-PI3K, p-p65 on endogenous expression of ICAM-1 in A549 cells

A549cells were pretreated with LY294002 (PI3K inhibitor), MK2206 (AKT inhibitor), or BAY (NF-κB inhibitor) for 1 h. ICAM-1 expression levels were determined by Western blot. *$P < 0.05$ compared to the untreated cells.
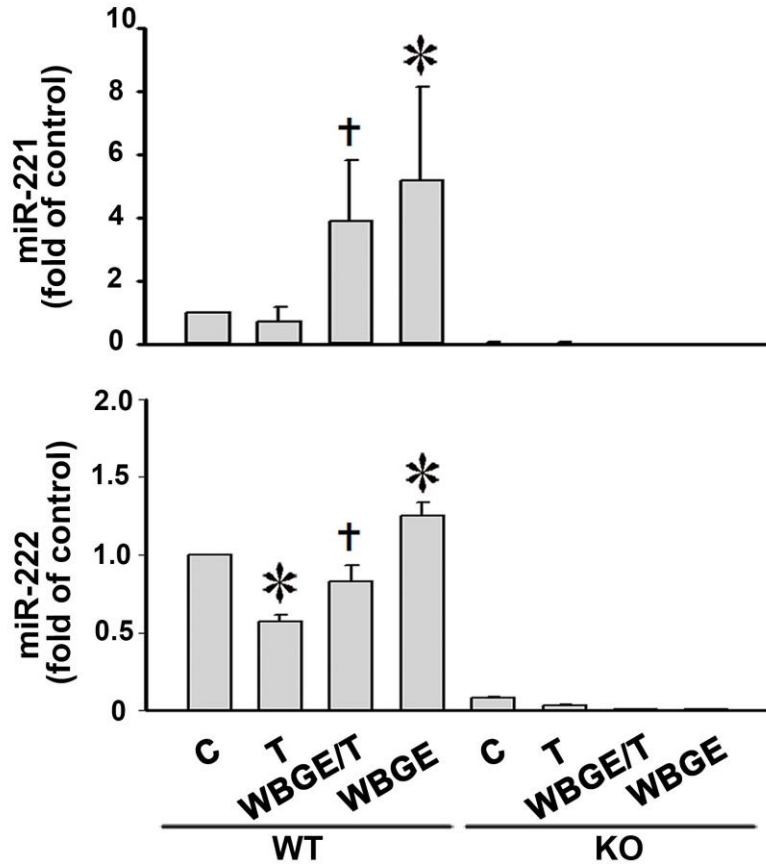
Figure 19

Figure 19: The effects of WBGE on the TNF-α-induced miRNA-221/-222 expression in lung tissues

The levels of miRNA-221/-222 expression were examined in lung tissues of WT mice and miR-221/-222 KO mice by RT-PCR. C: control mice; T: treated with TNF-α alone; WBGE/T: pretreated with WBGE and then stimulated with TNF-α; WBGE: treated with WBGE alone. The data are expressed as a fold value compared to the control value and are the means ± SEM for five separate experiments. $*P < 0.05$ compared to the untreated mice. $^{†}P < 0.05$ compared to the TNF-α-treated mice.
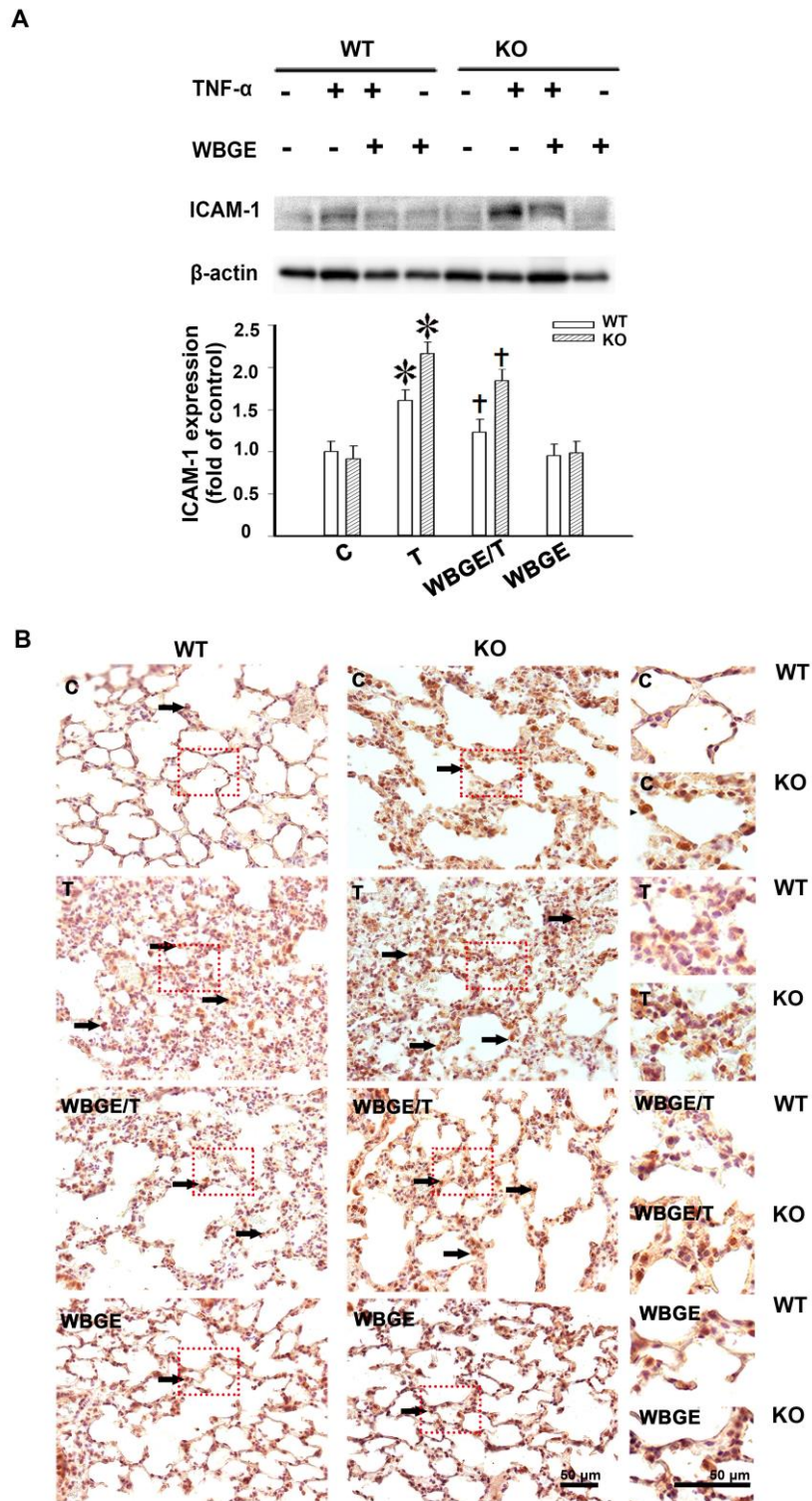
Figure 20

Figure 20: The effects of WBGE on the TNF-α-induced ICAM-1 expression in lung tissues
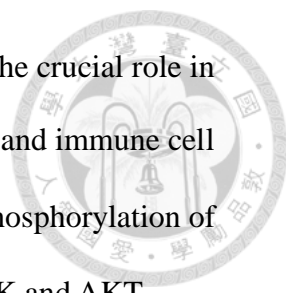
The levels of ICAM- 1 expression in lung tissues of WT mice and miR-221/-222 KO mice were examined by Western blot (A) and immunohistochemical staining (B). The reaction product is indicated by arrowheads. The boxed regions are enlarged and shown to the right line. C: control mice; T: treated with TNF-α alone; WBGE/T: pretreated with WBGE and then stimulated with TNF-α; WBGE: treated with WBGE alone. Bar= 50 μm. Values are means ±SEMs. $*P < 0.05$ compared to the untreated mice. $^{\dagger}P < 0.05$ compared to the TNF-α-treated mice.

結論

In the present study, our results showed that eupafolin and WBGE significantly reduced ICAM-1 expression and U937 adhesion onto TNF-α-treated A549 cells *in vitro*. The influence of eupafolin was partly mediated through the inhibition of AKT/ERK1/2/JNK phosphorylation and NF-κB activation. In addition, the influence of WBGE was partially mediated through inhibition of the phosphorylation of PI3K/AKT/NF-κB/IκB. Moreover, the effects of WBGE decreased phosphorylation of PI3K/AKT/p65/IκB were mediated through upregulation of miR-222 expression. Furthermore, eupafolin and WBGE attenuated ICAM-1 expression in lung tissues of TNF-α-treated mice *in vivo*. On the other hand, WBGE attenuated ICAM-1 expression and upregulated miR-221/-222 expression in the lung tissues of mice with or without TNF-α treatment but not in miR-221/-222 KO mice. Therefore, the protection of lung cells by WBGE was due to the inhibition of PI3K/AKT/p65/IκB and ICAM-1 by miR-221/-222.

MAPK pathways, such as phosphorylation of ERK, JNK, and p38 play the important role in the expressions of proinflammatory mediators (Lee et al., 2013). The present study demonstrated that TNF-α-induced activation of three MAPK subtypes in human alveolar epithelial A549 cells, as reported in previous studies (Lee et al., 2013; Jang et al., 2012; Oh and Kwon, 2009). Our results showed that eupafolin decreased TNF-α-induced ERK, JNK and p38 phosphorylation. The increase in ICAM-1 expression induced by TNF-α was markedly suppressed in the presence of an ERK inhibitor or a JNK inhibitor, but not a p38 inhibitor. However, WBGE had no effects on TNF-α-induced MAPK phosphorylation. These indicated that eupafolin and WBGE had different signaling pathway to attenuate the ICAM-1 expression.
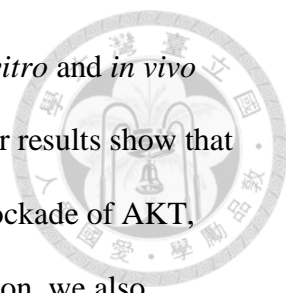
PI3K and AKT pathway have been implicated that they played the crucial role in activation of inflammatory mediators, inflammatory cell recruitment and immune cell function (Koyasu et al., 2003). We found that TNF-α activated the phosphorylation of PI3K and AKT. In addition, eupafolin decreased TNF-α-induced PI3K and AKT phosphorylation. However, eupafolin seems to have a more pronounced effect on AKT phosphorylation and subsequently reduced ICAM-1 expression. In addition, our results showed that WBGE significantly decreased TNF-α-induced PI3K and AKT phosphorylation. Thus, one of the mechanisms through which eupafolin and WBGE reduced TNF-α-induced ICAM-1 expression involves a reduction in PI3K/AKT activation.

The transcription factor NF-κB was served as the major activator in the regulation of inflammatory responses (Karin et al., 2002). Our results demonstrated that eupafolin and WBGE decreased ICAM-1 expression in TNF-α-treated A549 cells was mediated through inactivation of NF-κB binding activity. Moreover, the ICAM-1 expression was mediated through inhibition of IκB phosphorylation and NF-κB translocation.

We further investigate the effects of miRNA-221/-222. MicroRNAs have been reported to play a key role in mediating cellular responses under various stress conditions in lung diseases (Alipoor et al., 2016). We showed that overexpressed miRNA-222 levels significantly reduced the phosphorylation of PI3K/AKT and IκB /NFκB as well as the monocyte adhesion. Furthermore, the *in vivo* study demonstrated that WBGE pretreatment increased the miRNA-221/-222 levels and attenuated the ICAM-1 expression in lung tissues with or without TNF-α treatment. But WBGE had little effect on ICAM expression in lung tissues of miR-221/-222 KO mice with or without TNF-α treatment.

In summary, this study provides the first evidence that eupafolin and WBGE

reduces ICAM-1 expression under inflammatory conditions both *in vitro* and *in vivo* and also decreases leukocyte adhesion to alveolar epithelial cells. Our results show that the eupafolin inhibited ICAM-1 expression in A549 cells through blockade of AKT, ERK1/2, JNK, and NF-κB phosphorylation (Part I, Fig. 15). In addition, we also showed that the WBGE inhibited the endogenous ICAM-1 expression in A549 cells through blockade of PI3K/AKT/NF-κB/IκB phosphorylation and regulation of miRNA-222 expression. Both of eupafolin and WBGE exert the anti-inflammatory effect on pulmonary epithelial cells in the present study. Based on these findings, eupafolin and WBGE should be considered as a novel therapeutic agent targeting epithelial activation in pulmonary inflammation.

未來展望

In the future work, the research is designed to investigate whether the effects of eupafolin and WBGE on the expression of other inflammatory target protein such as IL-1β, MMP-9, COX-2. In addition, the research will be focused on the investigation of signaling pathways are involved in lung diseases and are associated with the function of eupafolin and WBGE. To get a deeper understanding of these effects and the related mechanisms can provide important insights into the therapy and prevention of pulmonary inflammation. Taken together, these findings can provide data to elucidate whether or not eupafolin and WBGE are used as the novel therapeutic agents in pulmonary inflammation.